

**GEOLOGY AND GEOCHEMISTRY OF GRANITOIDS OF KOKOONA  
AREA, IN RELATION TO MINERALIZATION, CENTRAL NIGERIA**

**By**

**Juliet Ugbede AKOH  
Msc/Scie/06161/09-10**

**A thesis submitted to the Postgraduate School, Ahmadu Bello University, Zaria, in  
partial fulfilment of the requirement for the award of the degree of Master of  
Science in Geology**

**Department of Geology  
Faculty of Science  
Ahmadu Bello University  
Zaria**

**May, 2014**

## DECLARATION

I declare that the work in this Thesis entitled “**GEOLOGY AND GEOCHEMISTRY OF GRANITOIDS OF KOKOONA AREA, IN RELATION TO MINERALIZATION, CENTRAL NIGERIA.**” has been carried out by me in the Department of Geology. The information derived from the literature has been duly acknowledged in the text and a list of references provided. No part of this thesis was previously presented for another degree or diploma at this or any other institution.

Akoh, Ugbede Juliet

---

Name of Student

---

Signature

---

Date

## CERTIFICATION

This thesis entitled “**GEOLOGY AND GEOCHEMISTRY OF GRANITOIDS OF KOKOONA AREA, IN RELATION TO MINERALIZATION, CENTRAL NIGERIA**” by Juliet Ugbede AKOH meets the regulations governing the award of degree of Master of Science [Geology (Mineral Exploration)] of the Ahmadu Bello University, and is approved for its contribution to knowledge and literary presentation.

\_\_\_\_\_  
Dr. P. O. Ogunleye  
Chairman, Supervisory Committee

\_\_\_\_\_  
Signature

\_\_\_\_\_  
Date

\_\_\_\_\_  
Dr. A. A. Ibrahim  
Member, Supervisory Committee

\_\_\_\_\_  
Signature

\_\_\_\_\_  
Date

\_\_\_\_\_  
Dr H. Hamza  
Head of Department

\_\_\_\_\_  
Signature

\_\_\_\_\_  
Date

\_\_\_\_\_  
Prof. A. A. Joshua  
Dean, School of Postgraduate Studies

\_\_\_\_\_  
Signature

\_\_\_\_\_  
Date

## **DEDICATION**

I dedicate this work to the Almighty God, the all-knowing, most gracious and most merciful for his faithfulness and love towards me (if not for God...).

## ACKNOWLEDGEMENTS

My foremost acknowledgement is to the Almighty God for His matchless grace and unfeigned love over my life, and for leading me thus far. He has given me all that I have needed to bring this work to a successful completion and I owe all that I am today and will ever be to Him. This work could not have been completed without the help and support of many specific persons, whom I would like to acknowledge here. First of all, I sincerely appreciate goes to the chairman of the supervisory committee, Dr. P. O. Ogunleye, my advisor and mentor, who was always available to give guidance, profound insight and assistance which have made this thesis a much better document than it might be without his input. For the very friendly and conducive atmosphere to learn under him, especially having a comfortable table and chair in his office for me to do my work, I say thank you Sir. My profound gratitude goes to the member supervisory committee Dr. A. A. Ibrahim for the profound assistance, his time, contributions, care and advice. I would also like to thank Professor E. C. Ike with whom this work was started but left the university service shortly thereafter.

My profound gratitude goes to the members of the internal examination committee, Prof. U. A. Danbatta and Dr. T. Najime for their timeless effort, careful and thoughtful review, which made this work better than it would have been, my appreciation sir.

Special note of appreciation is due also to the distinguished lecturers of the Department of Geology namely Drs. E.A Bala and S.A Alagbe especially for their fatherly advice and support, Mr. Shehu S. Magaji for his assistance and supply of academic materials, Drs. H. Hamza, E. O. Obiosio, A.E Ikpokonte, M. L. Garba, and I. Hamidu, Messrs A. Yola and I.I. Ahmed for their encouragement.. I am equally grateful

to Messrs R. Lamja and A. K. Abdulgafar who assisted with thin section preparation and Mr. E. Animashawun for helping in the sample preparation.

I also gratefully acknowledge my course-mates namely Messrs U. Ajose, T. Wandaku, F. Oche, Miss H. Onaji and Mrs. R. Adedayo for their friendship and willingness to rob minds over related academic issues or lend a hand, despite their tight schedule. My thanks also go to Mr Iyakwari and Mr Ibrahim both student of Nasarawa State University, Keffi for assisting me in the field.

My special thanks are due to Sir Akpabio Wilson Utin and his family for their financial assistance and support. Thank you for being there and for everything that you have done for me. God bless you sir. To others, who in one way or another have played a role in shaping my life and academic pursuit but too numerous to mention, I say thank you. Last, but far from the least, I would like to thank my family, especially mother and father Mr. and Mrs. Usman I. Akoh, for their love, prayer, encouragement and unalloyed support to ensure that I complete this work well. I am equally grateful to my siblings for the encouragement and their funny questions about rocks.

## ABSTRACT

The Angwa-Doka area, Kokoona LGA of Nasarawa State is underlain by migmatite, mica schist, granodiorite, topaz-bearing biotite granite and pegmatite. Geological and geochemical studies of the area were undertaken to determine processes of formation and the gemstone-bearing capacity of the pegmatites. Field mapping on a scale of 1:20,000 and petrographic studies were carried out while geochemical analysis of samples of the granitoid and muscovite selected from the different zones of the pegmatites were undertaken using a lithium metaborate/tetraborate fusion ICP-MS for the major, minor and trace elements. In addition, B and Li were analyzed in the muscovite samples using sodium peroxide fusion ICP-MS while fluorine was analyzed by fusion specific ion-electrode method. The results revealed a mineralogical zoning of these rocks from a metaluminous A/CNK ratio ( $<1$ ) to a more fractionated peraluminous (A/CNK  $> 1.1$ ) S-type variety. The K/Rb value suggests that biotite granite in Janta area is highly fractionated while chondrite normalized REE distribution patterns display distinct M-type tetrad effect and strong Eu depletion believed to be associated with late stage magmatic processes that brought about associated greisenization in the rock.

The pegmatites are commonly zoned and range from barren, simple to highly evolved lepidolite facies in the inner-most zone. Representative muscovite samples selected from different zones of pegmatites were studied to determine whether the pegmatites and the host granodiorite can be related by a common fractionation path. The geochemical data further reveals that Rb, Cs, Be, Li, F, B, Sn, Zn, Ta and Nb contents increase from the host granitoids inwards. In general, the Rb, Cs, Be, Li and F contents of the pegmatite increase with decreasing K/Rb and K/Cs ratios. The corresponding increase in Li, F and MnO contents from the border to the lepidolite unit is concomitant with decrease in  $\text{Fe}_2\text{O}_3$ , MgO,  $\text{Al}_2\text{O}_3$  and  $\text{TiO}_2$  from the border zone towards the core of the pegmatite. Li content of 0.213 wt% was recorded in the intermediate zone, increasing through the spodumene zone to 1.25-2.82 wt% in the core zone. F concentration also ranges from 0.43-0.62 wt% in the intermediate zone to 1.85-4.5wt% in the core zone. These variations are consistent with rare-element enrichment via fractionation processes, based on the degree of compatibility combined with partitioning of rare elements from the pegmatite melt into the minerals and volatile late stages. The pegmatite group in Angwan Doka, Kokoona district can be said to be "heterogeneous" consisting of the different types and subtypes of LCT family, Rare Element Class pegmatites of albite, spodumene, lepidolite to elbaite sub-class.

Tourmaline is essentially magmatic and display characteristic that indicate evolution from schorl-dravite series within the outer zones while the high activities of F, Li and B coincide with the abundant and quality of tourmaline (liddicoatite-rossmanite-elbaite solid solution series) encountered in the evolved zones of the pegmatite. Transfer of chemical components is probably one way; from the host rock to the pegmatite magma. The pegmatite dykes crystallized inwards from the wall-rock contact in a closed system. The systematic increase and replacement of biotite by muscovite in the fractionated granodiorite of Angwan Doka area, coupled with the increase in B, Li and F contents of the muscovite towards the lepidolite unit could serve as potential indicators of gem tourmaline mineralization in the pegmatite provinces of Nigeria.

## TABLE OF CONTENT

Declaration .....	ii
Certification.....	iii
Dedication .....	iv
Acknowledgements .....	v
Abstract .....	vii
Chapter 1	
INTRODUCTION	
1.1 Introduction .....	1
1.2 Statement of Research Problems .....	7
1.3 Location and Accessibility .....	9
1.4 Climate and Vegetation .....	9
1.5 Relief and Drainage .....	10
1.6 Previous Work .....	11
1.7 Objectives .....	14
1.8 Scope of Present Work.....	14
Chapter 2	
GEOLOGICAL SETTING	
2.1 Regional Geology.....	16
2.1.1 The Migmatite-Gneiss Complex (MGC) .....	18
2.1.2 The Schist Belts (metasedimentary and metavolcanic rocks).....	18
2.1.3 The Older Granites (Pan-African granitoids).....	19
2.1.4 Volcanics .....	20
2.1.5 The Younger Granites .....	21
2.2 Geology of Angwan Doka Area .....	22
2.2.2 Schist.....	24
2.2.3 Granodiorite .....	25
2.2.4 Granodiorite-Pegmatite Contact Rock .....	30
2.2.5 Aplite Zone .....	31
2.3 The Pegmatite Dykes .....	34
2.3.2 Angwan Doka Pegmatite body .....	38
Internal fabrics .....	38
2.3.3 Wallrock Alteration .....	45
2.3.4 Pocket Indicators.....	46



2.4	Geology of Janta Area .....	48
Chapter 3		
GEOCHEMISTRY OF THE GRANITOIDS		
3.1	Introduction .....	53
3.2	Geochemical Data .....	53
3.3.1	Granitoids .....	53
	Granodiorite .....	58
	Granite.....	60
3.4	Trace Element Characteristics of the Granitoids .....	62
Chapter 4		
PETROGENESIS OF THE GRANITOIDS AND PEGMATITES		
4.1	Rare Earth Elements .....	82
4.2	Niobium-tantalum Tin mineralization .....	89
4.3	Evolutional Trends and Gemstone Mineralisation Potential of the Angwan Doka Pegmatite .....	96
Chapter 5		
	DISCUSSION.....	105
Chapter 6		
CONCLUSION AND RECOMMENDATIONS		
6.1	Conclusions .....	115
6.2	Reccomendations .....	117
	REFERENCES .....	119

## LIST OF TABLES

Table 1.1	Classification of pegmatites according to Cerny, (1991).....	3
Table 1.2	Gemstones found in granitic pegmatite (after Simmons, 2007) .....	6
Table 3.1	Major elements data in granitoids and muscovite samples; (all values in wt %). .....	54
Table 3.2	Trace element data in granitoids and muscovite samples; (all values are in ppm except where stated otherwise) .....	56
Table 3.3	Rare earth elements data in the granitoids and mineral separates from pegmatites .....	57
Table 3.4.	Element ratios in granitoids and muscovite from Angwan Doka pegmatite group .....	58
Table 4.1	Chondrite normalized rare earth elements data in the granitoids and muscovite from Angwan Doka pegmatite group.....	86
Table 4.2	Absolute values of the REE tetrad effect in the granitoids .....	87

## LIST OF FIGURES

Fig. 1.1	Regional zoning in LCT pegmatite around a parental pluton (after Cerny, 1992) .....	5
Fig. 1.2	location map of study area .....	10
Fig. 2.1.	Map of Gondwana at the end of Neoproterozoic time showing the general arrangement of Pan African belts ( after Kusky <i>et al.</i> , 2003). .....	17
Fig. 2.2	Outline geological map of Nigeria .....	20
Fig. 2.3	Geological map of Kokoona area, north-central Nigeria .....	23
Fig. 2.4	Rose diagram with the general structural orientation of linearments within the study area .....	24
Fig. 2.5	Rose diagram of orientation of strike of the pegmatite dykes in the study area .....	35
Fig. 3.1	Classification of the granitoids according to TAS classification, after middlemost (1985) .....	58
Fig. 3.2	Bivariate plot of major element for granitoids. Symbols are same as in Fig, 3.1.. .....	59
Fig. 3.3	Chemical classification of the granitic rocks using the molecular ratio of alumina to alkalis [ $Al_2O_3/(Na_2O+K_2O)$ ] versus alumina to lime and alkalis $3I_2O_3/(CaO+Na_2O+K_2O)$ after Shand (1943).(b),A/CNK versus $SiO_2$ .....	60
Fig. 3.4	AFM classification of Irvin and Baraga (1971), (b), Peccerillo and Taylor (1976). .....	61
Fig. 3.5	Discriminant diagram for the granitoids after Batchelor and Bowden (1985). Symbols are same as in Figure 3.1. ....	62
Fig. 3.6	Discriminant diagram for the granitoids (after Pearce <i>et al.</i> , 1984). Symbols are same as in Fig.3.1 .....	63
Fig. 3.7	Rare earth elements pattern for granitic rocks. The chondrite normalizing values are those of Boynton (1984). Symbols are same as in Figure 3.1 .....	65
Fig. 3.8	Selected trace elements spider diagram relative to Upper Crust. The normalizing values are those of Taylor and McLennan, (1985). .....	67
Fig. 4.1	Plot of K/Rb versus Cs from individual pegmatites and pegmatite group from the Tanco pegmatite, Monitoba after Cerny (1985). .....	71
Fig. 4.2	K/Rb versus Cs variation plot in the granodiorite and pegmatite. ....	72
Fig. 4.3	K/Rb versus Rb plot of the samples. Symbols are same as in Figure 4.2 .....	73
Fig. 4.4	Plot of K/Cs versus Cs in samples showing the degree of fractionation and mineralization of the pegmatite. (Symbols are same as in Figure 4.2) .....	74
Fig. 4.5	Rb versus Sr plot of the samples from the study area. (Symbols are same as in Figure 4.2) .....	75

Fig. 4.6 Rb versus Ba plot of the samples from the study area. (Symbols are same as in Figure 4.2).....	76
Fig. 4.7 Plot of Fe <sub>2</sub> O <sub>3</sub> versus MgO of muscovite from Angwan-Doka area (Symbols same as in Figure 4.2). .....	77
Fig. 4.8 Bivariate plot of TiO <sub>2</sub> and MgO. Symbols are same as in Figure 4.2.....	79
Fig. 4.9 Bivariate plot of Li versus F indicating the gem elbaite potential within the inner most zones of the pegmatite. Symbols are same as in Figure 4.2.....	80
Fig. 4.10 Li and F values of muscovite from gemstone-rich pegmatite from other parts of the world (Jolliff <i>et al.</i> , 1986, Viana <i>et al.</i> , 2007, Roda <i>et al.</i> , 2005) .....	81
Fig. 4.11 Chondrite normalised REE pattern of the granitoids from the study area displaying the four segment of the lanthanide tetrad effect. ....	85
Fig. 4.12 Chondrite normalised REE patterns of the host granodiorite and muscovite samples from different zones of the pegmatite. ....	88
Fig. 4.13 The evolution of the Nb and Ta-oxides in the different pegmatite zones of Angwan Doka pegmatites (after Cerny <i>et al.</i> , 1985).....	90
Fig. 4.14 Variation plot Nb/Nb+Ta against Li. After Anderson (2013). Chondrite normalised REE patterns of the host granodiorite and muscovite samples from different zones of the pegmatite.....	91
Fig. 4.15 Ternary plots to demonstrate the association of Ta and Nb enrichments with the albite and muscovite rich parts of the pegmatite (after Kontak, 2006., Anderson,2013).....	92
Fig. 4.16 Variation in the B within the pegmatite zones. ....	99
Fig 4.17 Bivariate plot of MnO and Li .....	100

## LIST OF PLATES

Plate I.	Photograph of highly foliated N–S trending schist exposed at the NW quadrant of the study area .....	25
Plate II	Photomicrographs of schist composed of BIO=biotite, QTZ= quartz, PLF= plagioclase feldspar (A) with fractures cutting across foliation in the schist. Diameter of view = 3.2 X 40.....	25
Plate III	Photograph of outcrop of granodiorite at Jamalou area with cross-cutting fractures ....	26
Plate IV	Granodiorite, Angwan-Doka. (a) Crossed polarized light photomicrograph of plagioclase and microcline crystals exhibit displacement within the crystal. (b), Myrmekitic intergrowth of quartz and plagioclase replacing alkali feldspar.....	27
Plate V	Photomicrographs of the granodiorite at Jamaalu. The rock is composed of quartz, plagioclase, biotite and amphiboles with (a), Crossed polarized light QTZ= quartz displaying strains with pressure shadow, undulose extinction and (b) plane polarised light .....	28
Plate VI	Photomicrograph of granodiorite, Angwan-Doka; (a) Replacement of plagioclase by sericite and associated cordierite (b) Feldspar exhibiting different twinning styles of Carlsbad twinning, tweed texture with exsolution and alteration micro texture .....	29
Plate VII	Photomicrograph of granodiorite in Angwan-Doka (a) Crossed polarized light, biotite swerving around quartz and feldspar porphyroblast (b) stage rotated; diameter of view = 3.2 X 40. ....	29
Plate VIII	Photomicrograph of the granodiorite around Jamaalu; Crystals of biotite (Bio) associated with hornblende (Hbl) already undergoing alteration (a) Crossed polarised light, (b) Plane polarized light .....	30
Plate IX	Photomicrograph of granodiorite-pegmatite contact rock. (a) Alignment of biotite which impart a gneissic appearance (b) Replacement of biotite by muscovite and tourmaline, and feldspar by mica which occurs as blebs. Crossed nicols; diameter of view = 3.2 X 40.....	31
Plate X	(a) Photomicrograph of aplite, Angwan Doka, composed largely of albite, quartz, garnet, K-feldspar and muscovite. (b) Alteration of muscovite to tourmaline. (a) Crossed nicols, (b) Plane polarized light; diameter of view= 3.2 X 40 .....	32
Plate XI	(a) Photomicrograph of tourmaline crystals in pegmatite-contact rock. (a) Crossed polarised light, (b) Plane polarized light; diameter of view = 3.2 X 40.....	33
Plate XII	Photomicrograph of skeletal tourmaline (TUR) with inclusion of quartz (QTZ). Crossed polarised light; diameter of view = 3.2 X 40.....	34
Plate XIII	Photographs of pegmatite vein (a) and pods (b) in granitoids from study area.....	35
Plate XIV	Photograph of muscovite books hosted by quartz in a simple pegmatite, Angwan Doka .....	37

Plate XV Photograph of layered sacharoidal albitic aplite, with quartz, mica, garnet and Ta-oxide minerals .....	37
Plate XVI Hand specimen of border zone of pegmatite composed of albite containing biotite abuts in granodiorite, Angwan Doka .....	41
Plate XVII Photograph of hand specimen from the pegmatite wall zone, Angwan Doka. The rock is of composed K-feldspar, albite, graphic intergrowth of quartz and tourmaline with beryl and Ta-oxide mineral .....	41
Plate XVIII Photograph of the pegmatite wall zone, Angwan Doka, consisting of K-feldspar, albite, quartz, mica and inward flaring tourmaline .....	42
Plate XIX Crystals of schorl on quartz matrix .....	42
Plate XX Photograph of hand specimen containing crystals of Kunzit in groundmass of spodumene, (B) Pink beryl.....	43
Plate XXI Hand specimen of inner zone of pegmatite containing lithium aluminosilicate .....	43
Plate XXII Photograph of bicoloured water melon elbaite tourmaline in a massive lepidolite; the core pink colour surrounded by green colour .....	43
Plate XXIII Radial albite (A) attached to lepidolite and quartz unit at the base (B) base of albite unit attached to the upper lepidolite unit .....	44
Plate XXIV Crystals of tourmaline (elbaite) with green cap extracted from cavity in the lepidolite - albitic unit, Angwan Doka area .....	45
Plate XXV Sharp contact between pegmatite with the host rock.....	46
Plate XXVI photograph of muscovite rich replacement zone (B) part of the albitized wall zone (Mineralized in columbite-tantalite).....	46
Plate XXVII Dyke intersection in a mine pit at Angwan Doka .....	47
Plate XXVIII Typical pit from which alluvial gems and cassiterite minerals are won .....	49
Plate XXIX Topaz, Beryl and Aquamarine crystals from Janta alluvial-eluvial deposits.....	49
Plate XXX(a) Close up view of microcline altered to mica and clay, (b) Replacement of plagioclase by perthite. Crossed polarised light; diameter of view = 3.2 X 100 .....	51
Plate XXXI Exsolution within a plagioclase grain. Albite exsolved from microcline, the albite is light gray and display faint polysynthetic twinning while the microcline is mottled dark gray.....	51
Plate XXXII Photomicrograph of sericitized plagioclase crystals with deformational cracks within quartz and plagioclase .....	52

## CHAPTER ONE

### INTRODUCTION

#### 1.1 INTRODUCTION

Pegmatite is an exceptionally coarse grained igneous rock with interlocking crystals usually formed as irregular dykes, lenticular pod-like bodies, lenses or veins especially at the margin of deep-seated plutons, usually extending from the pluton itself into the surrounding country rocks. It represents the last and most hydrous portion of magma to crystallize hence it commonly contains high concentration of minerals present only in trace amount in granitic rocks. The pegmatite in the Angwan Doka area consists of discrete dykes, that generally coalesce to form a large N-S-trending dyke (or dykes), dipping moderately to the west. The dyke displays advanced fractionation, manifested by irregular spatial zonation of mineral assemblages, abundant rare-metal mineral phases and gemstones which are genetically linked to the late-orogenic Pan-African ( $\pm 550$  Ma) granodioritic host rock. It is a part of the rare-metal pegmatites occurring in a SW-NE trending broad belt extending for about 400 km from Ago-Iwoye in SW to Wamba, north-central Nigeria. Tourmaline, beryl and kunzite have been recorded in the pegmatite bodies. The tourmaline consist of dark-black, (schorl) in the outer unit of the pegmatite and varies from pale pink to deep pinkish red, greenish, violet green and blue varieties normally associated with the lepidolite, quartz and albite in the spodumene to core zone of the pegmatite. To the south of Angwan Doka area is the Janta biotite granite which is part of the Afu Complex, Younger Granites of Nigeria; and it is highly mineralized in topaz and beryl.

Crystallization mechanism of pegmatites has been a highly debated topic (Jahns and Burrham, 1969; London *et al.*, 1988; Morgan and London, 1999; Černý, 1991). Many hypotheses which include processes ranging from closed system fractional crystallization

of coexisting granitic and hydrous melt (Jahns and Burnham, 1969) to rapid cooling completely to a glass with subsequent development of pegmatitic textures by zone refinement which involves disequilibrium crystallization from an undercooled, flux-bearing granitic melt have been presented (Morgan and London, 1999). Černý (1991) described four plausible models for the development of pegmatites. These are:

- (i) Closed chamber crystallization,
- (ii) Open system deposition from flowing fluids,
- (iii) Recrystallization or metasomatism of finer-grained precursors, and
- (iv) Metasomatic replacement by fluids generated in the pegmatite or introduced from an external source, or some combination of all of these.

Of the four models presented by Černý (1991), the most prevalent view is crystallization of a volatile-rich, hydrous granitic melt under decreasing temperature in a relatively closed system with restricted exchange with the wall rock.

The very popular classification of pegmatite which combines depth of emplacement, metamorphic grade and minor constituent elements as proposed by Černý (1991) has four categories namely: the abyssal class, muscovite class, microlitic and rare element class (Table 1.1). Further subdivisions of the rare-element pegmatite, largely by their distinctive patterns of enrichment in rare-element (Li, Cs, and Ta; or Nb, Y, and F) are the Lithium-Cesium-Tantalum (LCT) and Niobium-Yttrium-Fluorine (NYF) families. LCT is a characteristic enrichment found exclusively in S-type granites that originate from metasedimentary rocks related to compressional tectonism. The peraluminous nature of LCT is expressed by the presence of muscovite, tourmaline, spessartine-rich garnet and topaz or andalusite. In addition to Li, Cs, and Ta, this pegmatite tends to be enriched in Be, B, F, P, Mn, Ga, Rb, Nb, Sn and Hf.



**Table 1.1: Classification of pegmatites according to Černý, (1991)**

CLASS	Family	Typical Minor Elements	Metamorphic Environment	Relation to Granite	Structural Features	Examples
ABYSSAL	_____	U, Th, Zr, Nb, Ti, Y, REE, Mo Poor (to moderate) mineralization	(Upper amphibolite to) to high- P granulite facies  ~4-9 kb  ~700-800 <sup>o</sup> C	None (segregation of anatectic leucosome)	Conformable to mobilized cross-cutting veins	Rae and Hearne province, Sask. (Tremblay, 1978); Aldan and Anabar shields Siberia (Bushev and Koplus, 1980); Eastern Baltic shield (Kalita, 1965)
	_____	Li, Be, Y, REE, Ti, U, TH, Nb>Ta  Poor (to moderate) mineralisation, micas and ceramic minerals.	High-P, Barrovian amphibolite facies (Kyanite-Sillimanite)  ~5-8 kb ~650-580 <sup>o</sup> C	None (anatectic bodies) to marginal and exterior	Quasi-conformable to cross-cutting	White Sea region, USSR (Gorlov, 1975); Appalachian Province (Jahns <i>et al.</i> , 1953); Rajahstan, India (Shmakin, 1976)
RARE-ELEMENT	LCT	Li, Rb, Cs, Be, Ga, Nb<>Ta, Sn, Hf, B, P, F  Poor to abundant mineralization gemstock industrial minerals.	Low-P, Abukuma amphibolite to upper greenschist facies (andalusite-sillimanite)  ~2-4 kb ~650-500 <sup>o</sup> C	(Interior to marginal) to exterior	Quasi-conformable to cross-cutting	Yellowknife, NWT (Meintzer, 1987); black Hills, South Dakota (Shearer <i>et al.</i> , 1987); cat Lake-Winnipeg river field, Monitoba (Cerny <i>et al.</i> , 1981)
	NYF	Y, REE, Ti, U, Th, Zr, Nb>Ta, F  Poor to abundat mineralization, ceramic minerals	variable	Interior to marginal	Interior pods, conformable to cross-cutting exterior bodies	Liano Co., Texas (Landes, 1932); South Plattes distric, Colorado (Simmons <i>et al.</i> , 1987); Western Keivy, Kola, USSR (Beus, 1960)

<b>MIAROLITIC</b>	<b>NYF</b>	Be, Y, REE, Ti, U, Th, Zr, Nb>Ta, F  Poor mineralization, gemstocks	Shallow to sub-volcanic  ~1-2 kb	Interior to marginal	Interior pods and cross-cutting dykes	Pikes Peak, Colorado (Foord, 1982); Sawtooth batholith, Idaho (Boggs, 1986); Korosten pluton, Ukrain (Lazarenko <i>et al.</i> , 1973)
-------------------	------------	---	--	----------------------	---------------------------------------	---

NYF is a characteristic suite of elements normally associated with A-type anorogenic granite and pegmatite within-plate granites. Apart from Nb, Y and F, the NYF pegmatites are enriched in heavy rare-earth elements (HREE). In the opinion of Černý and Ercit (2005), NYF pegmatites are associated with granite magmatism that is thought to originate from deep melting of crust within continental rift zones and usually with some chemical input from mantle sources.

According to Černý (1992), the peraluminous granite and pegmatite of LCT type commonly exhibit spatial sequence of zonations, fractionation and enrichment in Li dominant mineral, outward from their peraluminous source with respect to proximity of the related pluton as illustrated in Figure 1.1, while NYF pegmatites are generally clustered within the vicinity of the parent granite. Pegmatites are considered to be the source of the world's finest gemstones and are the main source of more than 40 gem minerals (Table 1.2).

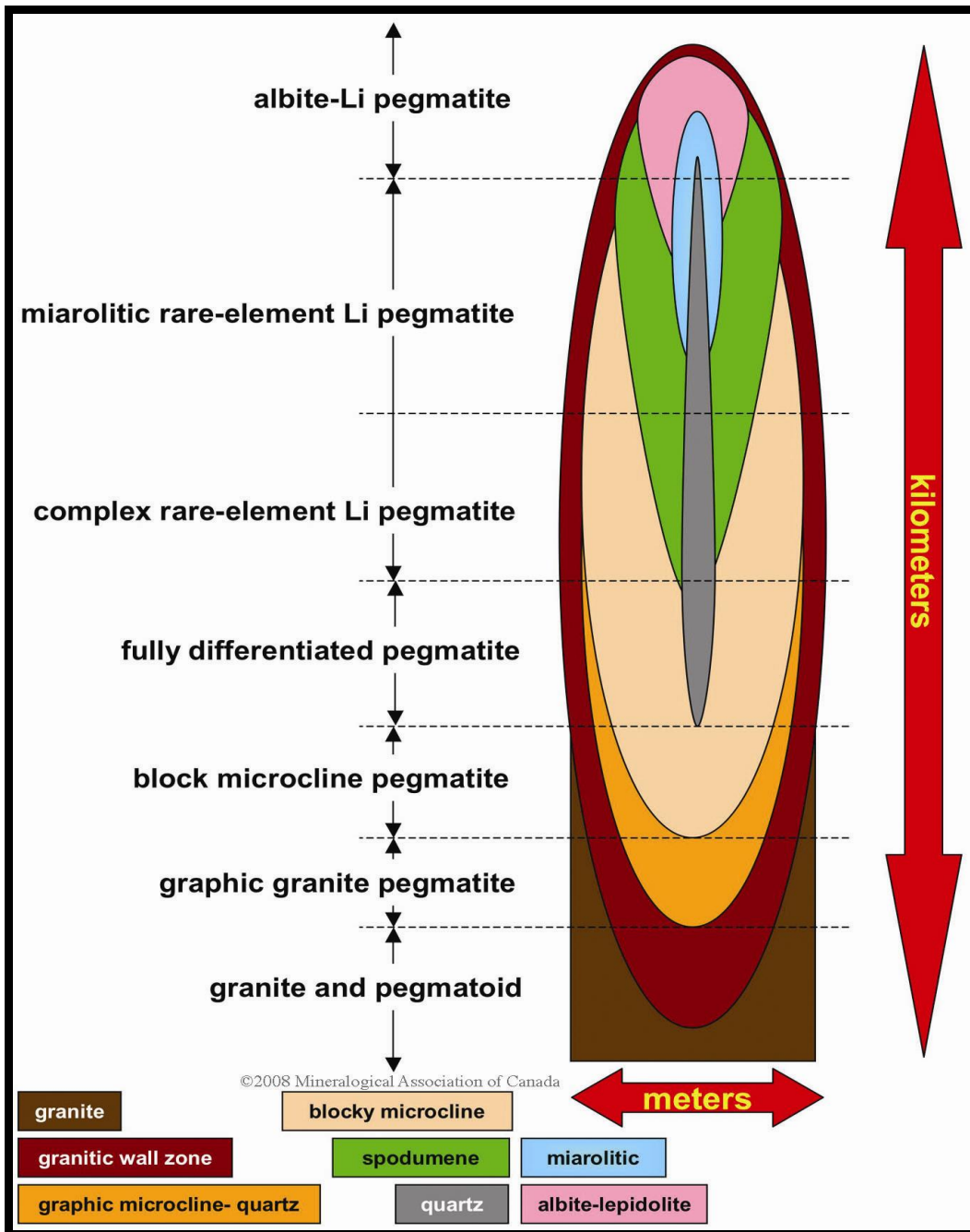


Figure 1.1: Regional zoning in LCT pegmatite around a parental pluton (after Černý 1992).

**Table: 1.2: Gemstones found in granitic pegmatite (after Simmons, 2007)**

GEMSTONES	COLOUR	MINERAL/GROUP	ABUNDANCE	PEGMATITE TYPE
Achroite	C	Tourmaline group	R	LCT
Albite	C	Plagioclase group	C	NYF&LCT
Amazonite	G	Alkali feldspar group	C	NYF>LCT
amblygonite	PL, Y,C	Amblygonite	R	LCT
Aquamarine	G-B	Beryl	C	NYF&LCT
Beryllonite	C,PL,Y	Beryllonite	VR	LCT
Brazilianite	Y-G	Brazilianite	VR	LCT
Chrysoberyl	g-y	Chrysoberyl	R	LCT
Danburite	C,Y	Danburite	R	LCT
Elbaite	C,P,G,B	Tourmaline group	C	LCT
Euclase	B-G	Euclase	VR	LCT
Flouropatite	B-P,PUR,G	Apatite group	C	NYF<LCT
Goshenite	C	Beryl	C	NYF<CLT
Hambergite	C,PL,Y	Hambergite	VR	NYF&LCT
Heliodor	Y	Beryl	R	NYF&LCT
Hiddinite	G-Y	Spodumene	VR	LCT
Hydroxylherderite	C,PL,Y,B	Hydroxylherderite	VR	LCT
Indicolite	B	Elbaite-schorl tourmaline	C	LCT
Jeremejevite	B	Jeremejevite	VR	NYF
Kunzite	P,PUR	Spodumene	R	LCT
Lazulite	B	Lazulite	R	LCT
lepidolite	PUR-P	Lepidolite	C	LCT
liddicoatite	P-R	Tourmaline group	R	LCT
londonite	Y-C	Londonite	VR	LCT
manganotantalite	R	Manganotantalite	VR	LCT
microlite	Y,R,BR	Microlite	VR	LCT
montebrasite	C,PL,P-Y	Montebrasite	R	LCT
morganite	P-O	Beryl	R	LCT
oligoclase	C	Plagioclase group	C	NYF&LCT
petalite	C	Petalite	R	LCT
pezzottaite	R	Beryl group	VR	LCT
phenakite	C,P,Y	Phanakite	R	NYF>LCT
pollucite	C	Pollucite	R	LCT
quartz	C,P,SM,PUR	quartz	C	NYF&LCT
rhodizite	Y-C	Rhodizite	VR	LCT
rossmanite	P-R,C,G	Tourmaline group	VR	LCT
rubellite	P-R	Elbaite –tourmaline	R	LCT
sanidine-orthoclase	Y,C	group	C	NYF
simpsonite	Y,O	Alkali feldspar group	VR	LCT
simpsonite	O	Simpsonite	C	LCT
spessartite	C-G	Garnet group	C	LCT
spodumene	Y	Spodumene	VR	LCT
stibiotantalite	B,C,P	Stibiotantalite	C	NYF&LCT
topaz	R,BR,P	Topaz	C	NYF
triplite	B-G	Triplite	R	LCT
triphylite	G	Triphylite	R	LCT
verdelite	C,P,BR,G	Elbaite-tourmaline group	C	NYF&LCT
zircon		Zircon		

**Colours:** C, colourless; G, green; Y, yellow; B, blue; P, pink; R, red; O, orange; Br, brown; Pur, purple; sm, smoky; Pl, pale. **Abundance in pegmatite:** C, common; R, rare; VR, very rare.

## 1.2 STATEMENT OF RESEARCH PROBLEMS

Gemstones have been prized for thousands of years for their colour, lustre, transparency, durability and high value to volume ratio. Gem deposits are rare because the geologic conditions necessary for the formation of gem-quality materials are rarely attained (Groat, 2007). These conditions include some or all of the following:

- i. Availability of major constituents, which in some cases are uncommon in nature.
- ii. Presence of adequate chromophore (elements responsible for colour in minerals) which can be rare in certain environments.
- iii. Limited concentrations of undesirable elements, which may be common either in nature or in a specific geologic environment (such elements can either impart an “off” colour or impede crystal formation).
- iv. Open space for crystals to grow unimpeded, which is rare in most geologic environments.
- v. Environment to form crystals of sufficient size and transparency.
- vi. Gem deposits also require specific thermobarometric conditions favourable for the crystallization and stability of the specific mineral.

Most gemstones have been reported to occur within pegmatites which display unique geological and mineralogical features (London, 2008; Simmons, 2007). Majority of the notable gem-producing pegmatite districts especially those in Brazil, Namibia,

Tanzania, Mozambique, and Madagascar are Neoproterozoic in age (870 - 550 Ma), Kroner (2004) and were formed during the closing stages of the tectono-metamorphic Pan-African event which occurred within the Gondwana paleocontinent. The Pan-African orogeny, between the West African craton and the Congo craton has been reported to be related to the Borborema (Brasiliano) and Pan-African provinces (Dada, 2006). One of the characteristic features of these provinces is the occurrence of a large number of granitoid bodies sporadically distributed in the basement. In Nigeria, these granitoids belong to the Older Granite suites, which have been dated  $600 \pm 150$  Ma by Matheis and Caen-Vachette (1983).

During the past few decades, many new gemstones and hitherto unknown, yet interesting gem quality minerals have been discovered and reported from different part of Nigeria (Aga and Ashano, 2008). The mineralogy of the gem deposits varies widely. Many of these gem minerals are unique and have recently been the subject of much research. The gem mineral deposit in Kokoona-Angwan Doka area comprise of tourmaline, beryl and topaz belonging to Li-Cs-Ta enriched group of the rare element bearing granitic pegmatites. The pegmatites have been reported to have formed in the late orogenic Pan-African Older Granites ( $600 \pm 150$  Ma) and schist (Matheis and Caen-Vachette, 1983; Jacobson and Webb, 1946).

A great majority of the previous work on the Nigeria pegmatites have concentrated on geochemistry, petrology and mineralogy all with emphasis on the ore bearing (metallic) potential of the pegmatites e.g. Küster (1990), Ekwueme and Matheis (1995), Garba (2002), Akintola and Adekeye (2007), Okunlola and Ocan, (2009). However, as far as can be ascertained no detail study has been solely devoted to the determination of the processes

of formation and the gemstone bearing capacity of these pegmatites. The pegmatites are currently being exploited for their gemstone and precious metals. This thesis examines the evolution and mineralization of the Angwan Doka granitic pegmatite, continuity of work aimed at a better understanding of how the gem deposits formed becomes essential in order to maintain and benefit from the cumulative investment in the knowledge of the geology and mineral resources of the country. Furthermore, efforts to update the existing geological data through systematic re-investigation of compositional trends, as it relates to the geochemical differentiation or evolution of the pegmatite which is the major source of gemstone will be in consonance with the drive to ensure availability of reliable exploration guide. This work is, therefore, a contribution towards the federal government tasks of developing the solid mineral sector and to ensuring a healthy supply of gems for the growing market both in the immediate and foreseeable future.

### **1.3 LOCATION AND ACCESSIBILITY**

The area of investigation is located on the Nigeria Sheet (209), Akwanga NW 209 – Akwanga SW 209 and Doma 230. It is bounded by latitude  $8^{\circ} 20'$  and  $8^{\circ} 50'$  N and longitude  $8^{\circ}$  and  $8^{\circ} 7'$  E (Figure 1.2) and covers an area of  $821.4 \text{ km}^2$ . Network of untarred roads that are linked to the major tarred road make the area quite accessible.

### **1.4 CLIMATE AND VEGETATION**

The area of study lies within the Guinea or tropical climate with distinct wet and dry season. The rainfall is concentrated in the short wet season which starts from mid-May to October whilst the dry season begins from November and last till April. An average

annual precipitation of about 1,200 mm have been recorded for the area with a generally high day time temperature while during the Harmattan the nights are very cold. The primary vegetation is characterized by grasses, shrubs and a few scattered trees, fringing forest with tall trees and well covered undergrowth along stream and river channels. The vegetation has been greatly modified by the agricultural activities of the inhabitants and consequently a mixture of grasses and short trees of the derived Guinea Savannah type now covers the area.

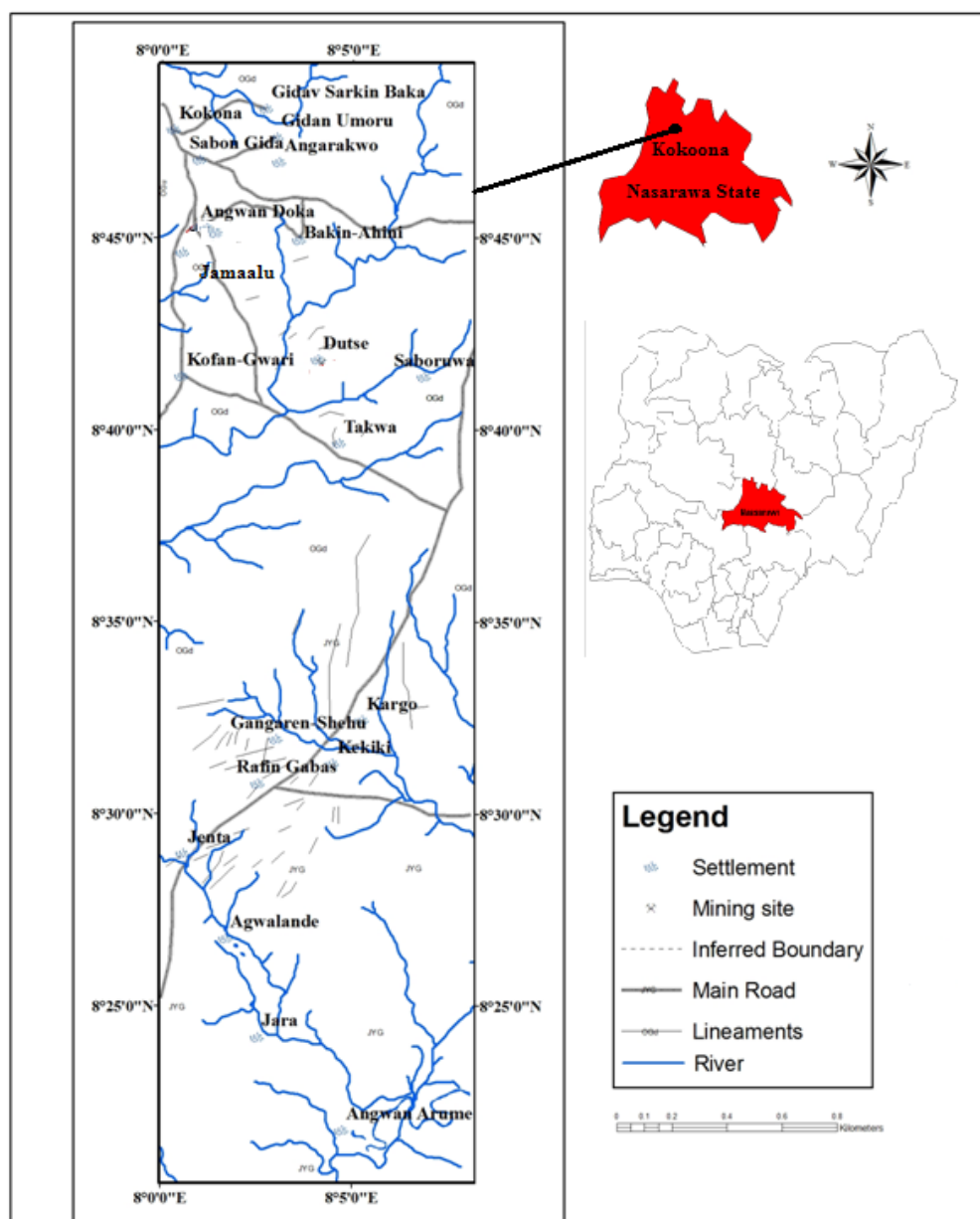




**Figure 1.2: Location map of study area. Inset: Political map of Nigeria indicating location of present Nasarawa State**

### **1.5 RELIEF AND DRAINAGE**

The area of study is gently undulating except where the pegmatite forms low ridges. The area is made up of pene-plain land and occasionally punctuated by hills measuring up to 400 m above sea level. All the streams draining the area flow southward and are mainly dendritic in pattern conforming to the topography of the area. The streams dry up during the long dry season.

### **1.6 PREVIOUS WORK**

Jacobson and Webber (1946) evaluated the rare-metal pegmatites of Nigeria and observed that the bulk of the tin, niobium and tantalum ores were formed during the late-stage albitization of the pegmatites. Their investigation covered a broad belt of the country extending south-west from Jema'a area of the Jos Plateau in the north to Egbe area in southwestern Nigeria. Matheis (1982) used the elemental ratios K/Rb and Rb/Sr to discriminate between barren and mineralized pegmatite and to identify fractional crystallization process that formed the pegmatite. Also Matheis and Caen Vachette (1983) used Sr isotopic ratios to determine the different ages and the cooling history of the pegmatite which formed over a time span from 562-534 Ma and suggested that the mineralized Egbe pegmatites are products of partial melting and leaching of the basement unit. He concluded that the Pan-African pegmatites are product of crustal recycling related to major tectonic lineaments and that there is no genetic link between the pegmatite and the Older Granites but that the pegmatite are product of high grade metamorphic conditions enhanced along a deep-seated reactivated continental lineament by high heat flow, with the host rock contributing significantly to the character of the pegmatite.

In addition the analysis of the fracture system of the Tuareg and Nigeria shield, McCurry (1971) and Ball (1980) reported that the end of the Pan-African tectonic event was marked by a conjugate fracture system of strike slip faults. Both authors noted that faults directions have a constant trend and sense of displacement i.e. a NNE-SSW trending system having a dextral sense of movement and a NW-SW trending system with a sinistral displacement. In her work on the Pan-African orogeny (McCurry, 1971) concludes that the pattern of those fracture system was probably established during the Pan-African event and that the main transcurrent movement probably occurred then. Wright (1970) was of the opinion that the regional faults had some influence on the direction of migration of hot spots within the mantle that culminated in the formation of the Mesozoic ring-complexes. Ajibade and Wright (1989), Küster (1990) and Garba (1996) further noted that both set cross-cut all the main Pan-African structures including older N-S trending shear zones (mylonites) and that other parallel Pan-African fracture system with structural trend (N 30° E and N 60° E) appears to have been precursors to the development of the Cretaceous Benue Trough and its associated volcanics.

Matheis and Caen-Vachette (1983) reported Rb/Sr age range of 562-535 Ma for barren and mineralized pegmatites of central and southwestern Nigeria and noted that the emplacement of the pegmatites in Nigeria occurred mainly after the peak of the Pan-African orogenic event. Geochronological data (Rb-Sr whole-rock, and U-Pb zircon) on Pan-African granitoids which intruded the reactivated Archean to Lower Proterozoic crust of central and south-western Nigeria proved that intrusive magmatic activity in these areas lasted from at least 630 to 530 Ma (Matheis and Caen-Vachette, 1983; Dada, 2006) .

Küster (1990), in his work on granites and granitic pegmatite from Wamba reported that enrichment of Rb, Cs, Sn, Nb and Ta in these rocks took place during both magmatic and postmagmatic evolution, with the highest contents of these elements occurring in early muscovite of the albitized and mineralized pegmatites.

Adekeye and Akintola, (2007) employed the degree of trace element correlation and K/Rb ratio versus Cs to determine the Ta-Nb-Sn ore-bearing potential of the pegmatite in Nasarawa area. These authors proposed that the late Pan-African tectonic granite which is parental to the highly mineralized pegmatites in this area originated from anatexis of undepleted mica-rich metasediments at depth, followed by a magmatic fractionation of the fluid rich melt as it ascended through reactivated ancient fractures. They also suggested that the heat for the partial melting might have been supplied mainly by the reactivation of ancient fractures, which controlled the emplacement of the fertile granites and the related pegmatites.

According to Okunlola and Ocan (2009), the pegmatite around Angwan-Doka can be divided into five mineralogical zones which are (i) Muscovite – quartz – microcline albite – Tourmaline (MQMIAT) zone, (ii) Lepidolite – Muscovite – Tourmaline (LMT) zone, (iii) Microcline – Albite (MIA) zone, (iv) Quartz – Muscovite – Albite (QMA) zone, and (v) Quartz – Beryl – Muscovite, Albite – tourmaline (QBMAT) zone. They reported the pegmatites to be Sn-Li rich with subordinate Ta-Nb concentration and that Sn is associated with the lepidolite, muscovite and albite rich zones.

The foregoing review of the previous work on the pegmatites in Nigeria shows that comparatively more attention has been focused on the rare metal potential of the Nigerian pegmatite zone. Detailed geochemical study is required to establish the gemstone bearing potential of the pegmatites associated with the granitoids in Angwan-Doka area.

The use of composition of muscovite in pegmatites to trace evolutionary and crystallization processes of tourmaline is not particularly new as Černý (1982); Jolliff *et al.*, (1987); London (2008); Roda *et al.*, (2005) and Viena *et al.*, (2007) have reported that the same fractionation trend of enrichment and substitution of element is commonly observed in both muscovite and tourmaline. By establishing and comparing the fractionation indices of the mineral, the sequence of crystallization of pegmatite zones and details of mineral paragenesis as it relates to gemstone formation can then be defined.

## 1.7 OBJECTIVES

The objectives of this work are:

- i. To investigate in detail the petrographic and chemical compositions in order to better understand the transformation sequences that affected the pegmatite and host rock.
- ii. To determine if the host rock (granodiorite) and the pegmatite are related by a common fractionation path.
- iii. To establish and describe mineralogically and chemically, compositional variation in a single pegmatite body (wall, intermediate and core zone).
- iv. To establish the geochemical signature of the pegmatites from Kokoona area and propose a petrogenetic model for evaluation of the pegmatite.
- v. To classify the pegmatite in line with current scheme of classification.

## **1.8 SCOPE AND METHODOLOGY**

The scope of the project is to use the geochemical composition especially Cs, Rb, K, Be, F, Li and B of the pegmatite to determine the trends of chemical fractionation that can aid in determining the gem mineralization potential and hence provide indices on favourable areas for further gemstones and rare-metal explorations.

In pursuance of the above stated objective, in-depth desk study and extensive review of journal articles, published and unpublished work, fieldwork and laboratory analyses were undertaken.

The fieldwork was carried out in two stages; first was the reconnaissance survey which was followed by geological mapping and collection of rocks and mineral samples for petrographic and laboratory studies. The area of investigation was mapped on a scale of 1:50,000. This was followed by mapping of the pegmatite bodies on a scale of 1:20,000 so as to determine the character of the individual pegmatite dyke and nature of the mineralization. Samples were collected from the least weathered zone. At each sampling site the coordinates were recorded as well as the strike and dip direction of the pegmatite dyke.

### ***Sampling and Analytical Methods***

Field mapping and rock sampling were carried out in February 2012. Care was taken to collect only fresh samples using geological hammer and sledge hammer, where appropriate. Altogether, 52 rocks and mineral samples were collected out of which 17 were selected for geochemical analysis. These comprise 6 samples (Doka 1, 5, 8, 15 and

Bah 1 and 2) believed to be representative of the host rocks of the pegmatite and gem minerals, while the remaining 11 samples (Doka 2, 3, 4, 6, 7, 9, 10, 11, 12, 13 and 14) are muscovite crystals extracted from the pegmatite dykes.

Preparation of thin section for petrographic studies was done at the Department of Geology Ahmadu Bello University. As part of the measure to ensure quality of the analytical data, the muscovite samples were cleaned by hand picking to remove contaminated grains. Samples of the granitoids and muscovite were then pulverized in a tungsten carbide mill at the Department of Geology, Ahmadu Bello University, Zaria. All the samples were thereafter analysed using a lithium metaborate/tetraborate fusion ICP-MS for major, minor and trace elements at the Activation Laboratory Ancaster, Ontario, Canada. In addition, B and Li were analyzed in the muscovite samples using sodium peroxide fusion ICP-MS while fluorine was analyzed by fusion specific ion-electrode method. The choice of fusion method ensures total metal dissolution, particularly for the REE in resistate minerals.

The analytical data generated were analysed using (GCDT 2.3 kit), a geochemical data treatment computer software for generating various discrimination diagrams.

## **CHAPTER TWO**

### **GEOLOGICAL SETTING**

#### **2.1 REGIONAL GEOLOGY**

Nigeria lies within the Pan-African reactivated mobile belt east of the West African Craton which has been stable since approximately 2.0 Ga (Küster, 1990). This mobile belt extends from Algeria across the southern Sahara into Nigeria, Benin and Cameroon. The Pan-African mobile belt continues southwest into northeast Brazil, and consist of a set of

orogenic cycles (the Brasiliano – Pan-African cycle) that lasted from about 850 to 550 Ma (Pinto and Pedrosa-Soares, 2001).

The Pan-African system of orogenic belts in Africa, Brazil and eastern Antarctica has been interpreted as a network surrounding older cratons (Figure 2.1) and essentially resulting from closure of several major Neoproterozoic oceans. In Nigeria, the granitoids associated with the Pan-African orogeny belong to the Older Granite suites (Jacobson and Webber, 1946; Grant 1970, Matheis 1979, Küster 1990), which have been dated  $600 \pm 150$  Ma old (Matheis and Caen-Vachette, 1983). While in Brazil, comparable granitoids especially in the Borborema province, have been associated with the Brasiliano Pan-African orogeny where analogous mineralized rare- metal pegmatite also occurs.

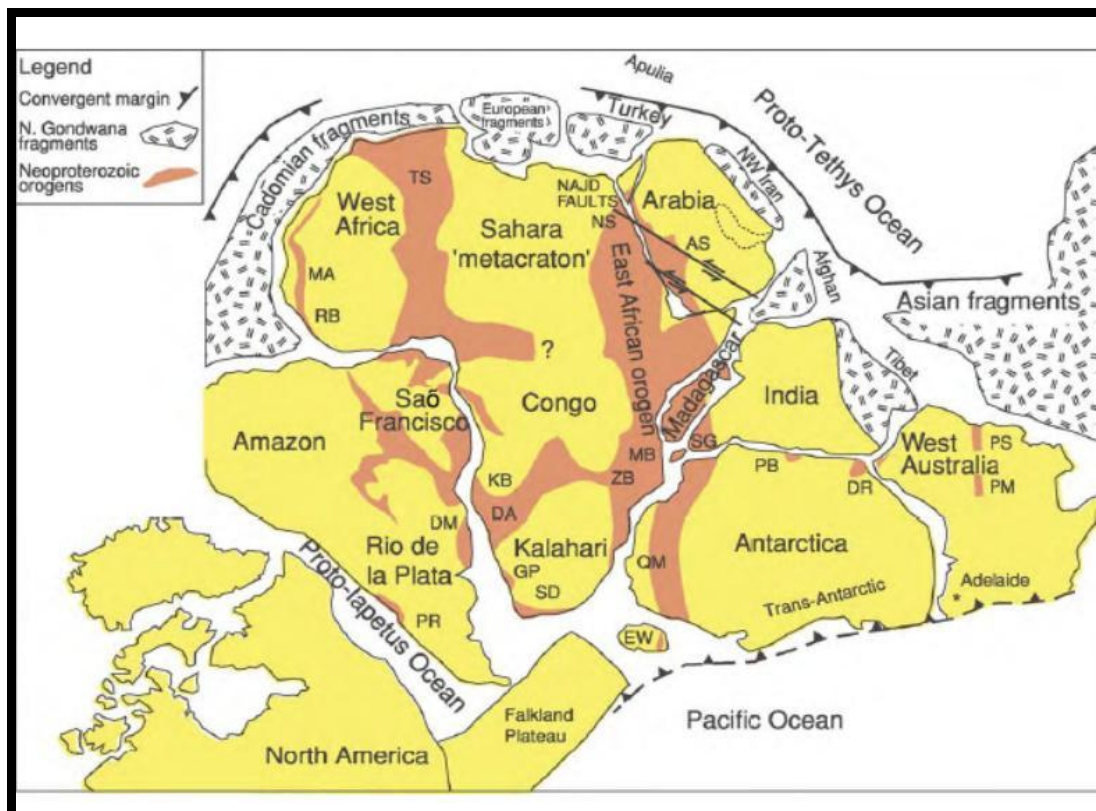


**Figure 2. 1: Map of Gondwana at the end of Neoproterozoic time showing the general arrangement of Pan African belts.** AS, Arabian Shield; BR, Brasiliano; DA, Damara; DM, Dom Feliciano; DR, Denman Darling; EW, Ellsworth Whitmore Mountains; GP, Gariep; KB, Kaoko; MA, Mauretanes; MB, Mozambique Belt; NS, Nubian Shield; PM, Peterman Ranges; PB, Pryolz Bay; PR, Pampean Ranges; PS, Paterson; QM, Queen Maud Land; RB, Rokelides; SD, Saldania; SG, Southern Granulite Terrane; TS, Trans Sahara Belt; WB, West Congo; ZB, Zambezi (after Kusky *et al.*, 2003).

The Nigerian basement rocks are believed to be the results of at least three major orogenic cycles of deformation, metamorphism and remobilization corresponding to the Liberian (2,700 Ma), the Eburnean (2,000 Ma), and the Pan-African cycles (600 Ma). The three cycles were characterized by intense deformation and isoclinal folding accompanied by regional metamorphism, which was further followed by extensive migmatization. Within the basement complex of Nigeria, four major petro-lithological units have been recognized. They are:

- i. the Migmatite-Gneiss Complex (MGC),
- ii. the Schist Belt (metasedimentary and metavolcanic rocks)
- iii. the Older Granites (Pan-African granitoids)
- iv. Volcanics

### **2.1.1 The Migmatite-Gneiss Complex (MGC)**

The Migmatite-Gneiss Complex is generally considered as the basement complex *sensu stricto* (Rahaman, 1988; Dada, 2006) and it is the most widespread of the component units in the Nigerian basement. It has a heterogeneous assemblage comprising migmatites, orthogneisses, paragneisses, and a series of basic and ultrabasic metamorphosed rocks. Petrographic evidence indicates that the Pan-African reworking led to recrystallization of many of the constituent minerals of the Migmatite – Gneiss Complex by partial melting with majority of the rock types displaying medium to upper amphibolite facies metamorphism (Dada, 2008). The Migmatite–Gneiss Complex has ages ranging from Pan-African to Liberian.



The Migmatite – Gneiss Complex of the Pan-African event not only structurally overprinted and re-set many geochronological clocks in the older rocks, but also gave rise to granite gneisses, migmatites and other similar lithological units (Rahaman, 1988).

### **2.1.2 The Schist Belts (Metasedimentary and Metavolcanic Rocks)**

The Schist Belts comprise low grade, metasediment-dominated belts trending N–S which are best developed in the western half of Nigeria, west of 8° E longitude, though smaller occurrences are found to the east but only sporadically. The belts are confined to a NNE-trending zone of about 300 km wide (Figure 2.2). The lithological variations of the schist belts include coarse to fine grained clastics, pelitic schists, phyllites, banded iron formation (Turner, 1964; Ajibade, 1980), Carbonate rocks (marbles/dolomitic marbles) and mafic metavolcanics (amphibolites) are also prominent members of the schist belts. Some may include fragments of ocean floor material from small back-arc basins (Rahaman, 1988).

The schist belts are believed to be relicts of a supracrustal cover which were infolded into the migmatite-quartzite gneiss complex, with the relicts of earlier structural event destroyed by the Pan-African (McCurry, 1973). Ajibade and Woakes, (1989) concluded that the schist belts are upper to late Proterozoic sediments and volcanic deformed and metamorphosed during the Pan-African event. Evolutionary model proposed for the schist include both the ensialic processes (with Algoma type BIF) that involve crustal extensional thinning and continental rifting at cratonic margin which led to deposition of sediments in graben-like structures while ensimatic (without BIF)

compression closure of basins led to deformation and metamorphism of the sediments and reactivation of older metasediment (Danbata, 2008).

### **2.1.3 The Older Granites (Pan-African Granitoids)**

The term “Older Granites” was introduced by Falconer (1911) to distinguish the deep-seated, often concordant or semi-concordant granites of the Basement Complex from the high-level, highly discordant tin-bearing granites of north central Nigeria. The Older Granites are believed to be pre-, syn- and post-tectonic rocks which cut both the migmatite-gneiss quartzite complex and the schist belts. They represent a varied and long lasting (750 – 450 Ma) magmatic cycle associated with the Pan-African orogeny. The rocks of this suite range in composition from tonalites and diorites through granodiorites to true granites and syenites. Charnockites form an important rock group emplaced during this period. They are generally high level intrusions and anatexis has played an important role (Rahaman, 1988). The Older Granites suite is noted for its general lack of associated mineralization although the thermal effects may play a role in the remobilization of mineralizing fluids. The suite have been dated severally at 750 – 500 Ma Breemen-Van *et al.*, 1977; Rahaman *et al.*, 1983; Fitches *et al.*, 1985; Ferre *et al.*, 1998; Ekwueme and Kroner, 1998).

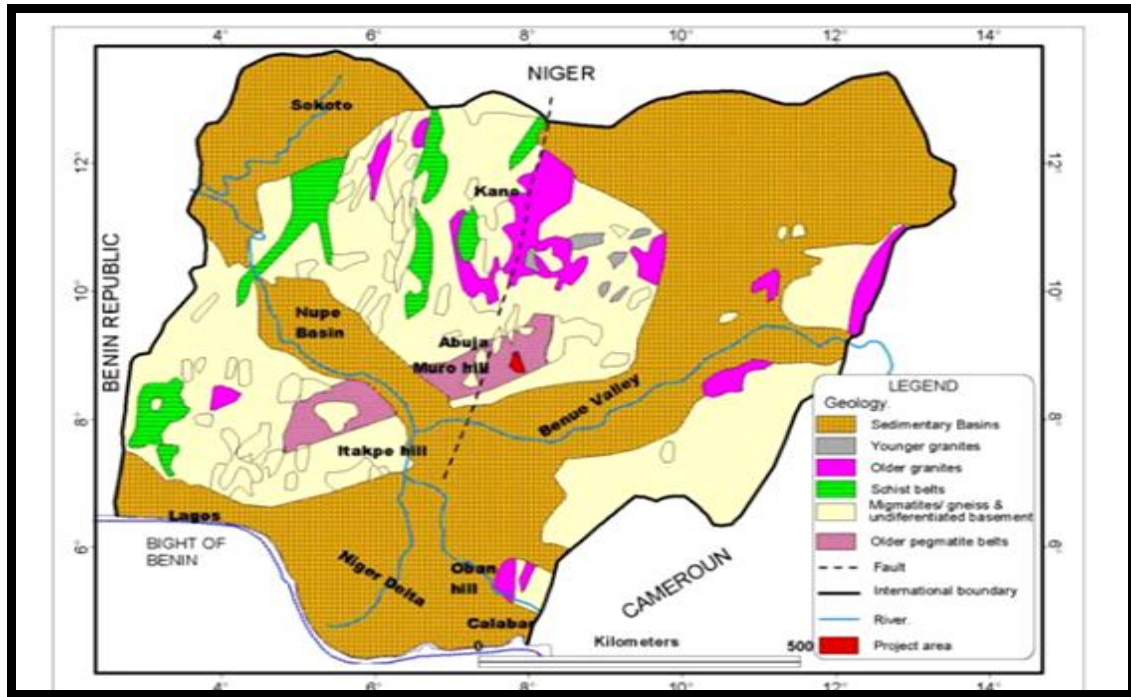


Figure 2.2 Outline geological map of Nigeria (after Okunlola and Ocan, 2009)

The Older Granits are the most obvious manifestation of the Pan-African orogeny and represent significant additions of materials of materials (up to 70 % in some places) to the crust (Rahaman, 1988). Attempt to classify the Older Granites with respect to timing during an orogenic event are valid over only short distances. Contact features between members of the Older Granites suite suggest the coexistence of several magmas. Granite magmatism is commonly associated with several tectonic settings and various stages during orogenic evolution (Pitcher, 1983; Pearce *et al.*, 1984; Maniar and Piccoli, 1989).

#### 2.1.4 Volcanics

The undeformed acid and basic dykes are high level magmatic rocks, intruded during epeirogenic uplift and fracturing in the final stages of the Pan-African orogeny.

The volcanics are the youngest rocks and belong to late to post-tectonic Pan-African intrusions, which cross-cut the Migmatite-Gneiss Complex, the Schist Belts and the Older Granites. The undeformed acid and basic dykes include:

- i. Felsic dykes that are associated with Pan-African granitoids on the terrain such as the muscovite-, tourmaline- and beryl-bearing pegmatites, microgranites, aplites and syenite dykes (Dada, 2006)
- ii. Basic dykes that are generally regarded as the youngest units in the Nigerian basement such as dolerite and the less common basaltic, felsite and lamprophyric dykes.

The age of the felsite dykes has been put at between 580 and 535 Ma from Rb-Sr studies on whole rocks (Matheis and Caen-Vachette, 1983; Dada, 2006), while the basic dykes have a much lower suggested age of ca. 500 Ma (Grant, 1971).

#### **2.1.5 The Younger Granites**

The Mesozoic Younger Granite ring-complexes of Nigeria (Fig.2.2) form part of a wider province of alkaline anorogenic magmatism. They occur in a zone 200 km wide and 1,600 km long extending from northern Niger to north central Nigeria. The most striking petrographic feature of the whole province is the overwhelmingly acid nature of the rocks and the similarity of the rock types found in all areas. Over 95% of the rocks can be classified as rhyolites, quartz-syenites or granites, with basic rocks forming the remaining 5%. Many of the rocks have strongly alkaline to peralkaline compositions, other are aluminous to peraluminous.

More than 50 complexes occur in Nigeria varying from <2 to >25 km in diameter (Kinnaird, 1981). The ring complexes cover a total area of about 7,500 km<sup>2</sup>. The granites of

the Younger Granites series are mainly in the form of ring complexes, of soda pyroxenes and amphiboles, biotite, and fayalite granites, syenites and trachytes with minor gabbros and dolerites. Rhyolites, tufts and ignimbrites are rarely preserved; they are associated with considerable cassiterite, wolframite, scheelite and zinc mineralization.

## **2.2 GEOLOGY OF ANGWAN DOKA AREA**

### **2.2.1 Introduction**

The Angwan Doka area is underlain by the Nigerian Basement Complex of Precambrian age affected mainly by the Pan-African orogeny. The major rock types in the area comprise metasediment (schist), granodiorite and pegmatite dykes (Figure 2.3). The pegmatite dykes are the late member of the Pan-African Older Granites suite which intruded the Basement Complex. The granodiorite forms the marginal portion of the pluton and therefore closer to the migmatite and metasedimentary rocks. There is an increase in deformation within the granodiorite, and it is more apparent especially at the contact with the pegmatite. The major mineral phases are plagioclase feldspars (sometimes perthitic), albite-oligoclase, biotite and less abundant late muscovite; biotite is the predominant ferromagnesian mineral within the pluton, whereas tourmaline predominates along the perimeter of the pegmatite intrusions.

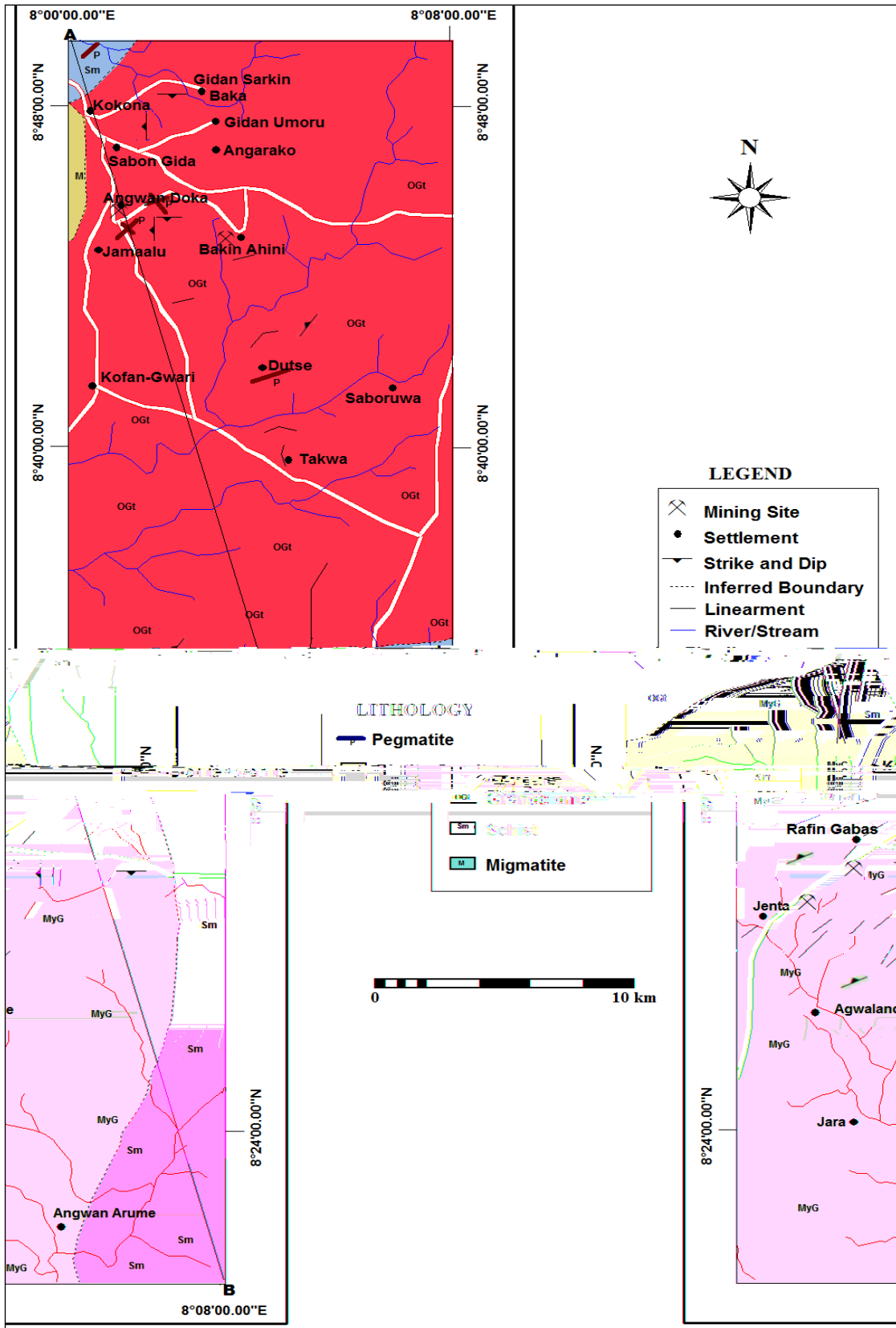


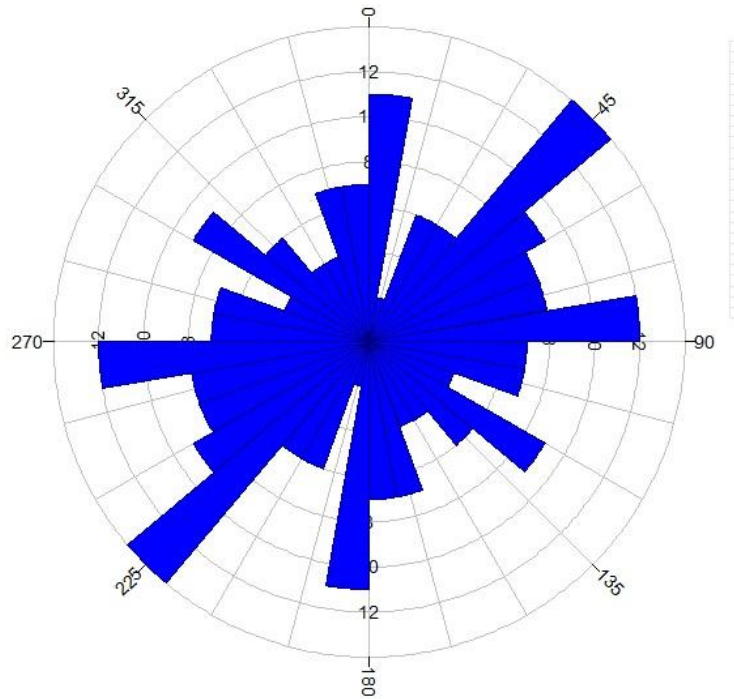
Figure 2.3: Geological map of Kokoona area, Central Nigeria





Figure 2.3 (b): Diagrammatic cross-section map of the study area





**Figure 2. 4: Rose diagram with the general structural orientation of linearments within the study area.**

### 2.2.2 Schist

The metasediment (mica-schist) form the northwest part of the study area and is strongly foliated. It is fine to medium grained with the foliation generally in the N-S direction defined by the alignment of biotite crystal which is the most common mafic minerals (Plate I). These have been interpreted to be Pan-African structure superimposed on earlier tectonic fabrics (Küster, 1990).

In hand specimen, the schist consists mainly of biotite, quartz, sodic plagioclase, K-feldspars and garnet as the main accessory minerals. Microscopically, development of quartz ribbons which is a product of mylonitisation is commonly observed in some of the schist (Plate II). Generally in areas where there is relatively high mica content, the rock appears darker while in zones where quartz-feldsparthic minerals are more, it becomes

lighter in colour. Biotite shows pleochroism from light to dark shades of brown, green-yellow to pink.



Plate I: Photograph of typical outcrop of schist with N-S foliation trend, NW of Kokoona

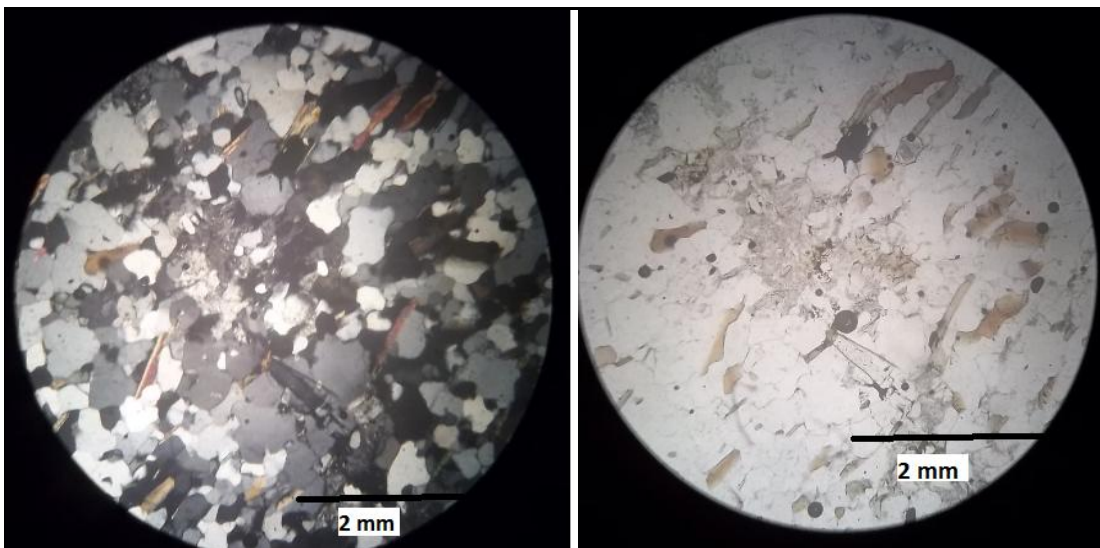


Plate II: Photomicrographs of mica schist composed of biotite (BIO), quartz (QTZ), plagioclase feldspar (PLF) with fractures cutting across foliation in the schist. (A) Crossed polarized light (B) Plane polarized. Diameter of view = 3.2 X 40.

### 2.2.3 Granodiorite

This rock occurs as low relief outcrop that are highly jointed, fractured with quartz and feldspathic veins. Several large granitic masses of the rock, especially around Jamaalu, occur as large whaleback and low lying outcrops (Plate III). Numerous cross-cutting fractures, veins and pegmatite dykes trending mainly NE-SW ( $40-50^{\circ}$  from N) mostly dipping west and varying in length from a few mm or stretching across the length of the outcrops were recorded in majority of the outcrop. The rock is dark grey in colour and usually medium to coarse-grained. It exhibits foliation defined by alignment of muscovite and biotite.

The granodiorite is composed of plagioclase (40%), quartz (25%), biotite (15%), microcline (15%) and accessory minerals mainly amphiboles, apatite,  $\pm$ andalusite,  $\pm$ cordierite  $\pm$  tourmaline and secondary minerals like chlorite, epidote and sphene making up the remaining 5% of the rock. Thin section study shows subhedral microcline with good polysynthetic cross-hatch twinning. Plagioclase also exhibits good polysynthetic normal albite twinning with twin lamellae parallel to the elongated crystal dimension (Plate IV). In addition, secondary quartz with characteristic cluster appearance and irregular cracks which are most probably the product of intense tectonism was recorded within this rock (Plate V). The deformation of quartz consists of development of subgrains, wavy-undulose extinction, sutured boundaries, pressure shadow and preferred orientation. Alteration typified by sericitisation as well as ductile and brittle deformation was observed in several outcrops especially in Jamaalu area.



**Plate III: Photograph of outcrop of granodiorite at Jamal area with cross-cutting fractures.**

Both biotite and muscovite are invariably present in the rock but with more biotite than muscovite. In addition, biotite occurs in different shades of colour from light brown to greenish blue and exhibit pleochroism while the muscovite shows birefringence of blue, green-yellow and pink in cross polarized light but generally colourless in plane polarised light. Evidence of tourmaline replacing biotite was revealed by irregular colour zoning and patches. Majority of the biotite, plagioclase and quartz crystals are fractured with the cracks filled by new minerals which are the product of alteration (Plate VI). Myrmekite, an intergrowth which is an evidence of replacement of alkali feldspar by plagioclase and quartz during the late stage of consolidation of the rock were seen on some sections. On the basis of anorthite contents, the main sodic plagioclase is albite. It is typically associated with certain gemstones and is the characteristic feldspar of gem-bearing pegmatites (London, 1986; Nabelek *et al.*, 1992).



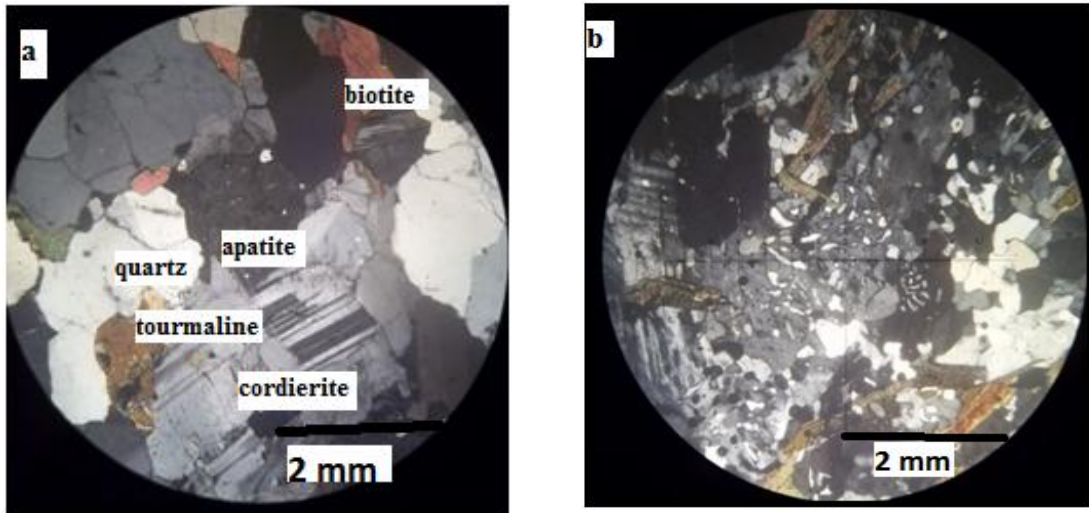


Plate IV: Photomicrograph of granodiorite, Angwan-Doka. (a) Cracked crystal of quartz, cordierite, tourmaline, (b) Myrmekitic intergrowth of quartz and plagioclase replacing alkali feldspar (Crossed polarized light; diameter of view = 3.2 X 40).

Several mono-mineralic veins (quartz) with banded or streaky structure occur in outcrops of the rock in Jamaalu area thus suggesting that the rock had experienced locally intense dynamic metamorphism which resulted in lenses of mylonite. Petrographic study of the rocks near the shear zones reveals evidence of brittle deformation and displacement along fault planes of different orientation.

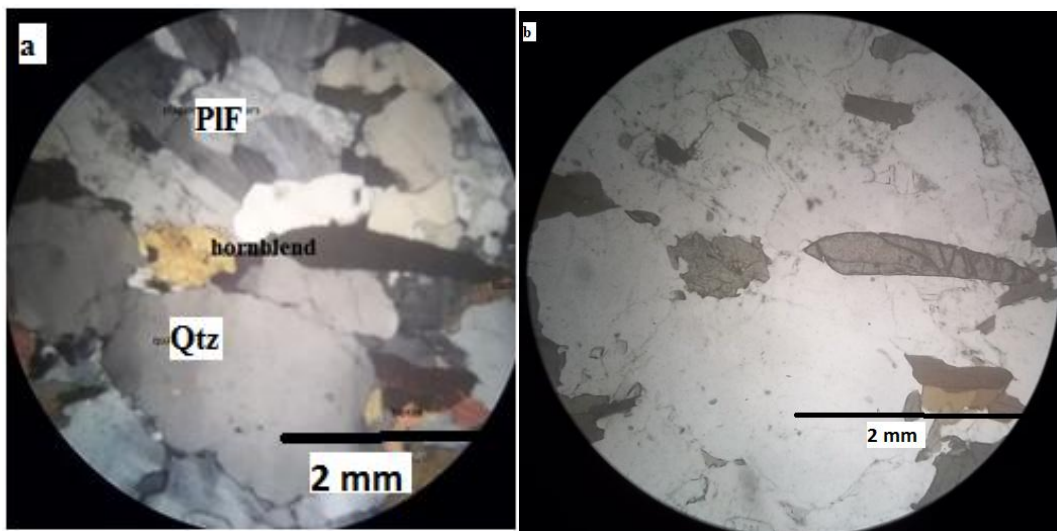
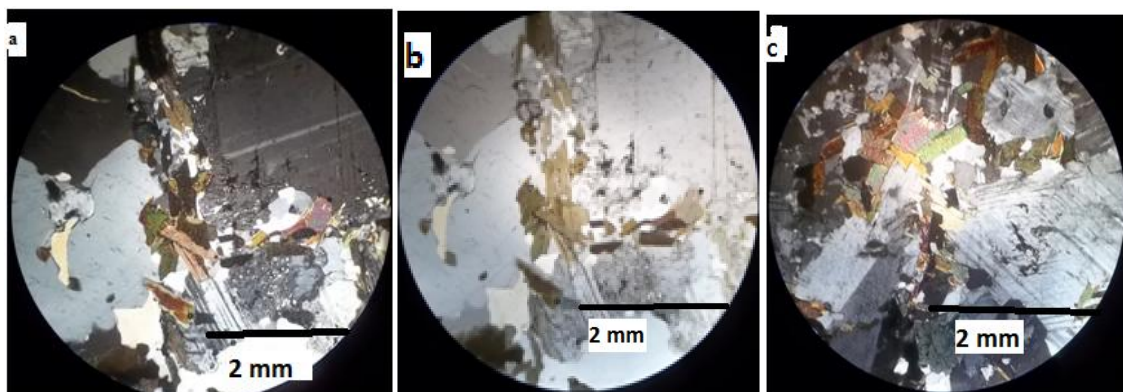


Plate V: Photomicrographs of the granodiorite at Jamaalu. The rock is composed of quartz, plagioclase, biotite and amphiboles with (a), Crossed polarized light QTZ= quartz

**displaying strains with pressure shadow, undulose extinction and (b) plane polarised light with diameter of view = 3.2 X 40).**

In Angwan Doka area, the granodiorite is composed mainly of quartz, plagioclase, K-feldspar, biotite and muscovite with minor amount of zircon, apatite and tourmaline. The presence of alumina-rich minerals like muscovite, tourmaline and cordierite in the granodiorite has been considered to be characteristic of peraluminous protolith (Chappell and White, 2001). Biotite is the predominant ferromagnesian mineral within the pluton, whereas tourmaline predominates along the perimeter of the pegmatite intrusions. Crystals of biotite, trending sub-parallel and swerving round the porphyroblastic grains of quartz and feldspar obviously show that the rocks have undergone late episode of shearing during a widespread tectono-metamorphic event (Plate VII). Quartz commonly occurs as granoblasts and in places. Quartz and feldspars also form strong stretching mineral lineation with various shape (rounded to elliptical) and size. Further, the quartz shows undulatory extinction and where deformation is more intense, quartz together with feldspar show complete recrystallization. The K-feldspar shows perthitic textures and sericitization (Plate V).



**Plate V: Photomicrographs of granodiorite, Angwan-Doka; (a) Replacement of plagioclase by sericite, biotite by muscovite with presence of apatite and cordierite (b) plane polarized image (c) Feldspar exhibiting different twinning styles of Carlsbad twinning, tweed texture with exsolution and alteration micro texture. Diameter of view = 3.2 X 40.**

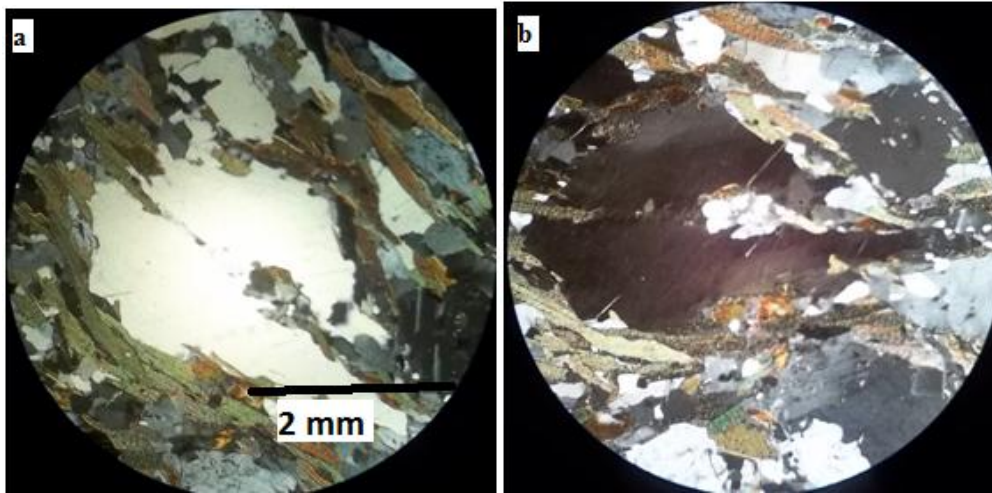


**Plate VII: Photomicrograph of granodiorite in Angwan-Doka; Biotite swerving around quartz and feldspar porphyroblast (a) Crossed polarized light, (b) stage rotated; diameter of view = 3.2 X 40.**

Under the microscope the granodiorite from Jamaalu consists of quartz, plagioclase, biotite, amphiboles (hornblende) and garnet and sphene. Quartz is fine to coarse grained and shows undulose extinction (Plate VIII). Biotite and hornblende are the main mafic minerals. Biotite being the dominant ferromagnesian mineral also occurs as small to medium-grained flakes. The granodiorite is weakly foliated with the foliation plane generally defined by the sub-parallel biotite and hornblende crystals. The mafic minerals are dark to light brown in colour with pleochroism from yellowish brown to reddish brown and some of the flakes are greenish brown in colour. The colour variation is probably indicative of the variation in chemical composition. In Bakin-aini area, however, the granitoid is finer grained with many large xenoliths of older rocks occurring as partially assimilated body within the granitoid.

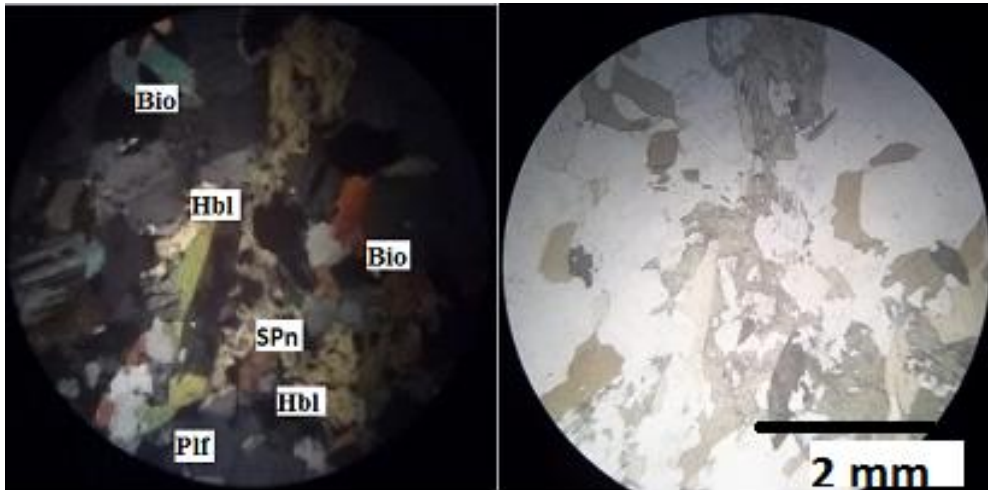


**Plate VIII: Photomicrograph of the granodiorite around Jamaalu; Crystals of biotite (Bio), Sphene (Spn), associated with hornblende (Hbl) already undergoing alteration (a) Crossed polarised light, (b) Plane polarized light; diameter of view = 3.2 X 40.**

#### **2.2.4 Granodiorite-Pegmatite Contact Rock**

The granodiorite-pegmatite contact consisting of dark coloured, medium to coarse grained gneissic rock. The rock is composed of quartz, biotite and muscovite trending sub-parallel which could be due to the intense activities associated with the surge of the pegmatite fluid (Plate IX). The melanocratic patches which are few cm wide occur directly in contact with the intrusive tourmaline-bearing pegmatite dyke and is regarded as moderately altered zone. The rock is obviously the only observable altered contact with the pegmatite, with expression of associated tourmalinization and process of metasomatism. In the thin section, chloritization of biotite as well as replacement of biotite with tourmaline were observed. Generally the tourmaline is skeletal with inclusions of quartz and irregular fractures with patches (Plate IX).



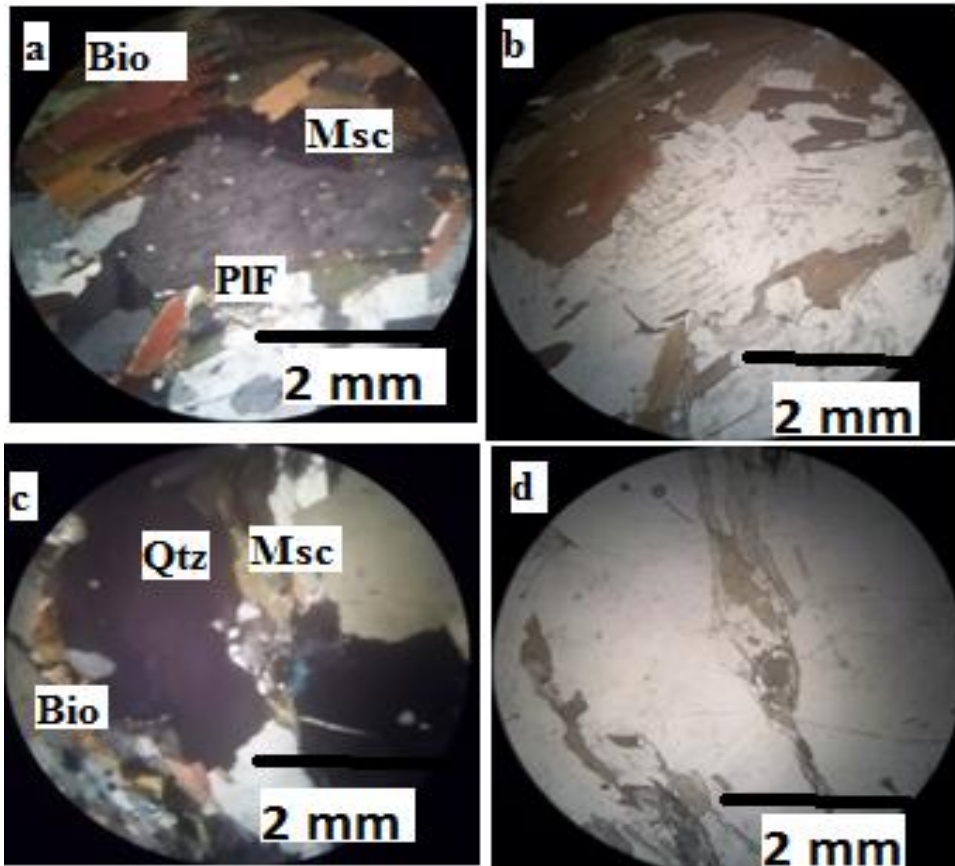


Plate IX: Photomicrographs of granodiorite-pegmatite contact rock; (a) Alignment of biotite (Bio) which imparts gneissic appearance, replacement of biotite by muscovite (Msc), and feldspar by mica, and disseminated grains of apatite (white specks) (b) Plane polarized image of (a). Plate (c) photomicrograph Quartz, biotite muscovite with a nodule Titanomagnetite or phosphate, (d) Plane polarized image of (c). Diameter of view = 3.2 X 40.

### 2.2.5 Aplitic Zone

The fine to medium-grained aplitic zone is more commonly massive and consists of sodic plagioclase (50%), quartz (15%), muscovite (15%), garnet (10%), and tourmaline (5%) with other accessory minerals (Plate X). The aplite is almost completely devoid of mafic minerals in hand specimen while the available micas occur as tiny flakes. Quartz is fine to medium grained, subhedral to anhedral and occasionally exhibit undulose extinction.

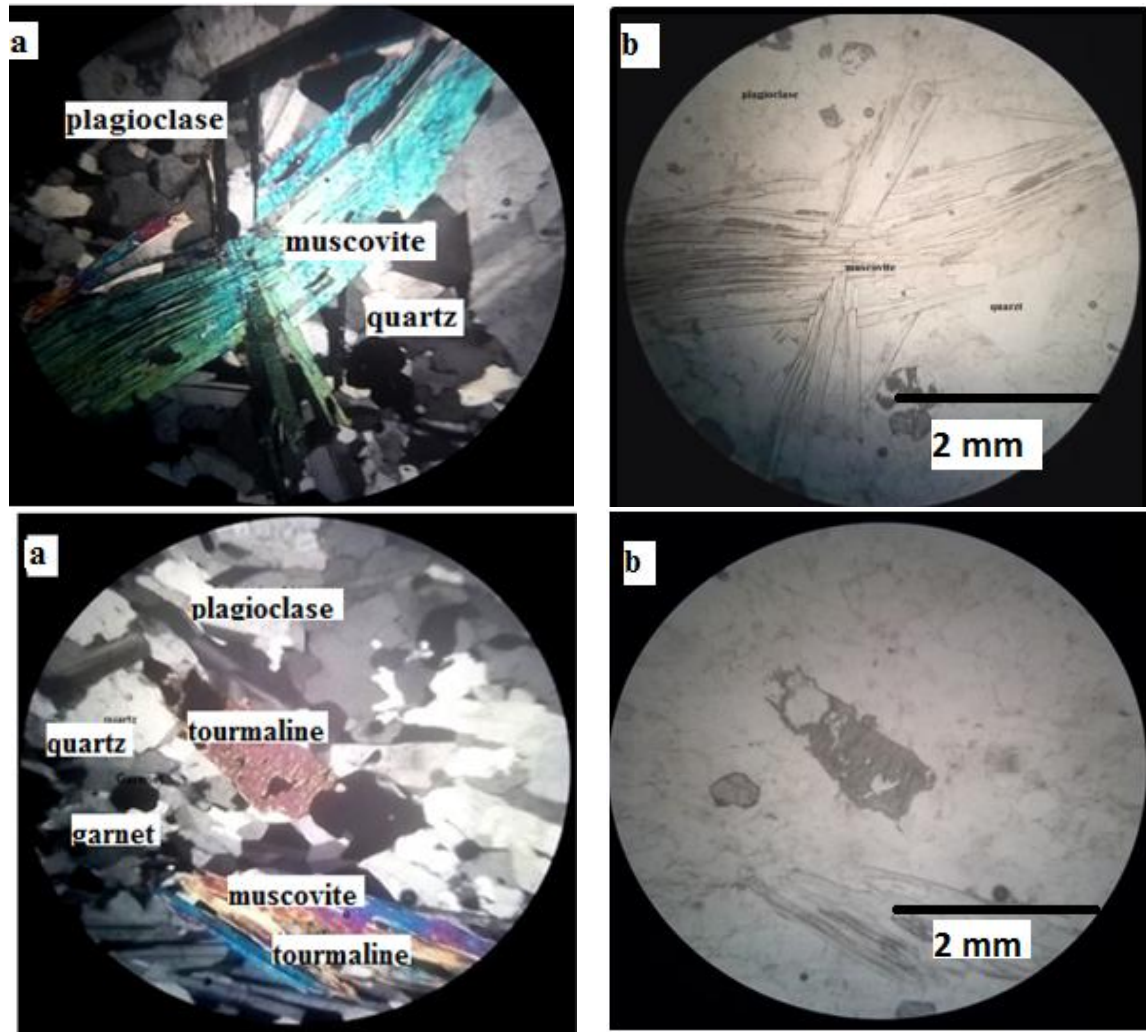
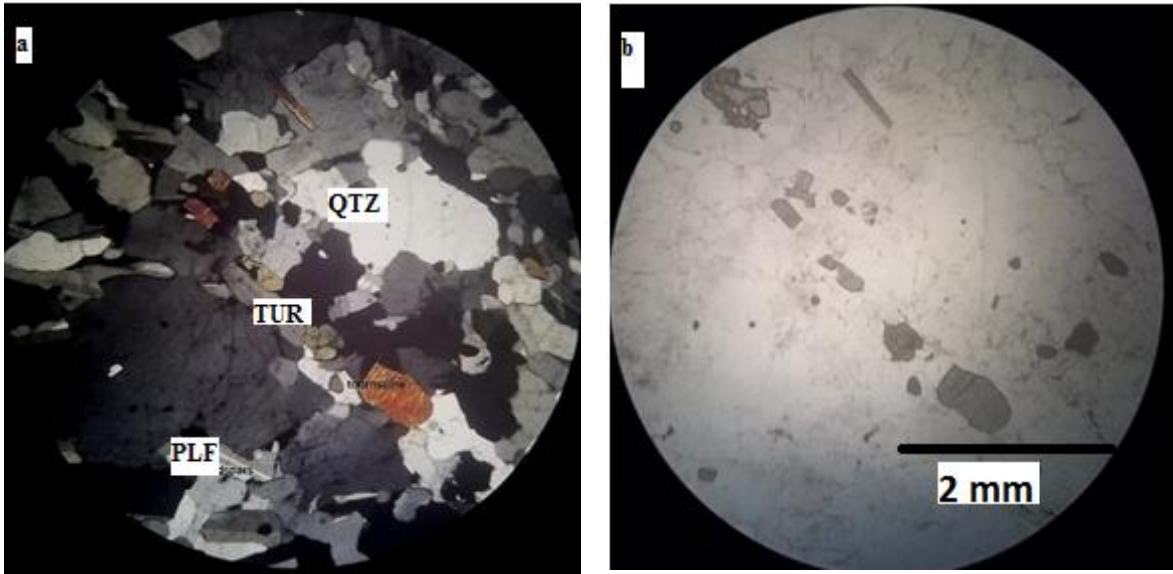


Plate X: (a) Photomicrograph of aplite, Angwan Doka, composed largely of albite, quartz, garnet, K-feldspar and muscovite. (b) Alteration of muscovite to tourmaline. (a) Crossed nicols, (b) Plane polarized light; diameter of view= 3.2 X 40.

Muscovite exhibit 3<sup>rd</sup> order interference colour under crossed polarized light and colourless in plane polarized light. Garnet occurs as very dark grain both in cross and plane polar light but exhibit high relief in plane polarized light with cleavages and inclusion seen in most garnet crystals (Plate X).

Crystals of quartz containing tiny flakes of muscovite as inclusion abound in parts of the sections. Plagioclase is subhedral to anhedral and shows characteristic lamella twinning and 18<sup>0</sup> extinction angle with reference to a twin plane suggesting it is albitic. The aplitic zone also shows layering, with alternate dark coloured bands rich in mica and schorl

and light coloured bands rich in sodic plagioclase, perthite, quartz, garnet bands and Ta-oxide minerals. The tourmaline crystals are relatively elongated, sub parallel oriented. In parts where disseminated, tourmaline also exhibit colour zonation (Plate XI).



**Plate XI: (a) Photomicrograph of tourmaline (colour zoned) crystals in pegmatite-contact rock. (a) Crossed polarised light, (b) Plane polarized light; diameter of view = 3.2 X 40.**

Tourmaline occurs in skeletal masses in some section with or without fracture. The skeletal crystals of tourmaline have a poorly defined euhedral outer form and a distinct hollow interior filled with quartz and feldspar (Plate XII). Inclusions of quartz are also present in feldspars, garnet, muscovite and the tourmaline. The tourmaline grains are strongly pleochroic and vary in colour (in plane-polarized light) from straw brown to deep brown, occasionally with a bluish to greenish or orange-brown core, they are best described as schorl,

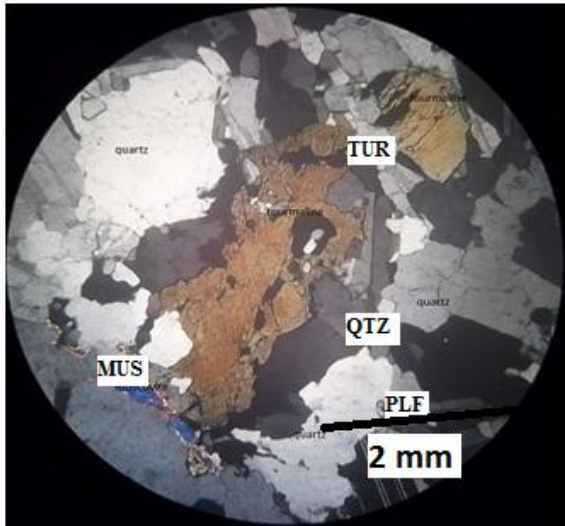


**Plate XII: Photomicrograph of skeletal tourmaline (TUR) with inclusion of quartz (QTZ). Crossed polarised light; diameter of view = 3.2 X 40.**

## **2.3 THE PEGMATITE**

### **2.3.1 Introduction**

Discrete dykes of pegmatite occur in the Pan-African granitoids especially the granodiorite. The dykes vary greatly in size (up to 2 m wide) and in mineral content from quartz, albite, K-feldspar, muscovite, tourmaline, beryl, and spodumene and rare-metals believed to have been injected into older rocks following zones of weakness. The most abundant pegmatite dyke has nearly vertical to steeply dipping disposition while some occur as pods in the granodiorite and as almost flat sill-like body especially within the schist (Plate XIII). The pegmatites are composed almost entirely of sodic plagioclase mainly albite with different varieties of phosphate mineral especially apatite including spodumene, petalite, amblygonite-monterbrasite, triphylite-lithiophilite, cookeite and lepidolite (Jacobson and Webb, 1946). The Angwan Doka pegmatite group consists of

zoned, layered or weakly zoned types and geochemically range from barren, simple to Ta, Nb, Be-bearing, Li, Be, Ta and Nb-enriched types with abundant Li, Rb and Cs.

Figure 2.3 shows about four strike directions of the pegmatite dykes, the most prominent of which is the NE-SW trend (20-50° from N). Minor sets occur in the E-W (60-80° From N), and NW-SE (170 – 350° from N).

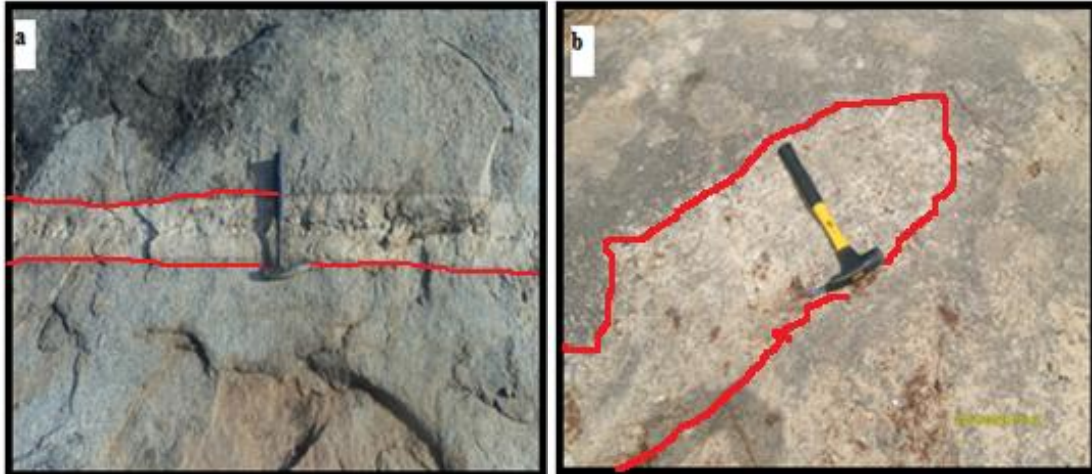


Plate XIII: Photographs of pegmatite vein (a) and pods (b) in granitoids from study area.

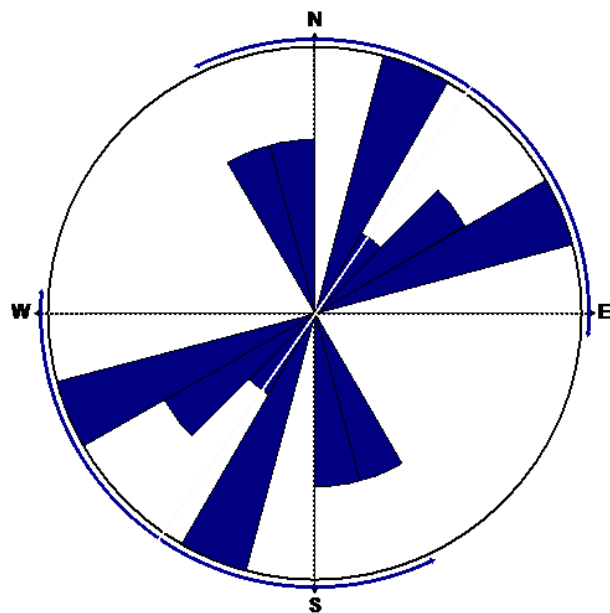


Figure 2.5: Rose diagram displaying the general orientation of pegmatite in the study area.



### **2.3.2 Angwan Doka Pegmatite body**

The Angwan Doka gemstone-bearing pegmatite is the westernmost extension of the rare-metal pegmatites of Wamba field described extensively by Küster (1990), Okunlola and Ocan (2009). The rare elements pegmatites generally occur as low lying ridges that are sometimes linked underground to form a "train" that is about 3 meters higher than the nearly flat-lying topography. Although poor exposure due to intense weathering and thick soil cover makes tracing the length and estimation of the transition from the host to the pegmatite difficult, a cross section of thin pegmatite are easily recognized from the trenches and pit dug by the artisanal miners. The pegmatites are of varying dimensions upto 2 meters in width and from a few meters to about 1 kilometer and sometimes more in length.

The dip of the pegmatite is highly variable and changes from nearly vertical to flat lying and undulating with pronounced pinch and swell structures; strike and dip may change in a pegmatite following planes of weakness. There is a generally sharp contact between the pegmatite and the country rock with contact phenomena restricted to a narrow zone of tourmalinization. Generally several varieties of pegmatite dykes, veins and pods were distinguished in the area; some are composed of feldspar and quartz with tourmaline while some are devoid of the mineral, tourmaline (see Plate XIII). The tourmaline-bearing pegmatite dykes are normally zoned from an outer, finer-grained aplitic zone composed of feldspar + quartz + skeletal tourmaline to an inner, coarse-grained pegmatitic zone of quartz + euhedral tourmaline. Some pegmatite dykes are mainly feldspatic and lack a quartz core therefore composed only of leucocratic mineral with some skeletal tourmaline. Crystallization of the skeletal tourmaline in the pegmatite

occurred at the expense of biotite, and resulted in the leucocratic biotite-free halo. Mica of variable size is common in all zones, mostly as pseudo hexagonal or fish-tail shaped books (Plate XIV).



**Plate XIV: Photograph of muscovite books hosted by quartz in a simple pegmatite, Angwan Doka**

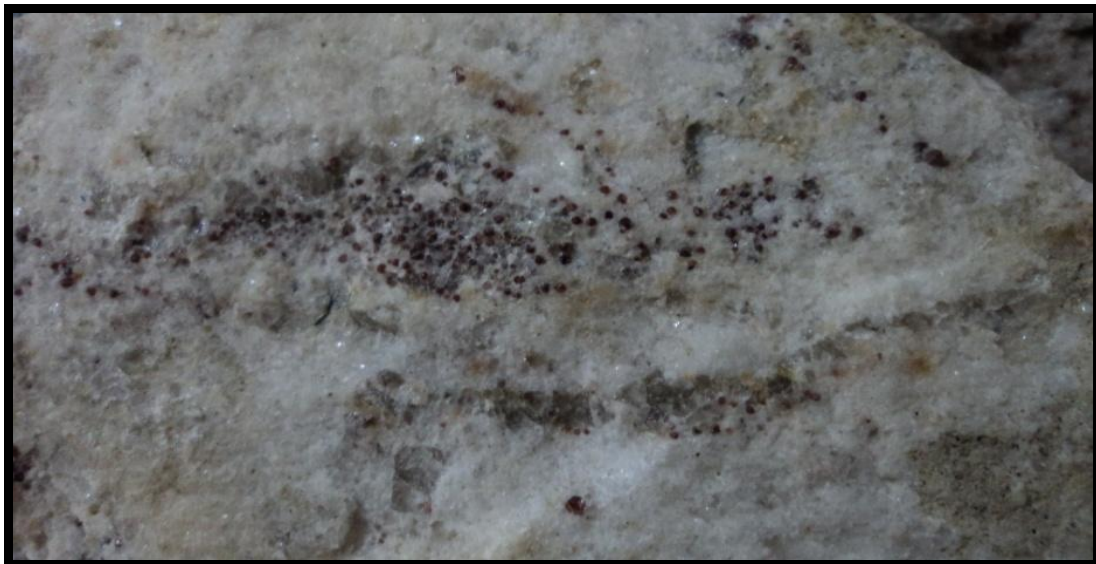


**Plate XV: Photograph of layered sacharoidal albitic aplite, with quartz, mica, garnet and Ta-oxide minerals.**

The pegmatites are very coarse-grained and are zoned. The coarseness increases from margin inwards indicating the direction and sequence of crystallization and symmetrical zoning. Zoned pegmatites are typified by border zone, wall zone, intermediate zone and central quartz zone. Gemstones are generally found in the spodumene and core zones. Albite is the most abundant mineral and it occurs as white or reticulated and nearly transparent variety in great masses of considerable size. Biotite is present in small amounts near the contact and within the border zone (Plate XVI). Muscovite occurs in three distinct forms. The first is clear coloured variety and gradually increase in colour intensity to light brown, second is the light green normally associated with albite and occur as books, pockets and flakes distributed through the pegmatite. The third varieties are associated with the pink lithium mica, lepidolite.

### ***Internal fabrics***

The volume and number of occurrences of pegmatite are highest within the contact zone of the granitic batholiths with the metasediment (shist) especially in Angwan Doka area and progressively reduce, away from the zone till an almost complete lack of the pegmatite is recorded at greater distances from Angwan-Doka area. The general character of the pegmatite dyke is continuous laterally along strike for almost a kilometre and down dip for more than 15 meters, compositional zoning is not very smooth and involves repetition of sequence in which the mineral mode appears to vary systematically from outer zones to inner zones with depth so that it is not possible to ascertain if the pegmatite is layered asymmetrically or zoned vertically asymmetrically with respect to the



central quartz core zones observed at a depth of about 12 -13 meters. Occasionally banded garnetiferous and albitic aplites were also noted within the main study area.

Mining is done by tunneling from the surface and later followed with explosives into the pegmatite as the pegmatite generally widen with depth. Muscovite occurs in all zones of the pegmatite dykes, and in thin pegmatitic and hydrothermal veins within the leucogranite adjacent to the pegmatitic bodies, Biotite is restricted to the border zone while muscovite “books” are common in the pegmatitic body.

Based on field observation, emplacement of the body, variation in texture with chemical composition, mineralogy and paragenetic characteristics that are visible in hand specimen and the degree of differentiation that increases from the host rock inwards towards the inner part of the pegmatite, the pegmatite samples were differentiated into six (6) zones, using the terminology of textural and zonal classification of Cameron *et al* 1949. These are:

- i. The simple pegmatite composed of white-milky quartz, large muscovite, feldspars accessory beryl, (Plate XIV) muscovite quartz pegmatite.
- ii. The border zone which consists mainly of sodic plagioclase (albite), apatite, tourmaline, quartz (lacerated quartz), biotite, augite and accessory, muscovite, columbite, Ta-oxide mineral (Plate XVI). Displays the transition from the granodiorite to the sodic pegmatite.
- iii. The wall zone, consisting of K-feldspars microcline, schorl, muscovite, albite, beryl. It is generally coarser grained and contain well developed tourmaline crystal, mainly schorl; the graphic intergrowth of tourmaline and quartz (Plates XVII and XVIII) is characteristic of this zone.

- iv. The intermediate zone. With the mineral assemblages consisting of muscovite, microcline-perthite (K-feldspars), quartz, albite, beryl, accessory cassiterite and Ta oxide minerals (Plates XXVI). This zone contains spodumene albite, microcline quartz intergrowth with greenish muscovite. It represents the main replacement unit observed with alteration of feldspars and spodumene. Composed mostly of green mica+ albite rich greisen alteration veins that are highly sporadic and the richest in cassiterite.
- v. The spodumene petalite unit (Plates XX and XXI), are composed of spodumene petalite, K-feldspar, Na-rich plagioclase, quartz, and lepidolite as major mineral phases while amblygonite and other phosphates occur as accessory minerals with cassiterite and Ta-oxide minerals.
- vi. The core zone or lepidolite unit composed of milky-clear quartz and plagioclase-muscovite intergrowth while the pocket consist of spherical radial masses of albite attached to massive lepidolite (Plates XXII and XXIII) spodumene, K-feldspars, quartz, elbaite tourmaline, topaz, and some beryl.

The Angwan-doka pegmatite represents a boron-rich system in which tourmaline and muscovite crystallized in all internal zones. It occurs in great abundance at the border zone, where it occurs as thick foliated masses of black prismatic grains up to 3-4 cm in length. Wall-zone also contains abundant black tourmaline intergrowth with quartz and muscovite, the intermediate and spodumene unit contain the lowest concentration of tourmaline while the lepidolite unit contains tourmaline.

Although miarolitic cavity (pocket) occurs within other zones of the pegmatite, concentrations of gem quality minerals occur mainly within two units. The units are albitized central spodumene zone which contains spodumene crystals while most of the

tourmaline is extracted from the lepidolite albite unit, (Plate XXIV). Lithian muscovite is the main component of this lepidolite unit with spodumene, subordinate quartz, albite and beryl.

Most of the pegmatite dykes are generally rich in lithium minerals petalite-lepidolite. The intermediate zone is rich in greenish muscovite. Purple lithian muscovite and lepidolite make up the inner-most zone around the core, the schorl are found commonly in the border-wall zone while beryl occurs as light greenish to white in the wall zone and extends into other inner zones. Cassiterite occupies outer wall-intermediate zones while Ta oxide increases from the border to intermediate and the core.



**Plate XVI: Hand specimen of border zone of pegmatite composed of albite containing biotite, schorl and Ta oxide minerals abuts the granodiorite, Angwan Doka**



**Plate XVII: Photograph of hand specimen from the pegmatite wall zone, Angwan Doka. The rock is composed K-feldspar, albite, graphic intergrowth of quartz and tourmaline with beryl and Ta-oxide mineral.**

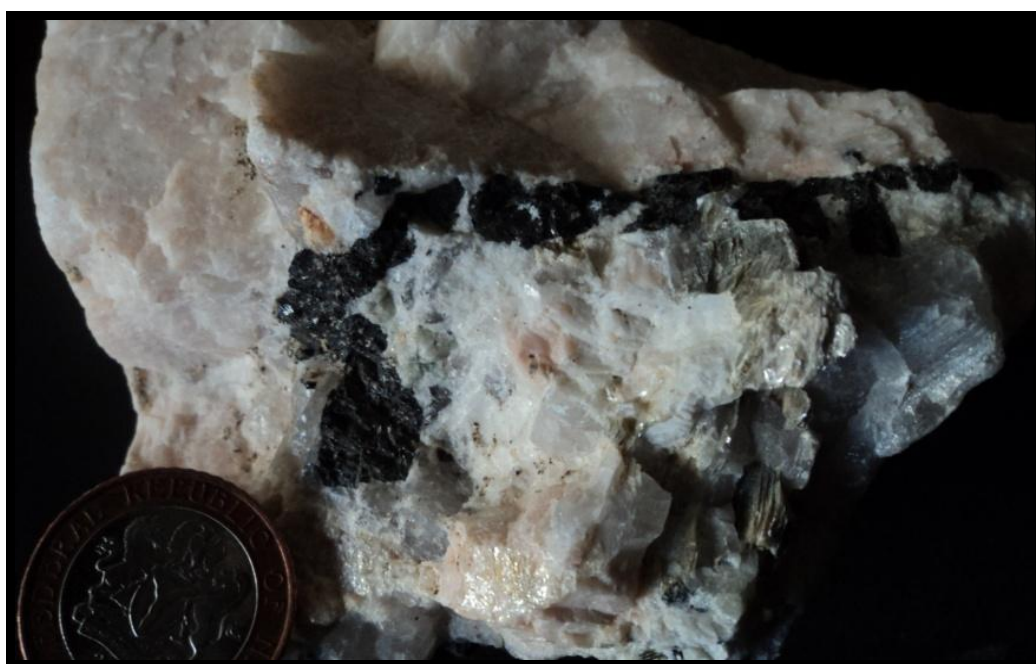


**Plate XVIII: Photograph of a pocket in the pegmatite wall zone, Angwan Doka, consisting of K-feldspar, albite, quartz, mica and inward flaring tourmaline and Ta-oxide minerals.**





Plate XIX: Crystals of schorl on quartz matrix

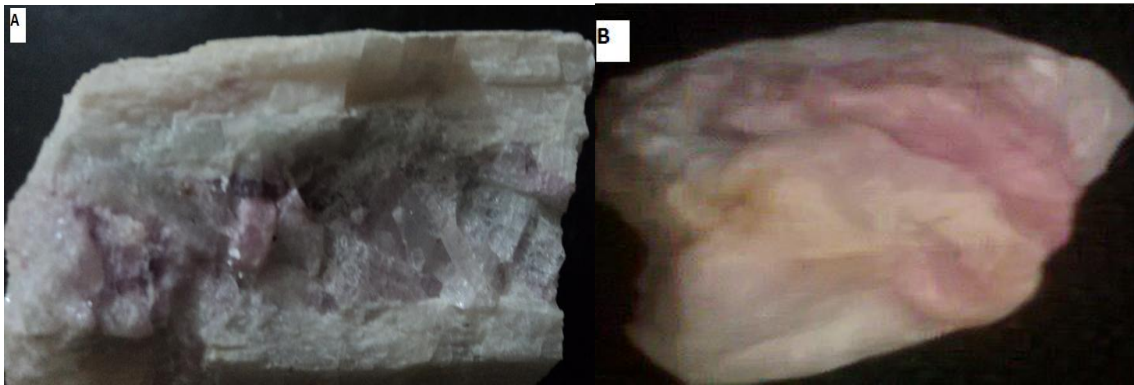


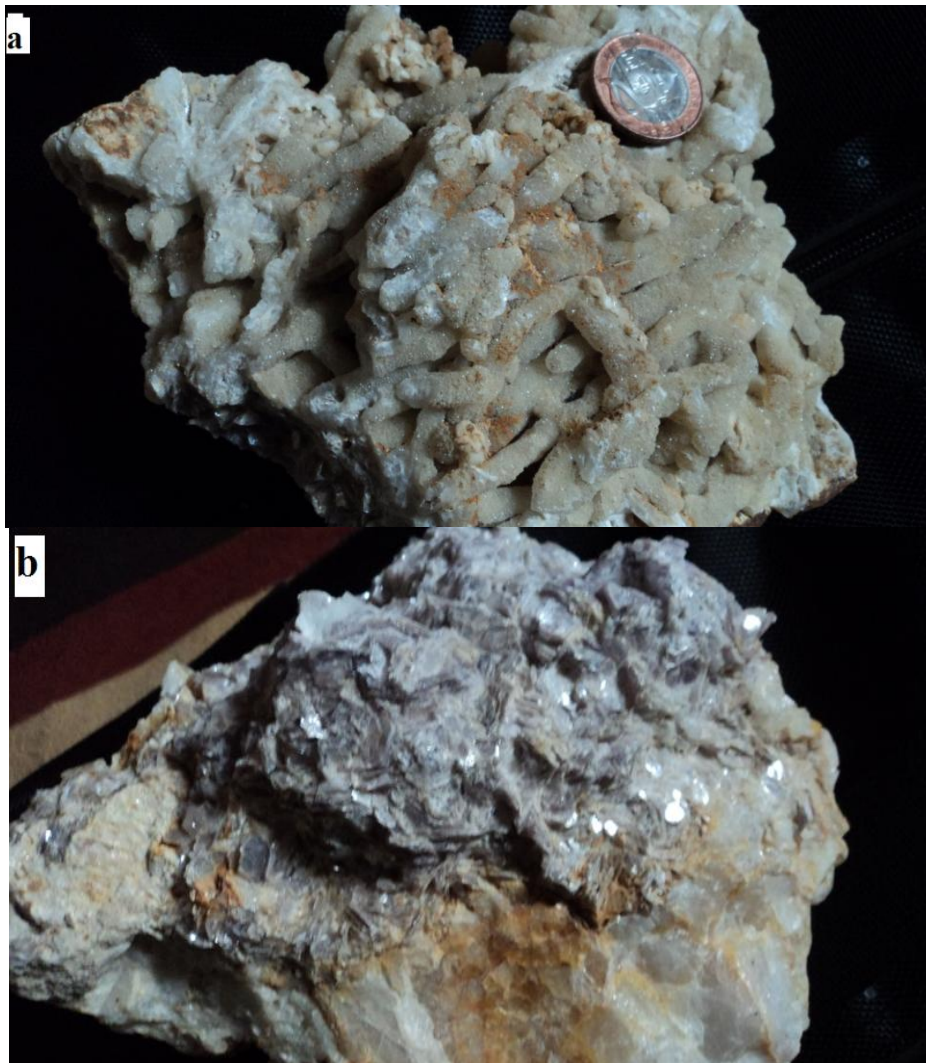
Plate XX: (A) Photograph of hand specimen containing crystals of Kunzite in groundmass of spodumene (B) Pink beryl.



Plate XXI: (a) Hand specimen of inner zone of pegmatite containing lithium aluminosilicate (b) part of spodumene zone



Plate XXII: Photograph of bicoloured water melon elbaite tourmaline in a massive lepidolite; the core pink colour surrounded by green colour.





**Plate XXIII: Radial albite (A) attached to lepidolite and quartz unit at the base (B) base of albite unit attached to the upper lepidolite unit**



**Plate XXIV: Crystals of tourmaline (elbaite) with green cap extracted from cavity in the lepidolite - albite unit, Angwan Doka area.**

### **2.3.3 Wall Rock Alteration**

The pegmatite dykes show effect of rock-fluid interaction in enclosing wall rock. Occurrence of tourmaline in the wall rock suggests that boron-bearing fluids reacted with mafic minerals in the rock to produce schorl or dravite. This phenomenon known as metasomatic alteration has been described as boron exomorphism (London, 2008). The metasomatic alteration is restricted to only a few (<2) cm in some areas and to region bordering the fractures, thus suggesting that fluid escaped from the pegmatite to alter country rock is negligible, the presence of narrow metasomatic aureoles is a common feature

of large rare-element pegmatites (London, 2008). This is more so as there was no obvious alteration halo in the host rock; the passage from pegmatite to country rock is generally rapid, giving sharp contact effect (Plate XXV).

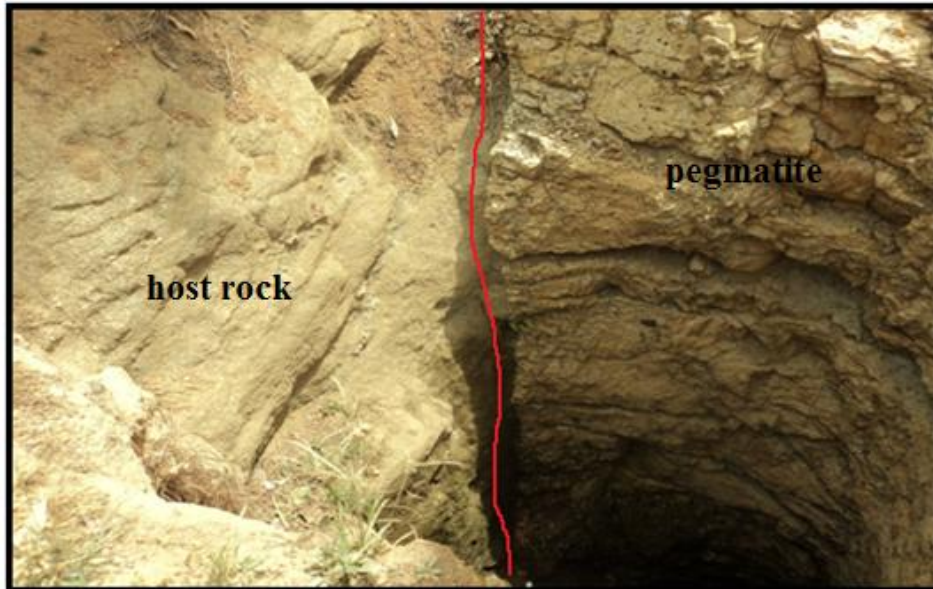


Plate XXV: Sharp contact between pegmatite with the host rock



Plate XXVI: (A) Photograph of muscovite rich replacement zone (B) part of the albitized wall zone (Mineralized in columbite-tantalite)



#### 2.3.4 Pocket Indicators

The most widely used indicator by the artisanal miners in the study area is dyke intersection where two dikes meet and form a T-junction or smaller dykes merge with a main dyke (Plate XXVII). According to Simmons (2007), development of pockets is enhanced at such location as a result of increase in volume and decrease in pressure within the pegmatite fluid during formation. The presence and quality of pathfinder minerals like quartz and schorl, as well as the orientation of the crystal encountered have also been used as indicator of the presence and quality of gem tourmaline in a pegmatite, euhedral crystal of clear or smoky quartz (lacerated quartz) and coarse mica flakes increases the prospect of a pocket. In deeply weathered pegmatite like the one encountered at Bakin-Aini and Janta areas, the miners use residual fragments of quartz as strong evidence that the weathered pegmatite contains gem topaz and beryl pocket.



## **Plate XXVII: Dyke intersection in a mine pit at Angwan Doka**

Other pocket indicators include clay filled fractures or clay enriched areas as pockets are mostly filled with clay. Small quartz crystals growing in parallel orientation on fracture surfaces while mineral alteration is also another good indicator used by the miners e.g. alteration of feldspars, tourmalinization and increase in grain size of crystal of minerals within the pegmatite.

### **2.4 GEOLOGY OF JANTA AREA**

The Janta area is underlain by topaz-bearing biotite granite. The granite is a part of the Afu Complex described by Kinnaird (1984, 1985), Küster, (1990), Adekeye and Akintola, (2007) and reported to have been derived from deep sources of magmatic origin and controlled by a series of NE-SW lineaments (Kinnaird, 1984). The Afu Complex is the southernmost of the nearly 50 multiphase granitic massifs, which are discordantly intrusive into the Pan-African basement of Nigeria between latitudes 8° and 12° N and longitude 8° and 10° E. Age determinations have shown that these granitic massifs are entirely Mesozoic (Jacobson *et al.*, 1963; Grant, 1971; Breemen and Bowden, 1973) and are collectively termed the Younger Granites of Nigeria.

The granite is composed mainly of quartz, alkali-feldspar (microcline-perthite), biotite and accessory minerals which include topaz, zircon, fluorite and hornblende. It is generally leucocratic with less biotite and more K-feldspar and range from medium to coarse grained. Outcrops of the granite occur as undulating hills generally trending NE-SW. Intense tropical weathering has decomposed and disintegrated the gem bearing rocks to

form sedimentary eluvial deposits within which mining of tin, aquamarine and topaz is currently going on by burrowing to a depth of 10-12 meters then tunneling to connect the pits underground (Plate XXVIII). Some gem minerals mined within the eluvial deposits are displayed in Plate XXIX.

The Janta alluvial and eluvial gem deposit field is composed of sub-recent alluvial with lenses of gravel, sand and streaks of heavy minerals like cassiterite and columbite associated with the gem deposits laid down in flood plains of stream, talus fan or at the foot of steep hill. The gem bearing layers in the alluvial deposits are markedly heterogeneous exhibiting a variety of shapes and sizes that indicate frequent change in stream courses and velocity. The heavy mineral constituents must have been deposited during period of intense flooding that caused the mechanical removal from the source area or from the eluvial areas.



**Plate XXVIII: Typical pit from which alluvial gems and cassiterite minerals are won.**



**Plate: XXIX: Topaz, beryl and aquamarine crystals from Janta alluvial-eluvial deposits.**

Unlike the Angwan Doka and Jamaalu area, this granite does not contain visible pegmatite dykes. The pegmatite veins exposed near Janta village are mainly quartzo-feldspathic.

It is important, however, to note that although the granites hosted pegmatites are rarely exposed, their gemstone samples were seen as transported materials within the eluvial mining district described above. The presence of miarolitic cavities and vugs indicate that late stage vapour phase separated from the residual melt to form the pegmatite and gemstones (Abaa 1991). This rock is extensively greisenized in some location with replacement and alteration of feldspar to mica, plagioclase to perthite, accompanied with replacement of biotite by chlorite. Greisenization is considered the most important factor for gemstone formation within the biotite granite complex of Nigeria (Abaa 1991). Unaltered plagioclase grains are also common and exhibit well-developed albite twinning (Plate XXX). The rock is generally decomposed almost to the



consistency of clay in some area thus making it impossible to sample muscovite for geochemical analysis

Microcline, which occurs as pinkish-white in hand specimen shows characteristic cross-hatched twinning in thin section and is the most abundant alkali feldspar. Exsolution of sodic plagioclase in a K-feldspar host is ubiquitous in this granite (Plate XXXI). Crystals of plagioclase are generally tabular to bladed. The sericitic alteration of feldspar is one of the most dominant characteristic of the granite which varies in grain size (Plate XXXII). The amount of mafic minerals is very low compared to the rock in Angwan-Doka area.

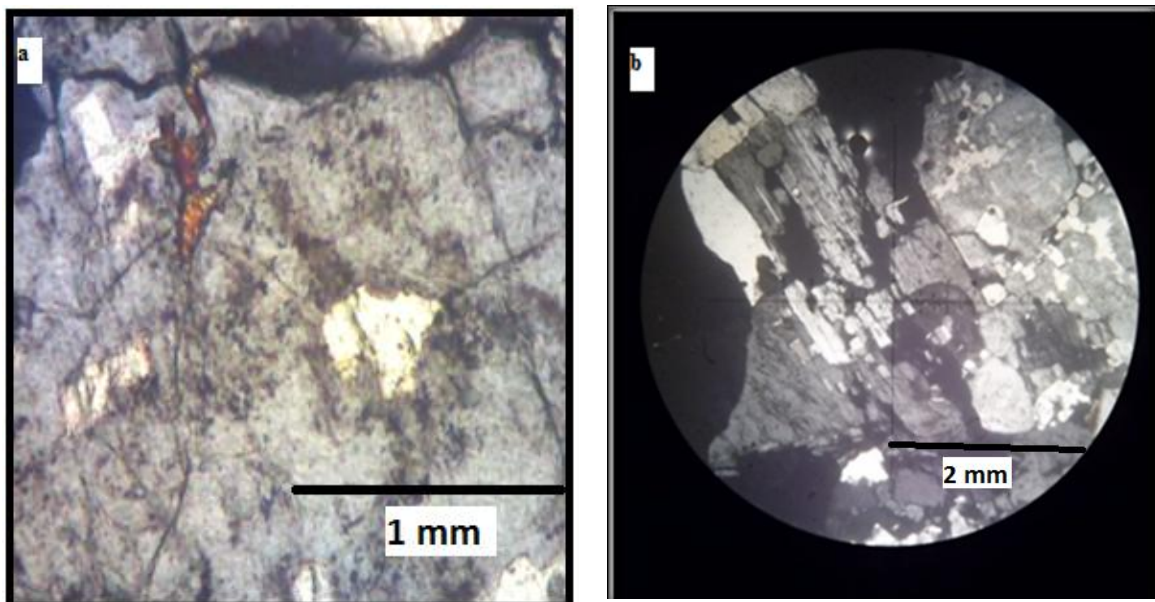


Plate XXX: (a) Close up view of microcline altered to mica and clay. (b) Replacement of plagioclase by perthite. Crossed polarised light; diameter of view = 3.2 X 40.

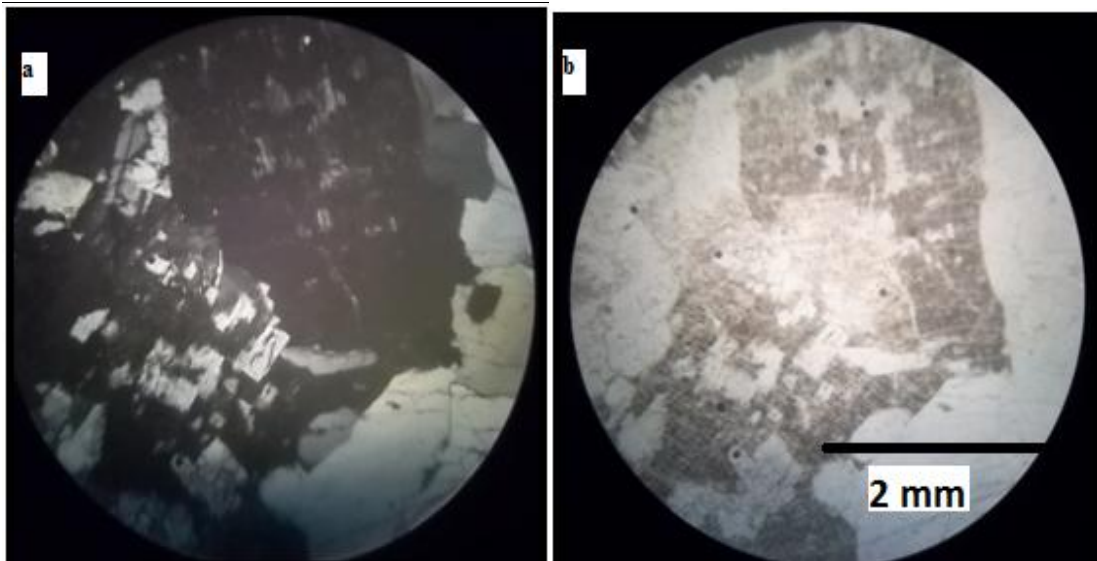


Plate XXXI: Exsolution within a plagioclase grain. Albite exsolved from microcline, the albite is light gray and display faint polysynthetic twinning while the microcline is mottled dark gray.

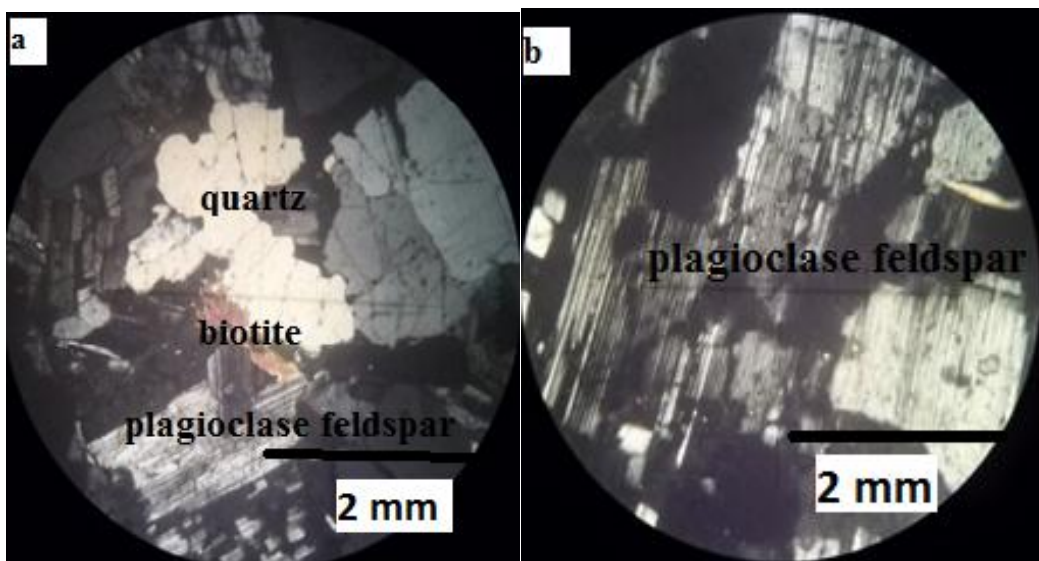


Plate XXXII: Photomicrograph of sericitized plagioclase crystals with deformational cracks within quartz and plagioclase. (b) Plagioclase feldspars Crossed polarized light, diameter of view = 3.2 X 40.

## **CHAPTER THREE**

### **GEOCHEMISTRY OF THE GRANITOIDS**

#### **3.1 INTRODUCTION**

Geochemistry is a tool generally used to establish how elements are distributed amongst the components of the Earth, why the elements are distributed the way they were and the principles that govern the distribution. Comparative evaluation of the geochemical data on the host granitoids and muscovite from different distinct zones of the pegmatite in the study area was carried out. This is to determine and use the chemical signature of the granitoids and the muscovite to establish gem mineralization potential, the differentiation degree and genesis of the pegmatite.

### **3.3 GEOCHEMICAL DATA**

The analytical data comprising major oxide, trace elements including REE in the rocks and muscovite samples are presented in Tables 3.1–3.4. The data were also presented on appropriate discrimination plots in order to clearly identify the main geochemical signatures of the rocks and muscovite. The data were then discussed on the basis of rock types and mineral paragenesis for better understanding of the variation in the composition and lithology.

#### **3.3.1 Granitoids**

The granitoids or granitic rocks in the area of study are coarse-medium-grained, and mineralogically composed predominantly of feldspar and quartz. On the O'Connor (1965) An-Ab-Or diagram, the granitoids from Angwan Doka (Doka 1, 5, 8, 15) and Janta



**Table 3.1: Major elements composition of granitoids and muscovite from Angwan Doka area (all values in wt %).**

Sample ID	Granitoids							Muscovite from pegmatites									
	Granodiorite				Granite		Aplite	Simple pegmatite	Border zone	Intermediate zone			Wall zone		Core zone		
	DOKA1	DOKA5	DOKA8	DOKA15	BAH1	BAH2	DOKA11	DOKA10	DOKA7	DOKA2	DOKA3	DOKA4	DOKA9	DOKA14	DOKA6	DOKA12	DOKA13
<b>SiO<sub>2</sub></b>	65.87	67.2	67.52	66.2	75.95	77.14	72.23	45.31	40.24	49.34	45.3	44.66	56.54	59.5	45.94	57.98	56.79
<b>TiO<sub>2</sub></b>	0.962	0.99	0.878	0.775	0.037	0.039	0.017	0.373	1.881	0.065	0.196	0.149	0.054	0.34	0.058	0.027	0.007
<b>Al<sub>2</sub>O<sub>3</sub></b>	15.16	14.5	14.42	14.72	12.37	12.48	16.83	34.51	19.06	32.65	33.87	34.24	27.32	23.9	34.13	23.96	21.48
<b>FeO(T)</b>	5.4	5.35	4.9	5.08	1.3	1.35	1.34	2.01	22.54	2.14	3.08	3.28	1.62	3.11	1.85	0.76	0.1
<b>MnO</b>	0.068	0.067	0.059	0.066	0.027	0.027	0.751	0.043	0.828	0.257	0.204	0.293	0.227	0.265	0.317	0.432	0.096
<b>MgO</b>	1.89	1.82	1.54	1.93	0.02	0.03	0.03	0.79	4.44	0.08	0.26	0.11	0.09	0.46	0.04	< 0.01	0.05
<b>CaO</b>	4.18	4.07	3.84	4.34	0.42	0.5	0.39	0.02	0.19	0.06	0.02	0.02	0.04	0.06	0.02	0.11	0.06
<b>Na<sub>2</sub>O</b>	2.72	2.43	2.4	3.03	3.51	3.85	8.28	0.74	0.79	0.6	0.56	0.56	0.41	0.75	0.54	2.24	0.28
<b>K<sub>2</sub>O</b>	2.13	2.06	1.89	2.9	4.66	4.77	0.31	9.94	7.51	9.5	10.07	10.06	8.06	8.04	10.11	7.64	9.61
<b>P<sub>2</sub>O<sub>5</sub></b>	0.19	0.17	0.17	0.15	< 0.01	< 0.01	0.26	< 0.01	0.08	0.03	0.02	< 0.01	0.01	0.04	0.02	0.1	0.01
<b>LOI</b>	1.09	-0.11	1.4	0.01	0.72	0.44	0.32	5.35	2.62	4.42	4.82	4.91	4.04	2.79	5.47	3.95	5.24
<b>Total</b>	99.68	98.56	99	99.18	99.02	100.6	100.8	99.09	100.2	99.14	98.4	98.29	98.39	99.24	98.48	97.21	93.72

**Table 3.2: Trace element composition of granitoids and muscovite samples from Angwan Doka area; (all values are in ppm except where**

	Granitoids							Muscovite from pegmatite									
Sample ID	Granodiorite				Granite		Aplite	Simple Pegmatite	Border zone	Intermediate			Wall zone		Core		
	DOKA1	DOKA5	DOKA8	DOKA15	BAH1	BAH2	DOKA11	DOKA10	DOKA7	DOKA2	DOKA3	DOKA4	DOKA9	DOKA14	DOKA6	DOKA12	DOKA13

stated otherwise).

	Granitoids							Muscovite from pegmatites								
--	------------	--	--	--	--	--	--	---------------------------	--	--	--	--	--	--	--	--

Sc	8	7	6	8	2	2	2	47	49	< 1	10	5	< 1	31	< 1	< 1	< 1
Be	4	6	3	2	7	16	125	18	10	24	23	24	20	19	27	22	41
V	66	60	53	65	< 5	< 5	< 5	25	70	< 5	< 5	6	< 5	9	< 5	< 5	< 5
Ba	510	558	555	608	20	11	< 3	44	36	20	20	13	20	60	16	3	26
Sr	190	182	193	202	6	5	4	4	10	13	7	8	8	9	15	17	24
Zr	219	208	187	178	98	106	74	5	54	< 4	< 4	< 4	< 4	30	< 4	< 4	21
Cr	50	40	40	60	< 20	< 20	< 20	< 20	< 20	< 20	< 20	< 20	< 20	< 20	< 20	< 20	< 20
Co	71	60	61	55	113	39	79	14	40	36	16	21	29	70	13	27	12
Cu	30	20	20	30	< 10	< 10	< 10	< 10	< 10	< 10	< 10	< 10	< 10	< 10	< 10	< 10	30
Zn	110	110	90	100	60	60	50	110	1260	680	380	520	510	210	590	620	< 30
Ga	24	24	20	22	38	38	39	172	112	176	201	217	149	124	215	105	45
Ge	1	2	1	1	3	3	10	3	8	10	5	6	9	5	9	14	66
Rb	223	308	202	111	519	459	58	1152	1245	3501	2946	3253	5891	6742	8127	9400	8801
Nb	11	15	17	9	67	76	98	236	630	113	262	229	90	216	198	92	211
Sn	11	9	16	3	17	31	10	191	573	510	825	886	427	771	553	269	97
Cs	122	243	109	14.6	11.5	12.2	54	28.9	347	712	190	302	555	255	662		

Table 3.2 (contd.)



Sample ID	Granodiorite				Granite		Aplite	Simple Pegmatite	Border zone	Intermediate zone			Wall zone		Core zone		
	DOKA1	DOKA5	DOKA8	DOKA15	BAH1	BAH2	DOKA11	DOKA10	DOKA7	DOKA2	DOKA3	DOKA4	DOKA9	DOKA14	DOKA6	DOKA12	DOKA13
La	32.1	30.6	20.8	33.1	17.9	22	1.6	0.2	2.7	0.2	0.3	0.8	0.2	1.7	6.4	0.2	4.7
Ce	64.9	60.7	43.6	63	34.6	48.7	1.7	0.7	4.8	0.2	0.2	1.2	< 0.1	2.4	6.8	< 0.1	9.5
Pr	7.94	7.38	5.39	7.42	5.48	6.33	0.14	< 0.05	0.52	< 0.05	< 0.05	0.2	< 0.05	0.3	1.36	< 0.05	1.29
Nd	30.3	28.3	21.6	27.2	20.7	23.8	0.4	0.1	1.8	0.2	0.2	0.7	0.1	1	4.8	< 0.1	4.7
Sm	6.2	5.7	4.6	5.3	7.7	8.1	< 0.1	< 0.1	0.5	< 0.1	< 0.1	0.1	< 0.1	0.2	0.7	< 0.1	0.8
Eu	1.41	1.31	1.13	1.22	0.08	0.06	< 0.05	< 0.05	0.05	< 0.05	< 0.05	< 0.05	< 0.05	< 0.05	0.18	< 0.05	0.18
Gd	4.7	4.5	3.7	4.2	9.2	9.5	< 0.1	< 0.1	0.5	< 0.1	< 0.1	< 0.1	< 0.1	0.2	0.5	< 0.1	0.5
Tb	0.7	0.6	0.5	0.6	2.2	2.2	< 0.1	< 0.1	0.1	< 0.1	< 0.1	< 0.1	< 0.1	< 0.1	< 0.1	< 0.1	< 0.1
Dy	3	2.8	2.5	2.9	14.2	14.2	< 0.1	< 0.1	0.9	< 0.1	< 0.1	< 0.1	< 0.1	0.2	0.2	< 0.1	0.4
Ho	0.5	0.4	0.4	0.5	3	3.1	< 0.1	< 0.1	0.2	< 0.1	< 0.1	< 0.1	< 0.1	< 0.1	< 0.1	< 0.1	< 0.1
Er	1	1	0.9	1.1	9	8.9	< 0.1	< 0.1	0.5	< 0.1	< 0.1	< 0.1	< 0.1	0.1	< 0.1	< 0.1	0.2
Tm	0.14	0.13	0.12	0.16	1.62	1.62	< 0.05	< 0.05	0.1	< 0.05	< 0.05	< 0.05	< 0.05	< 0.05	< 0.05	< 0.05	< 0.05
Yb	0.8	0.7	0.6	0.9	10.7	10.5	< 0.1	< 0.1	0.9	< 0.1	< 0.1	< 0.1	< 0.1	0.2	< 0.1	< 0.1	0.2
Lu	0.1	0.1	0.1	0.12	1.4	1.34	< 0.04	< 0.04	0.13	< 0.04	< 0.04	< 0.04	< 0.04	< 0.04	< 0.04	< 0.04	< 0.04
Y	12	11	10	11	108	108	< 2	< 2	4	< 2	< 2	< 2	< 2	< 2	< 2	< 2	< 2
ΣREE	163.09	155.22	115.94	158.8	245.8	268.4	-	-	17.7	-	-	-	-	-	-	-	-

Table 3.4 Elemental ratios of granitoids and muscovite from Angwan Doka pegmatite group

Sample ID	Granodiorite				Granite		Aplite	Simple pegmatite	Border zone	Intermediate zone			Wall zone		Core zone		
	DOKA1	DOKA5	DOKA8	DOKA15	BAH1	BAH2	DOKA11	DOKA10	DOKA7	DOKA2	DOKA3	DOKA4	DOKA9	DOKA14	DOKA6	DOKA12	DOKA13
<b>K/Rb</b>	79.29	55.52	77.67	216.88	74.53	86.4	44.36	71.62	50.03	13.38	12.7	12.38	19.11	20.51	10.32	6.74	9.04
<b>K/Cs</b>	144.93	70.37	143.93	1648.88	3363.83	3245.67	47.65	2855.18	179.66	110.76	439.96	276.52	120.55	261.73	126.77	52.85	70.28
<b>Rb/Sr</b>	1.17	1.69	1.04	0.54	86.50	91.81	14.51	288	124.60	269.3	420.85	407.37	736.37	749.11	541.81	552.94	366.70
<b>Rb/Ba</b>	0.43	0.55	0.36	0.18	25.95	41.72	19.33	26.18	34.61	294.55	329.05	518.61	175.05	54.21	507.93	3133.33	338.5
<b>Nb/Ta</b>	7.85	8.33	7.72	5.29	4.89	5.1	1.97	12.42	4.63	1.94	7.4	6.13	2.1	3.38	2.15	1.34	0.59
<b>Rb/Cs</b>	1.82	1.26	6.3	7.6	45.13	37.62	1.07	39.86	3.59	8.27	34.63	22.32	10.61	12.75	12.27	7.83	7.75
<b>Y/Nb</b>	1.09	0.73	0.59	1.22	1.61	1.42	0.02	0.01	0.01	0.02	0.01	0.01	0.02	0.01	0.01	0.02	0.01
<b>Al/Ga</b>	0.63	0.6	0.72	0.66	0.32	0.32	0.43	0.2	0.17	0.18	0.16	0.15	0.18	0.19	0.15	0.22	0.47
<b>Fe/Mn</b>	79.41	79.85	83.05	76.96	48.14	50	1.78	46.74	27.22	8.32	15.09	11.19	7.13	11.73	5.83	1.75	1.04
<b>Zr/Hf</b>	41.33	40	42.5	38.71	16.07	14.72	12.98	25	20.77	20	2.35	20	20	15	20	8	42
<b>Li/Cs</b>	0.0004	N/A	N/A	0.001	N/A	N/A	0.0003	0.002	0.001	0.0003	0.002	0.007	0.0002	0.0004	0.001	0.001	0.003
<b>Li/F</b>	0.33	N/A	N/A	0.4	N/A	N/A	0.6	0.15	0.32	0.48	0.48	0.5	0.37	0.33	0.6	0.68	0.63

area (Bah 1 and 2) plot distinctly into granodiorite and granite fields respectively (Figure 3.1).

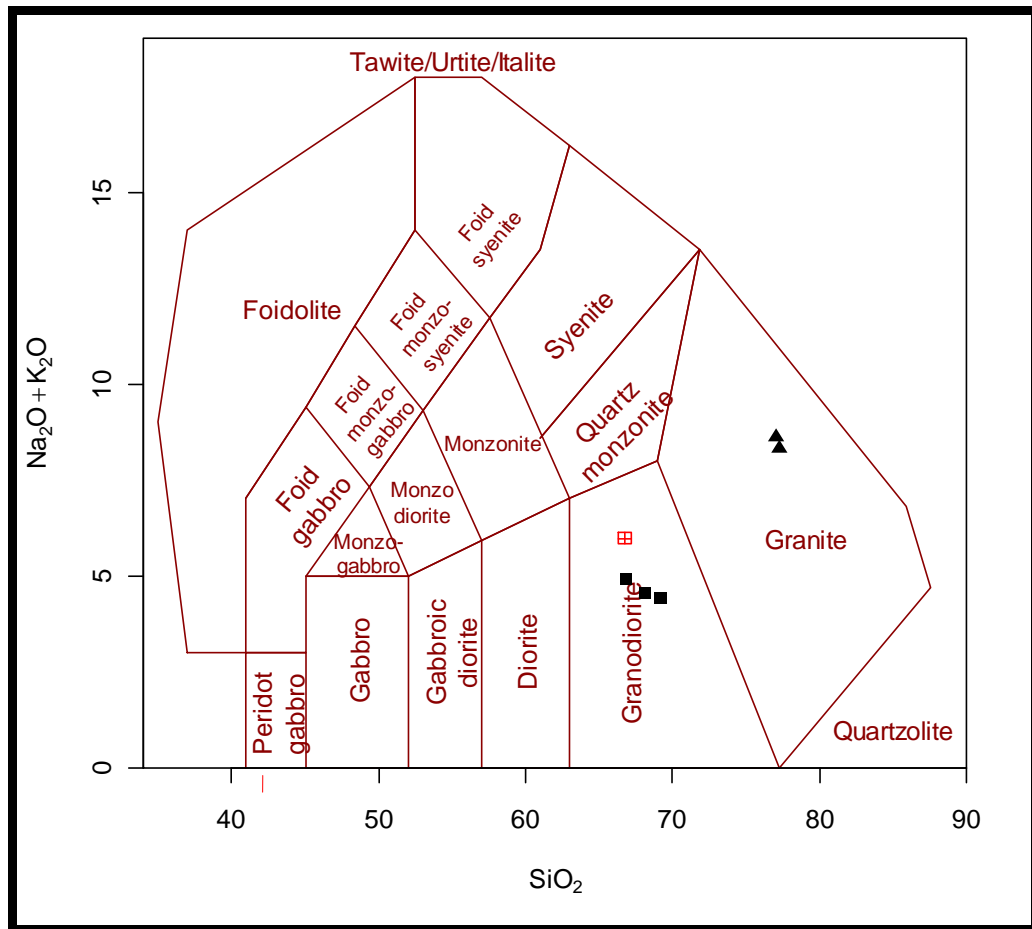


**Figure 3.1: Whole-rock geochemical data plotted on the TAS classification diagram ( $\text{SiO}_2$  versus  $\text{Na}_2\text{O} + \text{K}_2\text{O}$ ) after Middlemost (1985),  $\boxplus$  Graniorite from Jamaalu,  $\blacktriangle$  Biotite granite from Janta,  $\blacksquare$  Granodiorite from Angwan Doka.**

### **Granodiorite**

All samples of granodiorite from Angwan Doka (Doka 1, 5, 8) have moderate enrichment in  $\text{Al}_2\text{O}_3$  and higher concentration of  $\text{MgO}$ ,  $\text{CaO}$  and  $\text{TiO}_2$ . The  $\text{SiO}_2$  content of the granodiorite is generally less than 68 % whereas it is higher than 70 % in the aplite (Doka 11). The granodiorite also has higher concentration ( $\sim 5$  wt %) of  $\text{FeO}$  (t) than the aplite. Major element variations in terms of wt % oxide versus wt %  $\text{SiO}_2$  for example,  $\text{TiO}_2$

show somewhat scattered plot in contrast to linear trend for CaO, Na<sub>2</sub>O, Al<sub>2</sub>O<sub>3</sub>, Fe<sub>2</sub>O<sub>3</sub>, P<sub>2</sub>O<sub>5</sub> and MgO (Figure 3.2).

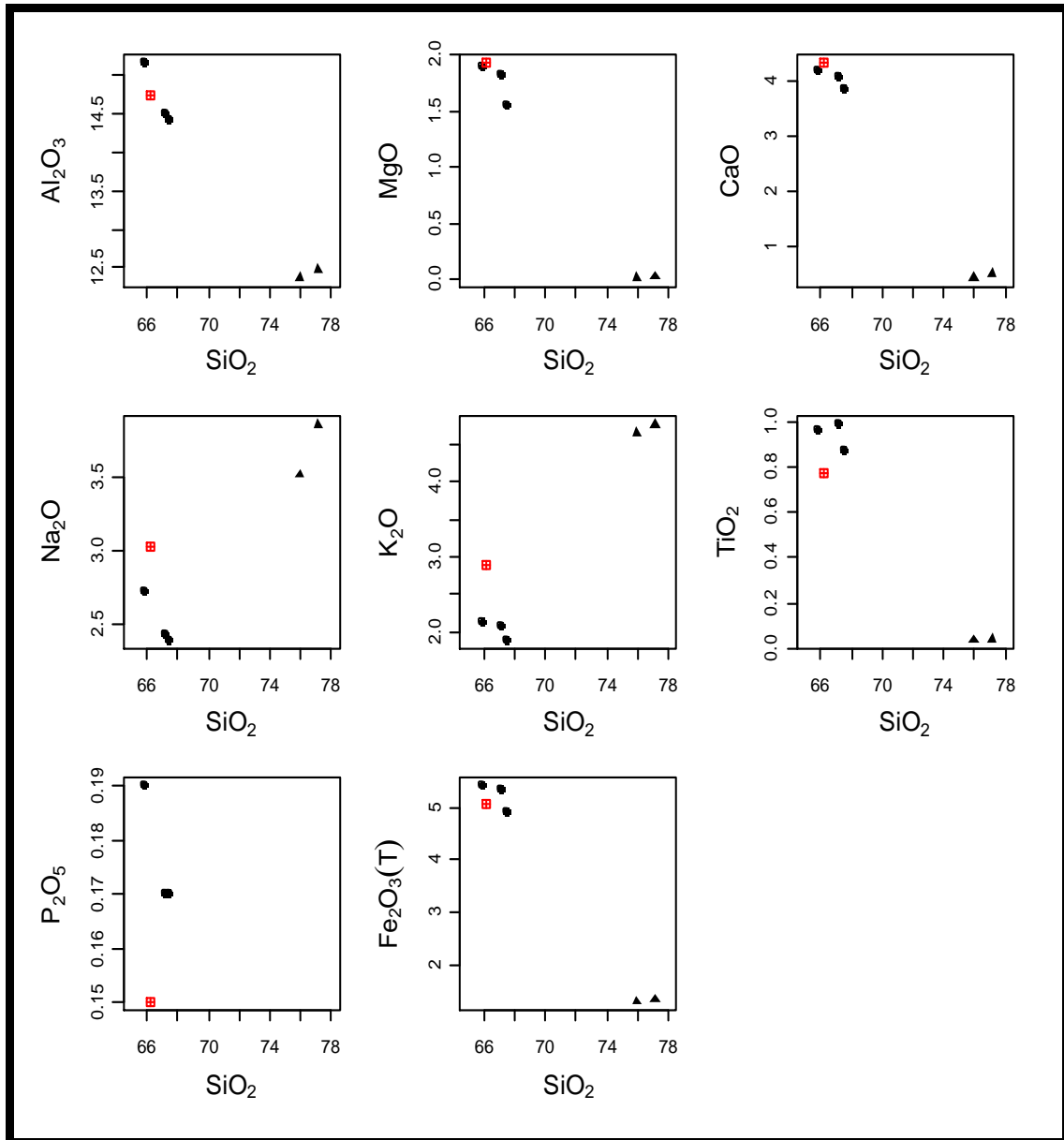


**Figure 3.2: Bivariate plot of major element for granitoids.** ■ Granodiorite from Jamaalu, ▲ Biotite granite from Janta, ■ Granodiorite from Angwan.

In addition, Al<sub>2</sub>O<sub>3</sub> is greater than CaO+Na<sub>2</sub>O+K<sub>2</sub>O (in molecular proportions). Discrimination based upon the molecular ratio alumina to alkalis [Al<sub>2</sub>O<sub>3</sub>/(Na<sub>2</sub>O+K<sub>2</sub>O)] versus alumina to lime and the alkalis [Al<sub>2</sub>O<sub>3</sub>/CaO+Na<sub>2</sub>O+K<sub>2</sub>O] after Shand (1943) indicate that the granodiorite is distinctly peraluminous in Angwan Doka area, whereas it is



metaluminous in Jamalul [Al<sub>2</sub>O<sub>3</sub>/CaO+Na<sub>2</sub>O+K<sub>2</sub>O), A/CNK > 1.1 (Figure 3.3). In the plot of A/CNK versus SiO<sub>2</sub>, the granodiorite was discriminated into I- and S- types in Jamalul and Angwan Doka respectively. The metaluminous affinity of this granite is also supported by the presence of titanite and hornblende (Chappell and White, 1974).

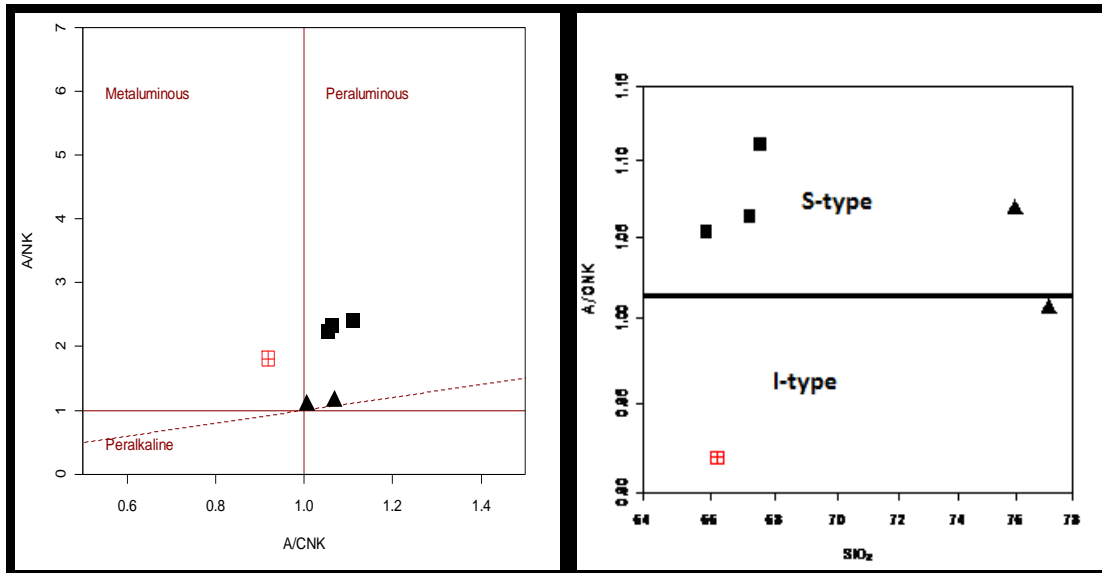


**Figure 3.3: Chemical classification of the granitic rocks using the molecular ratio of alumina to alkalis [Al<sub>2</sub>O<sub>3</sub>/(Na<sub>2</sub>O+K<sub>2</sub>O)] versus alumina to lime and alkalis Al<sub>2</sub>O<sub>3</sub>/(CaO+Na<sub>2</sub>O+K<sub>2</sub>O) after Shand (1943). (b) A/CNK versus SiO<sub>2</sub> discrimination diagram after (Chappell and White 1974). Symbols are same as in Fig 3.1.**

### *Granite*

The granite is characterized by relatively high alkali and low CaO contents (at SiO<sub>2</sub> = 77.14%: Na<sub>2</sub>O + K<sub>2</sub>O = 8.62%, CaO = 0.5%), high Fe<sub>2</sub>O<sub>3</sub>/MgO ratio (SiO<sub>2</sub> = 77.14%: Fe<sub>2</sub>O<sub>3</sub>/MgO = 45-65). MnO and P<sub>2</sub>O<sub>5</sub> are extremely low (generally less than 0.03 %) and both oxides are as much minor as TiO<sub>2</sub>. The Al<sub>2</sub>O<sub>3</sub> content is about 12.4%. Figure 3.3 reveals that the granite is weakly peraluminous [Al<sub>2</sub>O<sub>3</sub>/(CaO+N<sub>2</sub>O+K<sub>2</sub>O), ASI. Plots of the analytical data on the ternary AFM plot of (Irvin and Baraga 1971), based on (Na<sub>2</sub>O+ K<sub>2</sub>O =A) + (FeO= F) + (MgO= M) is used to classify the rocks into calcic-alkaline, while the K<sub>2</sub>O versus SiO<sub>2</sub> shows the degree of alkalinity of the biotite granite from Janta area. The plot

expresses the composition of the feldspars in the rocks which can be used to determine sources of magma, the ternary variation diagrams which give information on the differentiation history of a granitic magma reveals compositional change in the granitoids (Figure 3.4). The beryl-topaz bearing biotite granite from Janta area (sample BAH 1 and BAH 2) has higher contents of alkalis and lower mafic content therefor plotted in high-K-calcium-alkaline series by contrast, the Angwan Doka granodiorite Doka (1, 5, 8 and 15) is relatively less potassic than the biotite granite from Janta and therefore plots in the calcic-alkaline series.

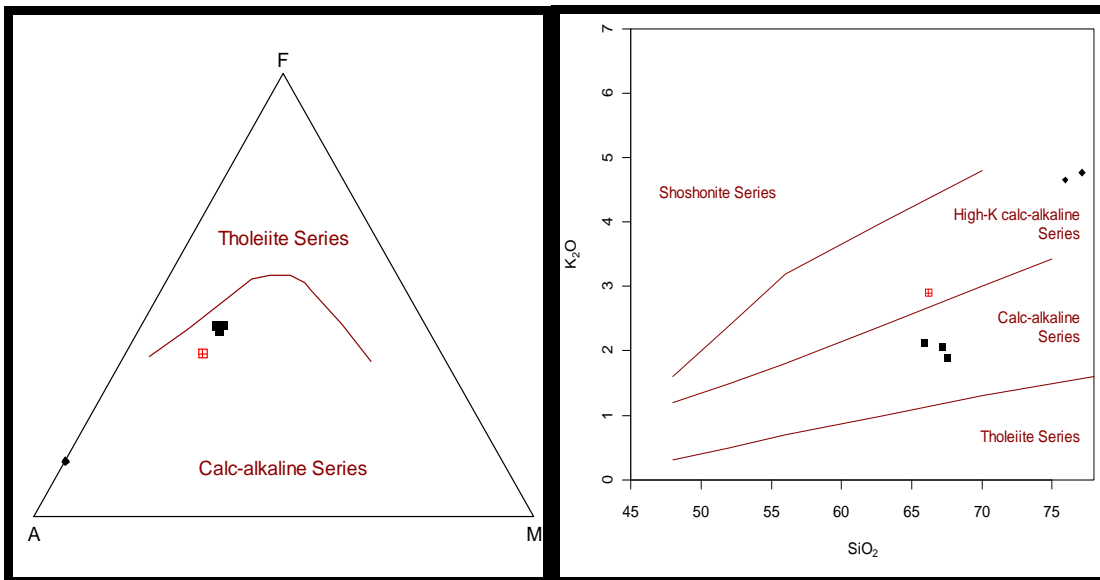


**Figure 3.4: AFM classification plots of (Irvin and Baragar 1971) and (Peccerillo and Taylor 1976) indicating a high-K calc-alkaline for the biotite granite with a decrease in mafic content and calc-alkaline for the granodiorites. (Symbols are same as in Fig. 3).**

In the discriminant diagram after Batchelor and Bowden (1985), the granodiorite in Angwan Doka area, which is host to the tourmaline-bearing pegmatite dykes plots distinctly within the mantle fractionates field whereas the biotite granite from Janta straddled on the post orogenic field and not fully within the anorogenic field indicating it is

either a very late orogenic or highly contaminated by the Older Granite and metasediment within the study area (Figure 3.5).

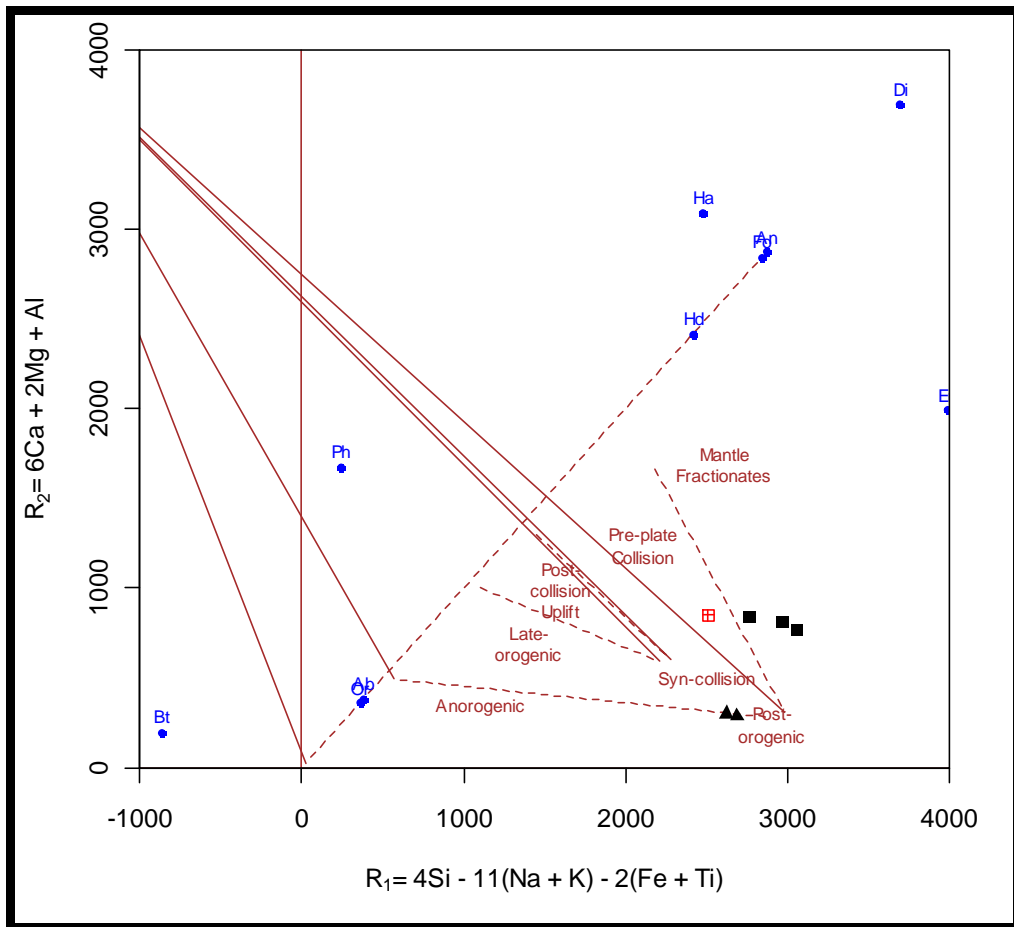


**Figure 3.5: Discriminant diagram for the granitoids after Batchelor and Bowden (1985).** Symbols are same as in Figure 3.1.

### 3.4 TRACE ELEMENT CHARACTERISTICS OF THE GRANITOIDS

The geochemical signatures of the granite samples from Janta are similar to anorogenic granitoids of the Younger Granite province. The main chemical characteristics of the granite are its high concentrations of  $SiO_2$  (>73.9 wt%), elevated contents of F, Li, and Rb, and low contents of Ba, MgO,  $TiO_2$  Sr and Zr which are characteristics for geochemically specialized tin-bearing granites (Haapala,1997). Y/Nb and Yb/Ta ratios are

relatively constant with  $Y/Nb > 1.2$  which suggests that the granite was probably generated from interaction between mantle-derived magma and continental crust (Eby, 1990).

The granite is considered to be a part of or peripheral to the Younger Granite ring-complexes province of Nigeria and only exposed in the area as erosion has removed the volcanic rocks and other evidence of rifting. Discrimination plot after Pearce *et al.*, (1984) clearly distinguish the rock, tectonically into granite formed within plate field (anorogenic) and granite associated with tectonic activities (Figure 3.6)

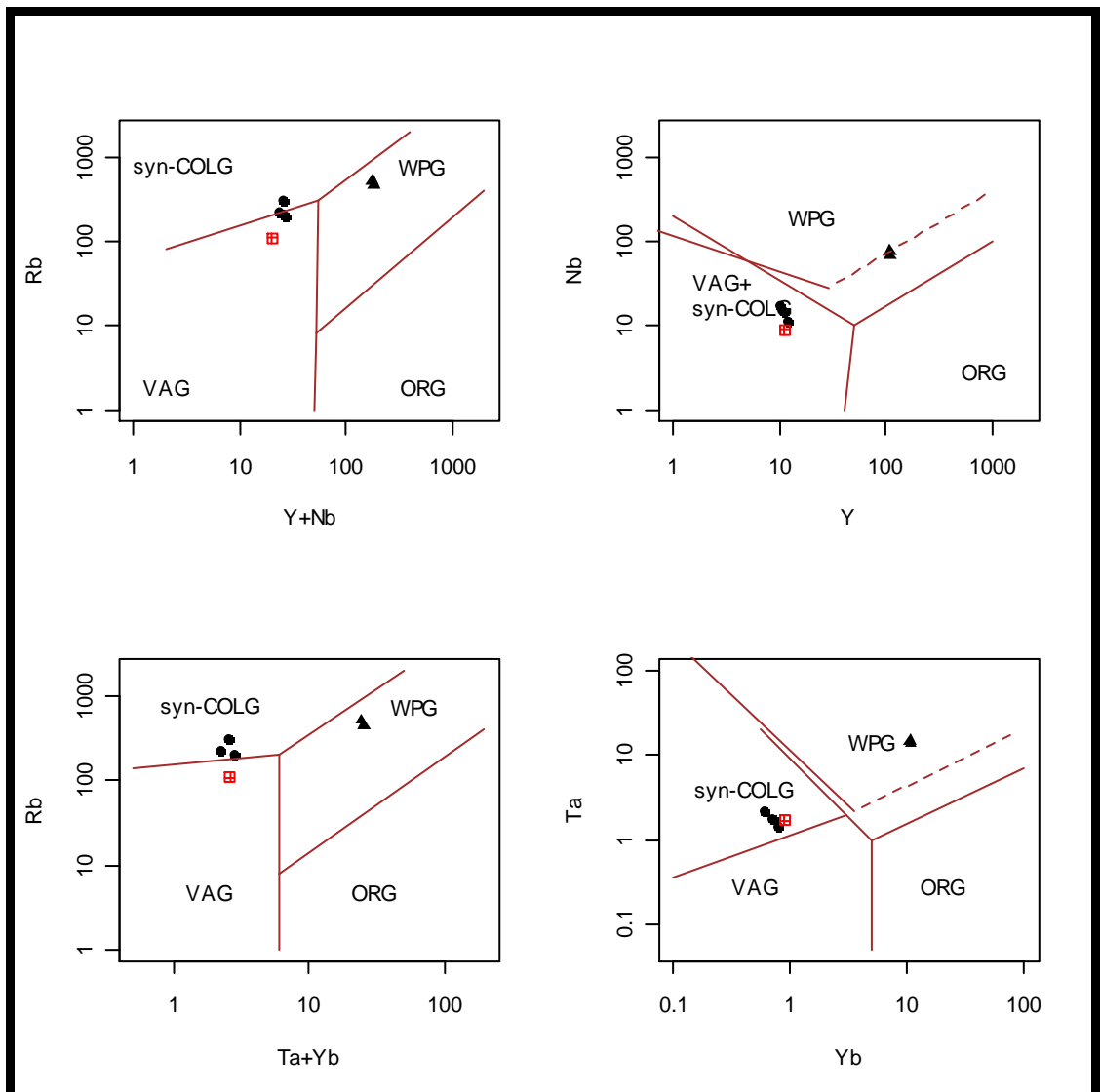


**Figure 3.6: Discriminant diagram for the granitoids (after Pearce *et al.*, 1984).** ■ Granodiorite from Jamaalu, ▲ Biotite granite from Jenta, ● Granodiorite from Angwan Doka

The REE contents in the granitoids relative to chondritic abundances and compared with the average of about 250 ppm for granitic rocks in general given by Emmermann *et al.*, (1975) are low (Table 3.3). The REE abundance pattern relative to chondrite revealed that the granodiorite at Angwan-Doka (Doka 1, 5, 8) and Jamaalu, (Doka 15) are very similar in chemical composition despite the large spatial distance between the areas sampled (Figure 3.7). The gentle slope with a relatively small negative Eu anomaly pattern is typical of the Older Granites of Nigeria (Okunlola, 2005; Akintola and Adekeye, 2008; Garba, 2003). Albitization of earlier formed plagioclase during partial melting may have generated the Eu anomaly within the pegmatite granite of Angwan Doka area. By contrast, the REE abundance pattern in granite from Janta area reveals a strong relative enrichment in REE content which easily partition into apatite, zircon, monazite, fluorite and alkaline feldspar of the rocks (Ercit, 2005; London, 2008). The highly negative Eu anomaly can be interpreted as evidence of earlier separation of the mineral phase, plagioclase, in unoxidized magma or (plagioclase fractionation) thus suggesting that the rock forming material was produced in a reduced environment. The process of albitization which affected the feldspar would have contributed significantly to the extremely negative Eu anomaly in Janta area.

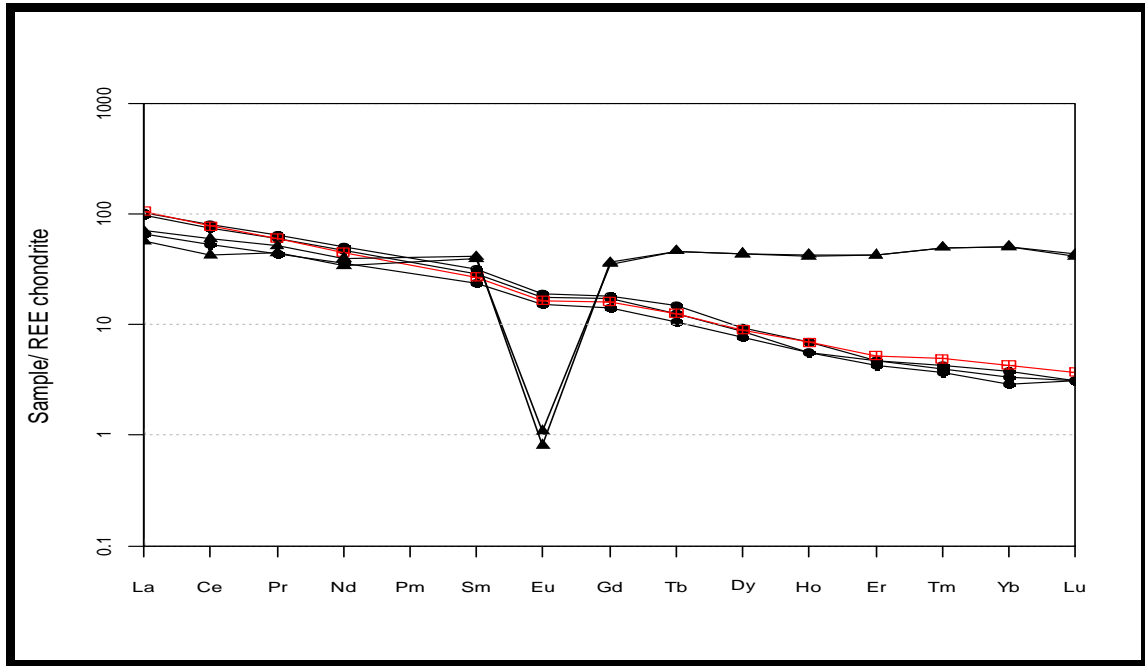


**Figure 3.7: Rare earth elements pattern for granitic rocks. The chondrite normalizing values are those of Boynton (1984). Symbols are same as in Figure 3.1.**

The granite from Janta area (BAH 1 and BAH 2) is enriched in both the LREE and HREE with a significant depletion in Eu; typical of the Nigerian Younger Granite of (Ogunleye, 2003). This granite also contains higher values of Nb, Y, F, Be, U, Ti, Pb, Th and Ta relative to the granodiorite from Angwan Doka area, typical of the A-type granite believed to be associated with granite magmatism that originates by deep melting of crust within the continental rift zones and usually with some input from the mantle source (Černý, 1991; Ercit, 2005; Martin and Devito, 2005).

The NYF family of pegmatite, described by Černý (1991) is derived from A-type granite with the designations 'A' standing for anorogenic and 'NYF' for niobium, yttrium and fluorine respectively. Although fluorine was not analysed in the biotite granite, the high fluorine content in the granite was attested to by the moderate enrichment in topaz, a fluorine-bearing mineral, Ogunleye *et al.*, (2006) also reported high fluorine bearing

minerals like cryolite and thomsenolite from the Younger Granite province of Nigeria. According to Samson and Wood (2005), the heavy REE are normally associated with rocks rich in fluorine while the high niobium and yttrium values (Figure 3.2) attest to the magmatic signature of the granite (Martin and de Vito, 2005). The granite is also marked with high Li, Rb, low Sr and Ba and very low concentration of phosphorus which are characteristics of A-type granite (Bircket and Sinclair, 1998). The variations in the trace elements content in the granitoids are graphically displayed in Figure 3.2 taking the upper crust as a reference to which the data are normalized.

The similarity of Sr and Eu is shown by an almost coherent behaviour in the granitic systems but Eu is more sensitive in ionic size to oxygen fugacity and temperature. The low Sr and Ba value in the granite from Janta suggests that the source of the granite is magmatic. With an advanced fractionation of feldspars in upper crust, fractionation of the feldspar would also cause decrease in MgO and TiO<sub>2</sub> contents. The advanced fractionation characteristic of the rocks was attested to from the depletion of Ca and Sr by separation of oligoclase; fractionation of the feldspars would have resulted into the reduced Ba, Sr, TiO<sub>2</sub>, Mg and the negative Eu anomaly observed with a simultaneous increase in Rb.

With onset of crystallization of K-feldspar and biotite and subsequent removal of plagioclase in the magma, the pegmatite and early granite became depleted in Ba and Sr as a response to changes in bulk chemical composition of crystallizing magma (Kolbe and Taylor, (1966). Černý, (1985) reported that with evolution of NYF granitic pegmatite, Ti content would drop with concomitant increase in Si, F, Li and Ga. The value of Nb predominates over Ta while Y value is moderately high in the NYF granite from Janta area (BAH 1 and BAH 2).

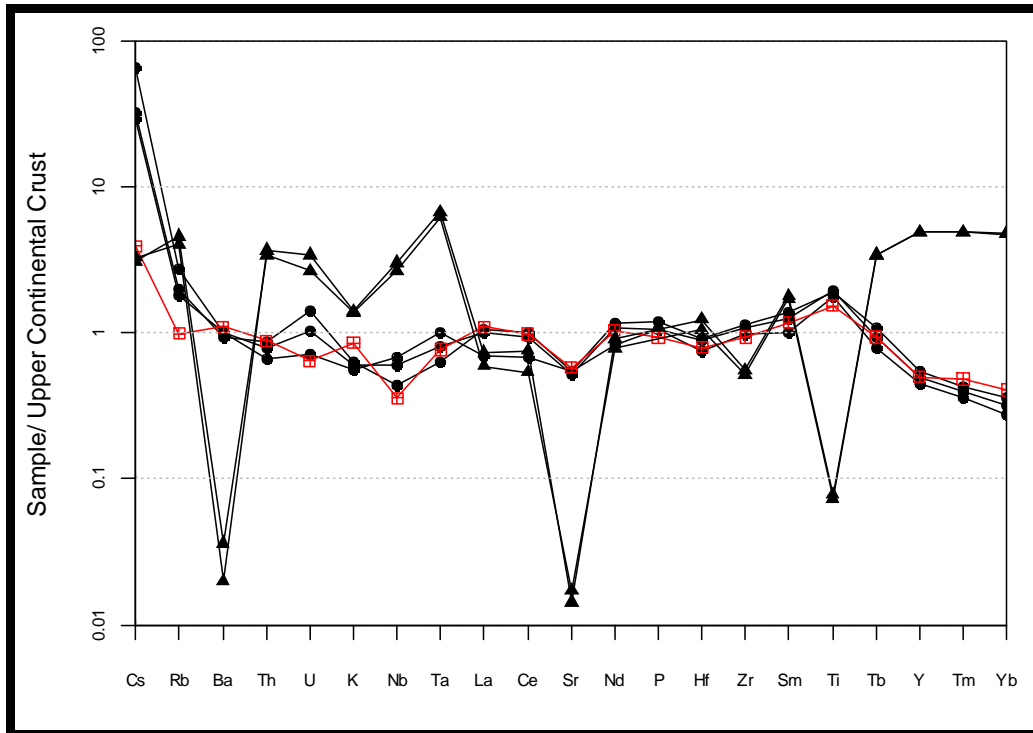


Figure 3.8: Selected trace elements spider diagram relative to Upper Crust. The normalizing values are those of Taylor and McLennan, (1985). Symbols are same as in Fig.3.1

## CHAPTER FOUR

### PETROGENESIS OF THE GRANITOIDS AND PEGMATITES OF ANGWAN DOKA AREA

#### 4.1 INTRODUCTION

Muscovite is a common rock forming minerals in the terrestrial crust. In granitic pegmatite, it is the fourth major mineral after quartz, K-feldspars and plagioclase with chemical formula as  $KAl_2(Si_3Al)O_{10}(OH)_2$ . Due to its crystal structure, muscovite may incorporate several trace elements many of which are potential indicator of the fractionation degree of an evolving pegmatite melt. The indicator elements reported in



literature mainly by Černý (1982) are mobile element such as Na, Ba and Cs which occur preferably in the X-site while others like Ti, V, Cr, Ga, Zn, Y, Nb, Sn, La and Ce are incorporated in the Y-site.

The importance of muscovite composition as a clue to internal evolution of pegmatite magma has been discussed by Černý (1982), Černý and Burt (1984), and Joliff *et al.*, (1987). The K/Cs and the K/Rb ratios in muscovite are considered as the best indicator of pegmatite evolution (Černý *et al.*, 1985; Joliff *et al.*, 1987). These indicators are used in assessment of rare element pegmatites before expensive drill programs are carried out. Micas from pegmatite derived from granitic precursor by fractionation normally show a gradual enrichment in Li, Rb, Cs and F with a decrease in Fe, Mg, Ti and K/Cs, K/Rb ratio from internal to external zones.

Crystals of muscovite from different zones of selected granitic pegmatites belonging to the known gem-producing Angwan Doka pegmatite group were analyzed for major, minor and trace elements. Analysis of the compositional trend as it relates to the geochemical differentiation or evolution of the pegmatites, with particular emphasis on coexisting micas and tourmaline was also done so as to establish and delineate the fractionation indices of these minerals, the sequence of crystallization of pegmatite zones and details of mineral parageneses.

Pegmatites commonly display extreme fractionation and accumulation of rare lithophile elements beyond the limit observable in the granitic rocks. Cs, Li, B, F and Rb are incompatible within common silicate so they partition into the melt (London *et al.*, 1999). The enrichment of these elements leads to their precipitation in highly fractionated pegmatite.

Potassium (K) and rubidium (Rb) have similar ionization potentials and electronegativities; therefore the geochemical behaviour of Rb is closely similar to K. Potassium (K) is the only major element for which cesium (Cs) can substitute. The electronegativity and ionization potential of Cs is lower than K, with a slightly larger ionic radius (Černý et al., 1985). Although, Cs and Rb are incompatible in the most important silicate mineral during magma fractionation, Cs is commonly enriched in rare alkalis in fractionated liquid while Rb is highly compatible in mica (Černý, 1985). Cs increases gradually from the host granitoids (Doka 1, 5, 8 and 15) to the pegmatite (Doka 7, 10, 11) and increasing towards the inner-most fractionated zones of the pegmatite (Doka 2, 3, 4, 6, 12, 13), (Table 3.4). The high Li, Cs, Ta and Rb values of the muscovite and the positive correlation between those elements in the muscovite suggest that the pegmatite belong to the lithium-cesium-tantalum (LCT) family of the rare elements. Continuous increases in Cs occur only in the most complex bodies of pegmatite on the outskirts of cogenetic granitic pegmatite swarms, furthest away from their plutonic sources. In order of increasing concentration, the main carriers of Cs are K-feldspar, micas, beryl and pollucite (Černý, 1985).

Leucogranites and pegmatitic granites parental to groups and fields of complex rare-element pegmatites have been reported to commonly contain between 170 and 735 ppm Rb, and have a K/Rb ratio as low as 41. In addition, the Rb content of pegmatites reaches 4.98 wt. % in K-feldspar, 6.35 wt. % in muscovite and 4.72 wt % in lepidolite (Černý et al., 1982, Černý, 1982).

Figure 4.1 (Shown for comparison with figure 4.2) is a plot of K/Rb versus Cs of Černý (1985) modified by London (2008) to illustrate the fractionation level from a granite-host to the rare-element pegmatite fields of central Manitoba, Canada, in which K/Rb

reaches the value of 4.0 in K-feldspar and Sr 170 to 8 ppm in the more primitive pegmatites while lepidolite record K/Rb ratio of 2.1. Rb/Cs decreases to 8.0 in K-feldspars and 4.5 in lepidolite respectively (Rb < 5,500 ppm) (Jahns 1982). Al/Ga ratios range from 1100 in feldspar to 260 in the mica while Fe/Mn ratio drops from 4.57 in early muscovites to 0.13 in lithian mica, (Černý 1985), a distinct increase in Sr in the spodumene-bearing bodies with increasing Rb content was also observed (Shmakin 1979, Černý *et al.*, 1985).

The degree of fractionation is important in determining the potential for mineralisation and the type of mineralisation with which a granite suite is associated. Fractional crystallisation can be measured with the use of compatible/incompatible element ratios and the behaviour of selected trace elements that indicate the incoming or outgoing of crystallising phases. The K/Rb and K/Cs ratios of the muscovite from the study area (Table 3.4) decrease from the outer zone towards the innermost zone, thus reflecting the increasing differentiation degree as well as mineralization potential of the pegmatite from the outer zone to innermost zone. This is consistent with the observation of Černý (1985) and London (2008). Plots of K/Rb Versus Cs, K/Rb versus Rb and K/Cs versus Cs respectively as Figures 4.2, 4.3 and 4.4 have been employed in order to provide pictorial view of changes in absolute abundance of those elements within the pegmatite during the process of fractionation.

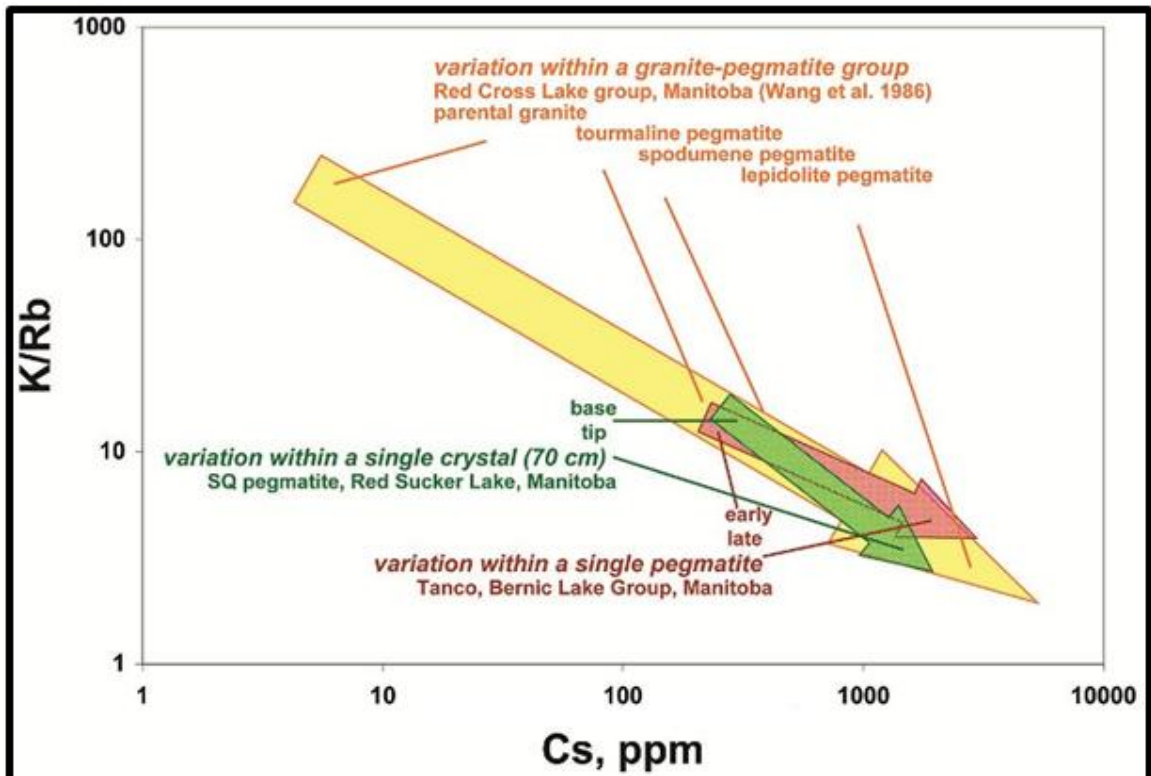


Figure 4.1: Plot of K/Rb versus Cs from individual pegmatites and pegmatite group from the Tanco pegmatite, Manitoba (after Černý *et al.*, (1985).

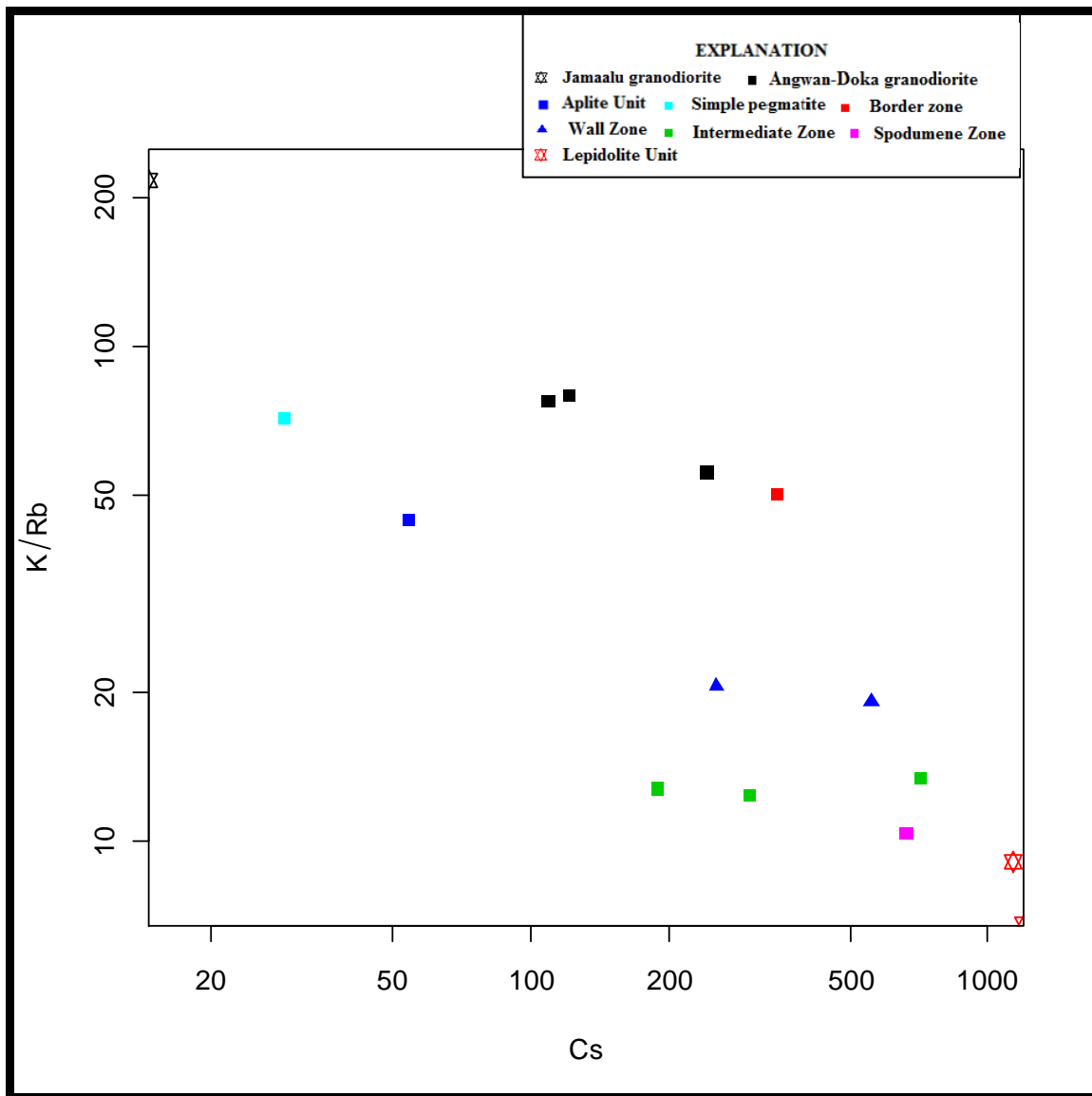


Figure 4.2: Plot of K/Rb versus Cs showing the degree of fractionation from rocks to pegmatite and mineralization of pegmatite in the study (after Černý *et al.*, (1985))

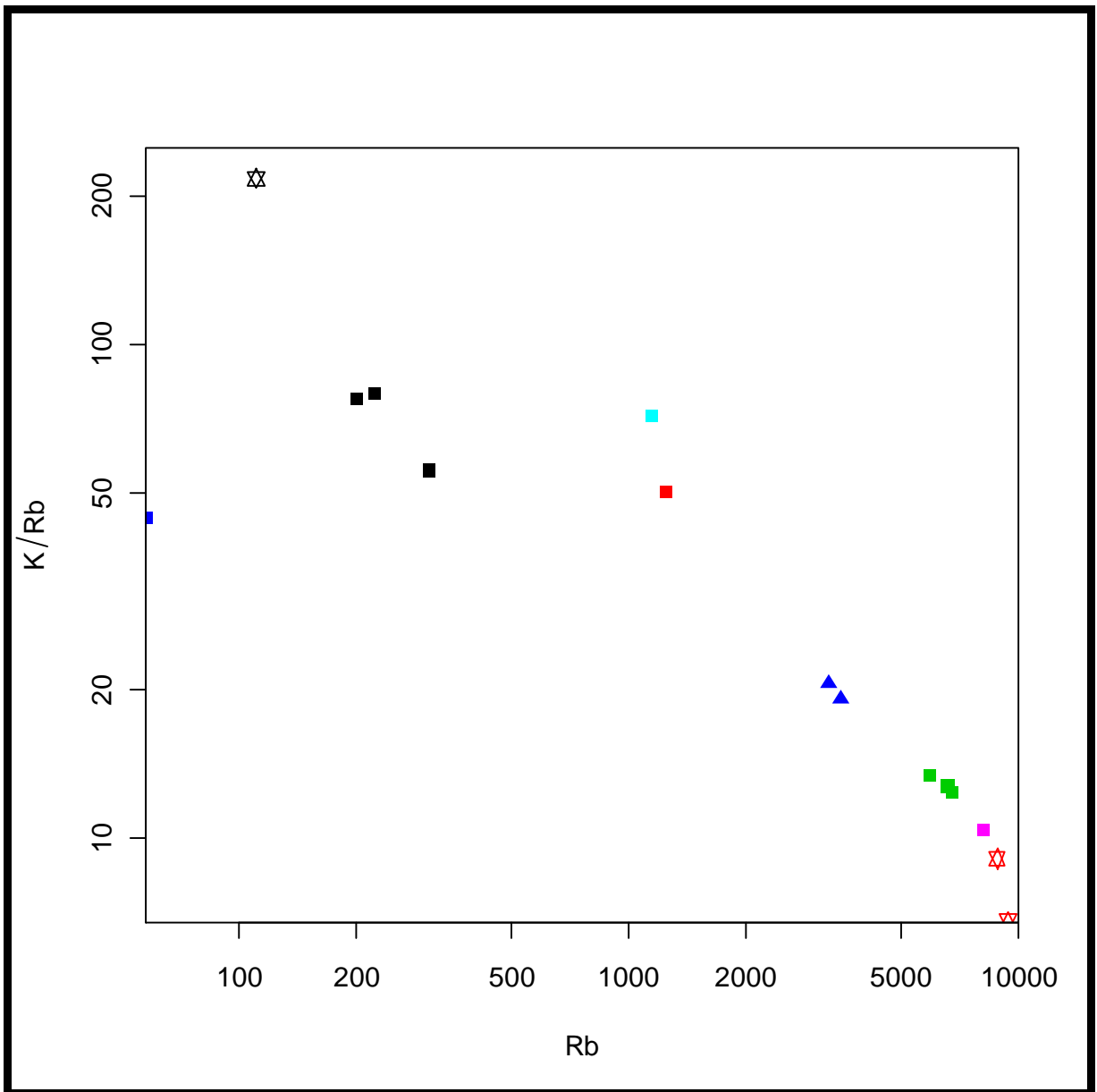
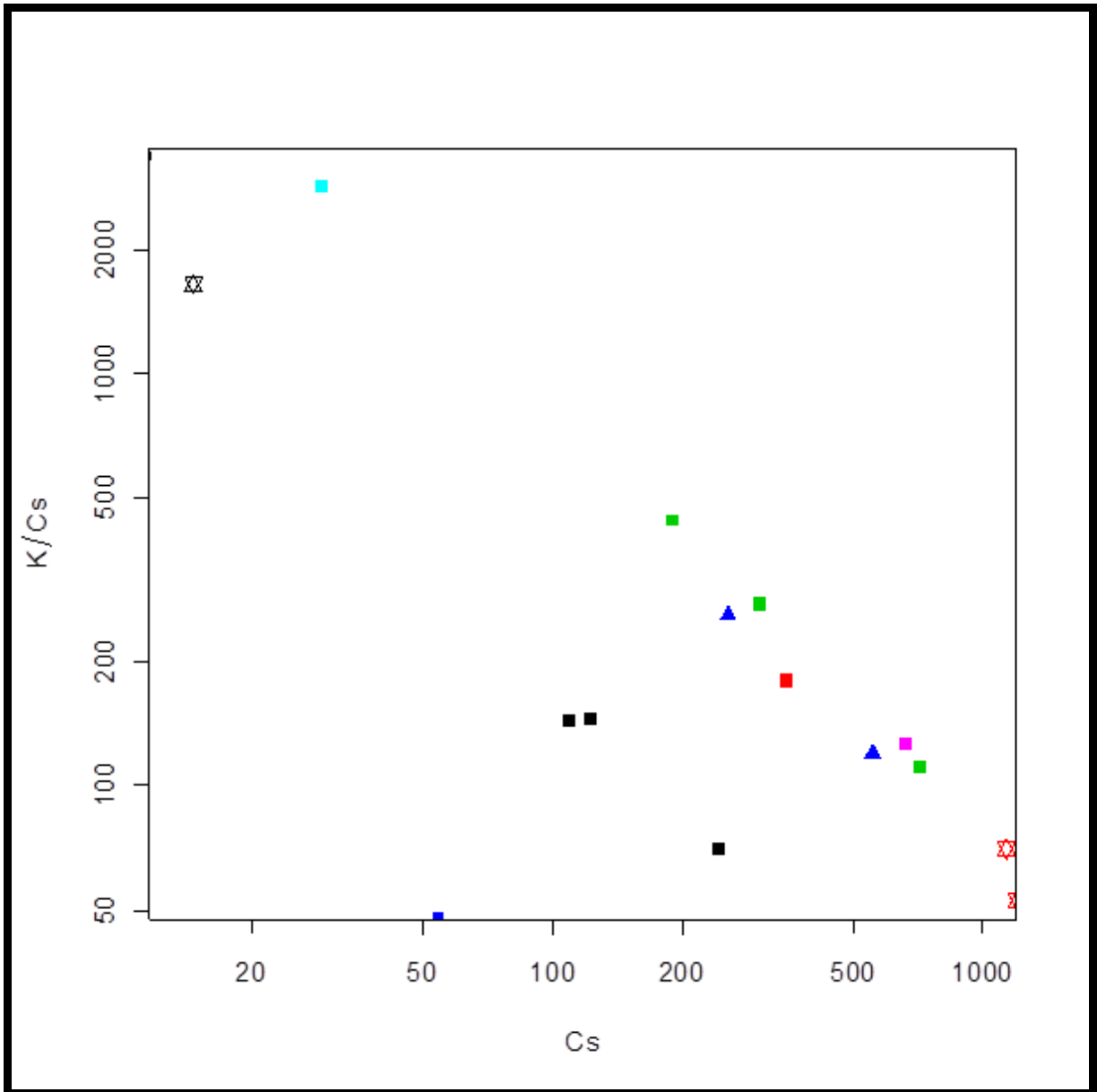


Figure 4.3: K/Rb versus Rb plot of rocks and minerals making up the pegmatite, in the study area (after Černý *et al*, (1985)). Symbols are same as in Figure 4.2.



**Figure 4.4: K/Cs versus Cs variation plot in the granodiorite and pegmatite (after Černý *et al.*, (1985)). (Symbols are same as in Figure 4.2).**

Rb and Sr are more compatible in plagioclase and alkaline feldspars (London 2005) while Ba is highly compatible in micas and the K-feldspars. Because mica hosts most of the Ba in igneous rocks, the Rb/Ba ratio of micas should increase with crystallization of micas. This trend is observed in samples from the wall zone (Doka 14) to intermediate zone (Doka 2, 3, 4) and increased up to 3133 in the core zone represented by Doka 12 (Table 3.4).

The value of Ba in the highly fractionated Li, Rb and Cs enriched granodiorite host rock from Angwan-Doka area range from 510 to 608 ppm while Sr range from 182 to 202 ppm (Table 3.2). There is an observable increase in the Sr due to the high Rb value with advanced crystallization within the granitoids (Figures 4.5 and 4.6).

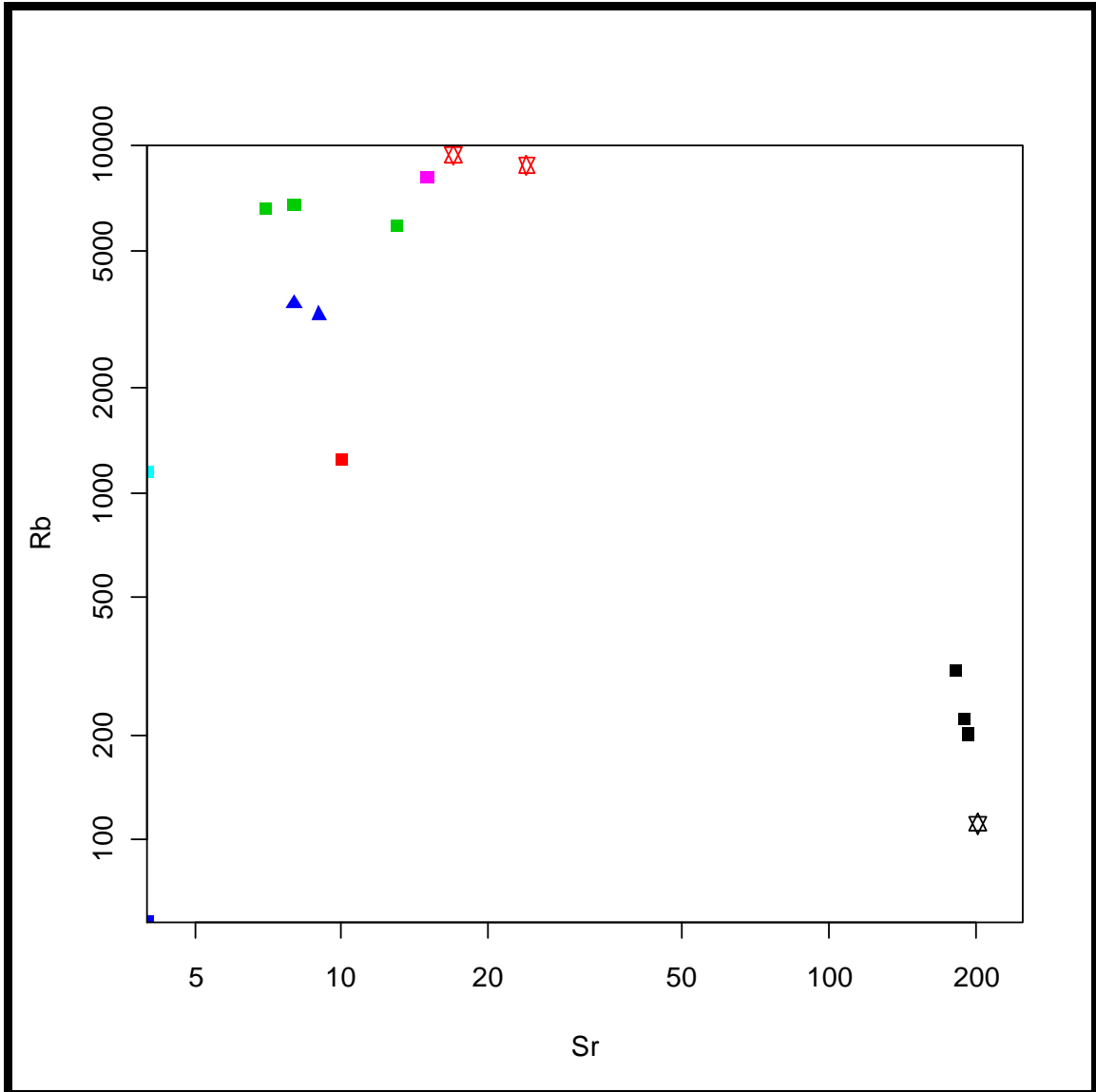
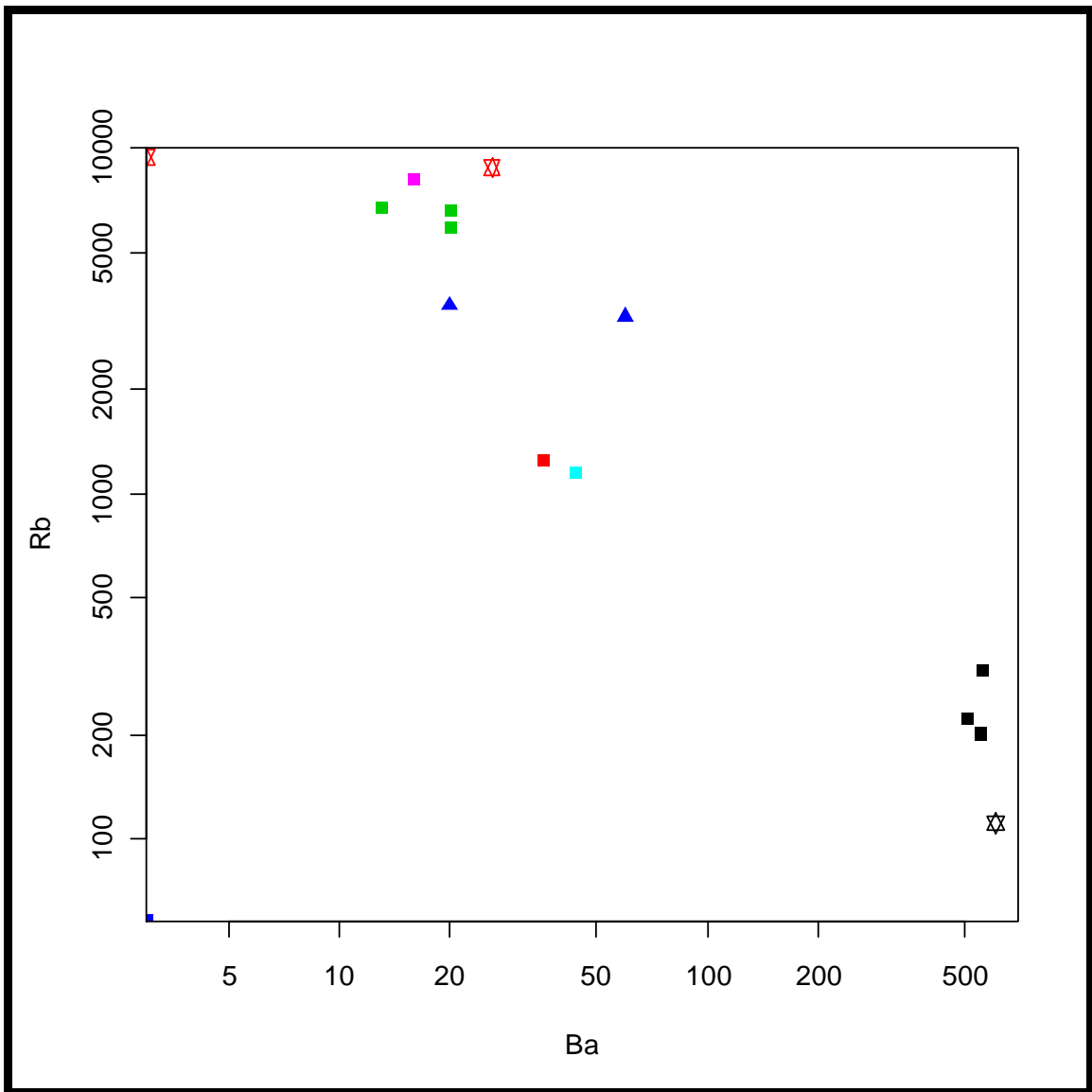


Figure 4.5: Rb versus Sr plot of the samples from the study area (after Černý *et al.*, (1985). (Symbols are same as in Figure 4.2).





**Figure 4.6: Rb versus Ba plots from the study area (after Černý *et al.*, (1985)).** (Symbols are same as in Figure 4.2).

The plot of  $\text{Fe}_2\text{O}_3$  versus MgO (Figure 4.7) and the  $\text{FeO} + \text{MgO}$  ratio (Table 3.4), in muscovite show a linear trend from the core zone towards the granodiorite with a strongly positive correlation coefficient ( $R= 0.9$ ). The value of  $\text{Fe}_2\text{O}_3$  and MgO decreases

with fractionation through the pegmatite except for the border zone (Doka 7) which has the highest value of 22.5 % for  $\text{Fe}_2\text{O}_3$  and MgO of 4.44%, while the  $\text{Al}_2\text{O}_3$  content seems not to have changed significantly, probably due to the peraluminous nature of the host (Table 3.1). The ratio of MgO to FeO and  $\text{Al}_2\text{O}_3$  in the pegmatite is not related to the paragenesis but to the degree of differentiation or contamination of the mica from studied pegmatite.

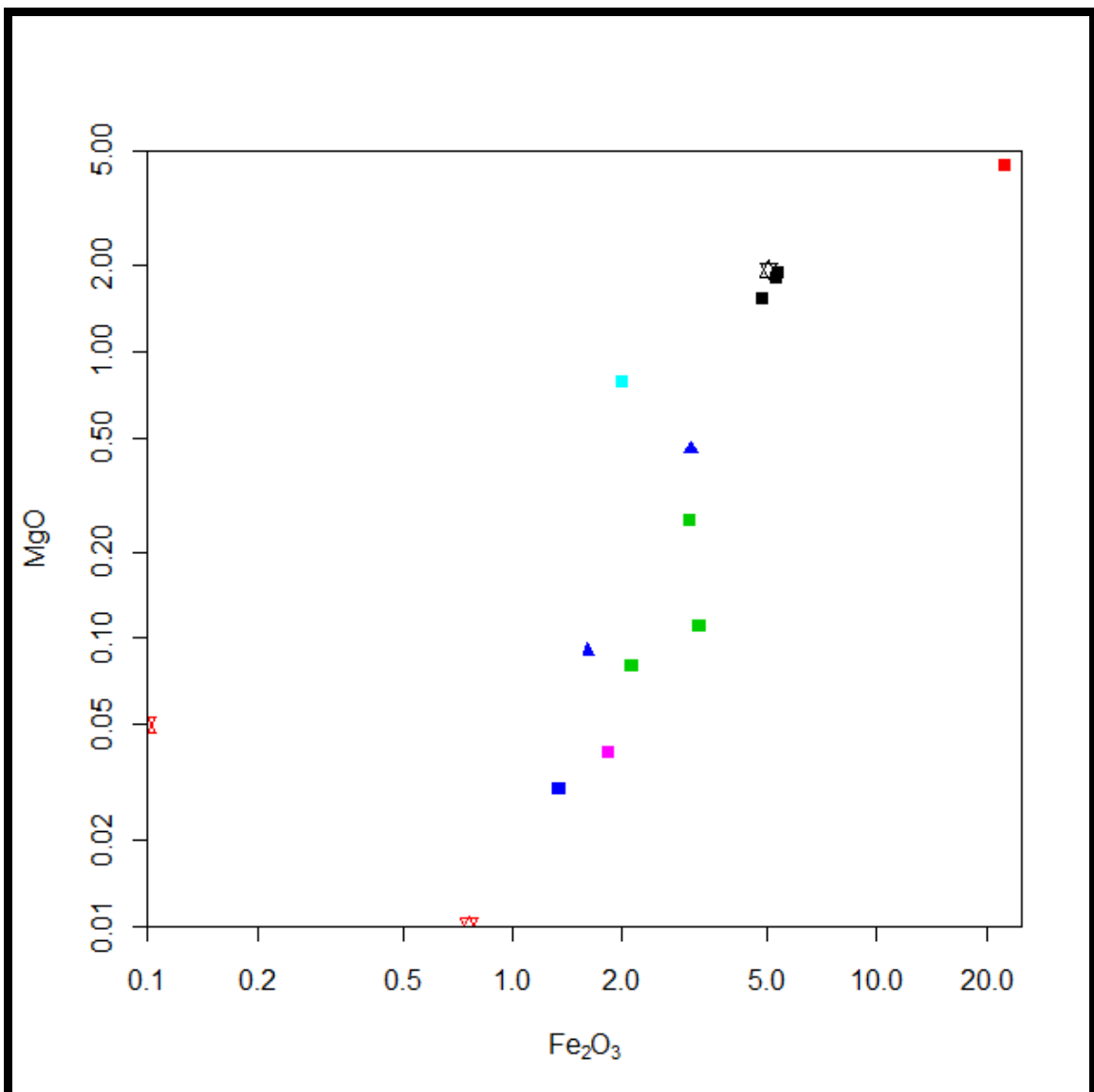
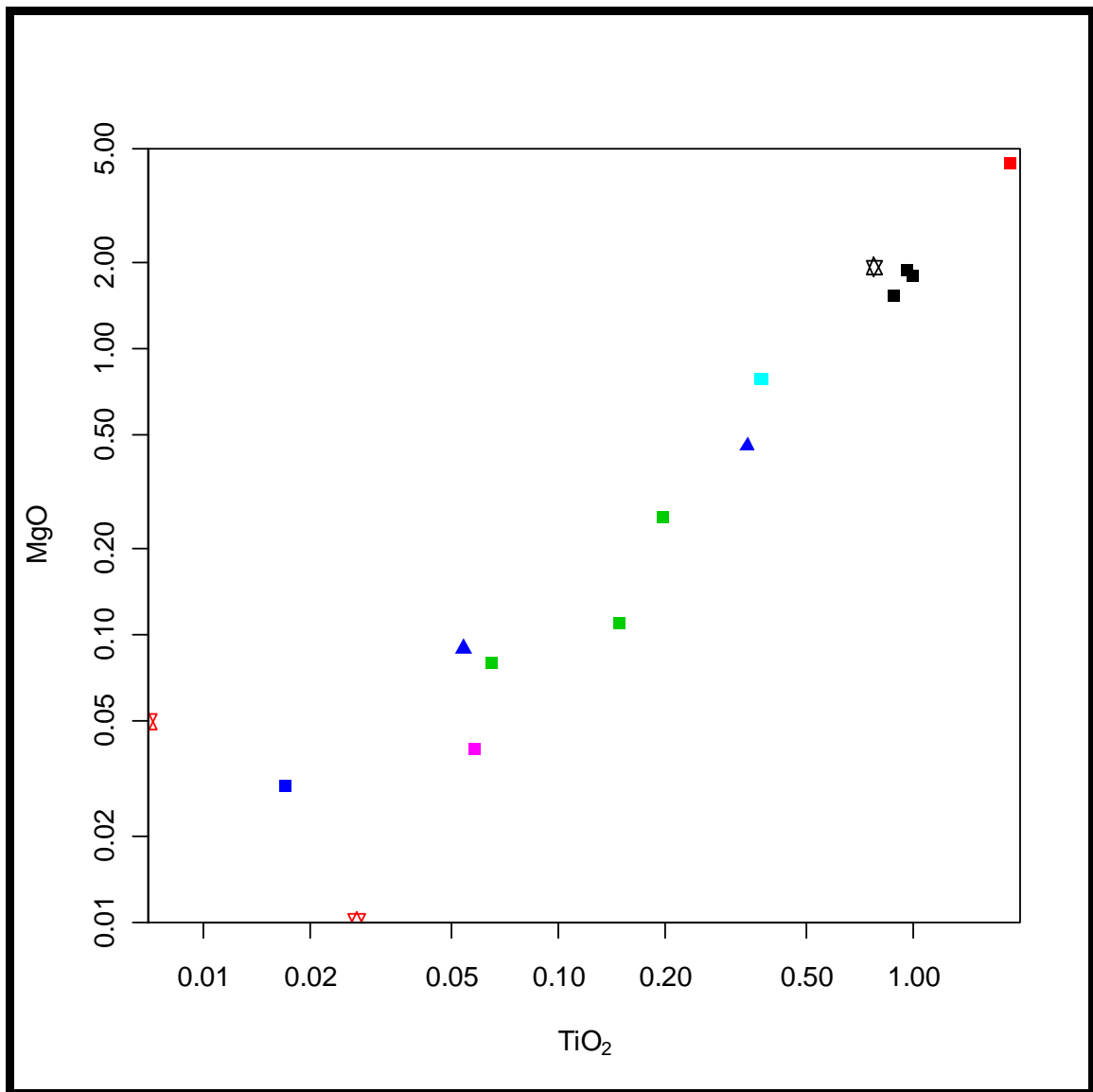


Figure 4.7: Plot of  $\text{Fe}_2\text{O}_3$  versus MgO of granodiorite and muscovite from Angwan-Doka area (after Černý *et al.*, 1985). (Symbols same as in Figure 4.2)

The granodiorite from Angwan Doka with high biotite content recorded higher  $\text{TiO}_2$  and MgO values of 0.77 - 0.96 wt% and 1.54 - 1.93 wt% respectively, compared to the biotite granite from Janta area with 0.037 - 0.039 wt%  $\text{TiO}_2$  and 0.02 - 0.03 wt% MgO. The border zone in the pegmatite dyke from Angwan Doka, which is composed of plagioclase and biotite (Doka 7) has  $\text{TiO}_2$  1.88 wt%, MgO 4.44 wt% while the simple unmineralized pegmatite (Doka10) composed of quartz and biotite has  $\text{TiO}_2$  0.373 wt% and MgO 0.79 wt% values, and the inner zone that does not contain biotite recorded lower values of MgO and  $\text{TiO}_2$ . This trend is observed traversing from the wall zone to the core thus reflecting the differentiation degree of the pegmatite and stabilization of tourmaline with respect to biotite in the inner zone of the pegmatite (Figure 4.8).

The Ti and Mg value in the granodiorite from Angwan-Doka area is higher than that of the biotite granite from Janta area. Some researchers have argued that Ti concentration in granitic melts is as important as boron concentration in controlling the relative stability of biotite and tourmaline. According to Nabelek *et al.*, (1992), Ti may stabilize biotite at the expense of tourmaline. These authors suggested that high  $\text{TiO}_2$  contents in the melt preferentially stabilize biotite instead of tourmaline, even at high B content in the granitic melts.



**Figure 4.8: Bivariate plot of TiO<sub>2</sub> and MgO (after Černý *et al.*, 1985).** Symbols are same as in Figure 4.2.

A strong positive correlation of Li with F in the muscovite from Angwan Doka pegmatite indicates increased Li and F activity as fractionation progressed in the pegmatite (Figure 4.9). The extreme enrichments of Li in the pegmatite from Angwan Doka area is supported by the occurrence of Li-rich minerals, such as elbaite tourmaline, spodumene, amblygonite-montebrazite and lepidolite. Muscovite from the simple unmineralized pegmatite and the aplitic-line rock has the lowest Li concentration, 0.018-0.045 ppm while

Li concentration in the pegmatitic zone is significantly higher ranging from 0.021-0.029 ppm in the intermediate zone, with the highest Li content in the lepidolite zone 1.25-2.82 ppm. The probable substitution of Li in the octahedral sites of micas is reflected in increasing concentration of Li in the pegmatite melt/fluid system. In general, the increasing activity of Li in pegmatitic magma with progressive crystallization resulted in melt saturation with the lithium aluminosilicate component and Li dominant tourmaline elbaite, rossmanite and liddicoatite which are restricted to innermost zone. Fluorine which readily substitutes for the hydroxyl group in tourmaline and topaz also increased from the outer zone to the innermost zone. This trend is consistent with the observation of London and Burt (1982).

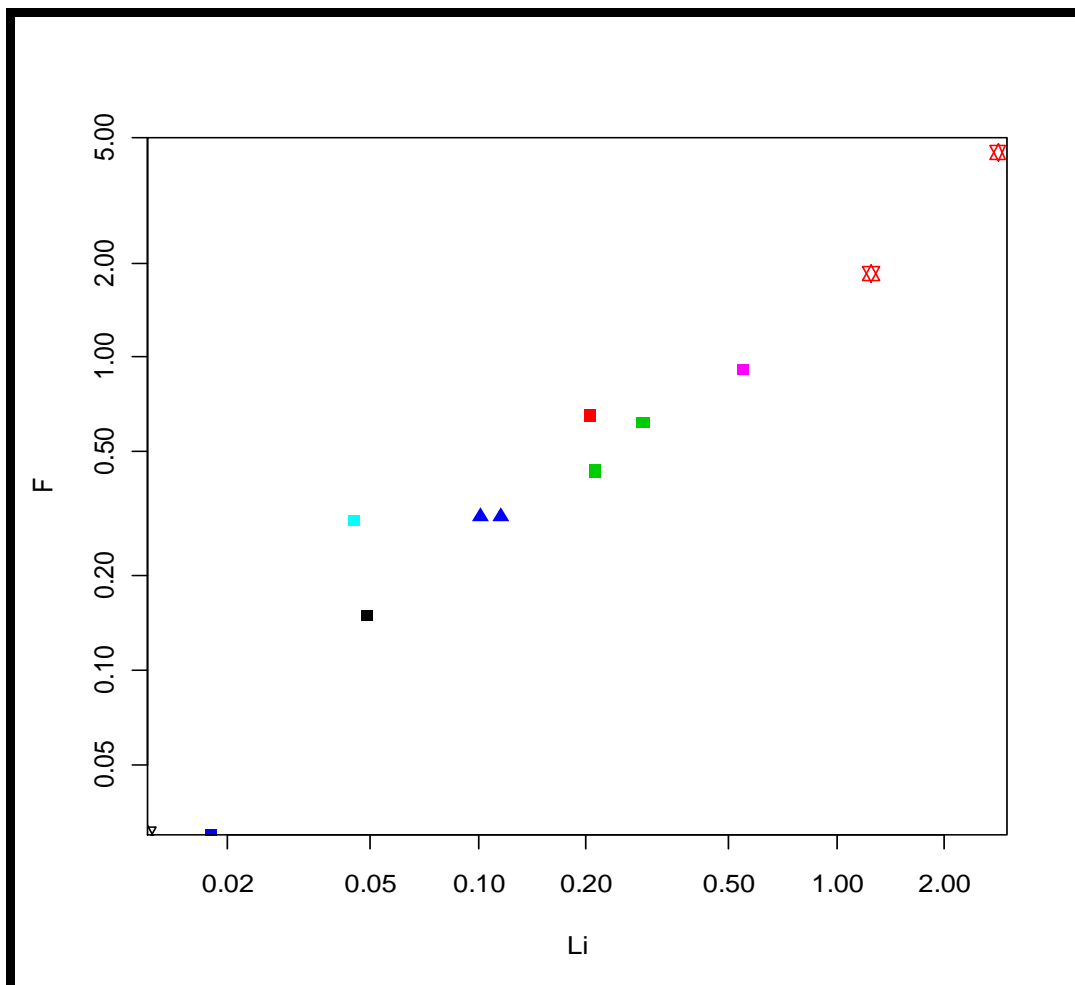


**Figure 4.9: Bivariate plot of Li versus F indicating the gem elbaite potential within the inner most zones of the pegmatite (after Tindle *et al.*, (2005)). Symbols are same as in Figure 4.2.**

A plot of Li and F content in the muscovite from Angwan Doka pegmatite, (Figure 4.10) against other highly differentiated gem tourmaline bearing pegmatite from (1) EBPP of Brazil (2) Li, F, Be, B, P-bearing pegmatite of central Iberian zone, Zamora, Spain (3) Bob Ingersol pegmatite, South Dakota USA reveals that the highly differentiated pegmatite from Angwan Doka is similar to the Bob Ingersol pegmatite from USA and comparable to the Brazilian, Spain and USA tourmaline-bearing pegmatite. Variation trend in Li, B and F content in the muscovite could serve as a measure of the gem tourmaline-bearing potential of the pegmatites.

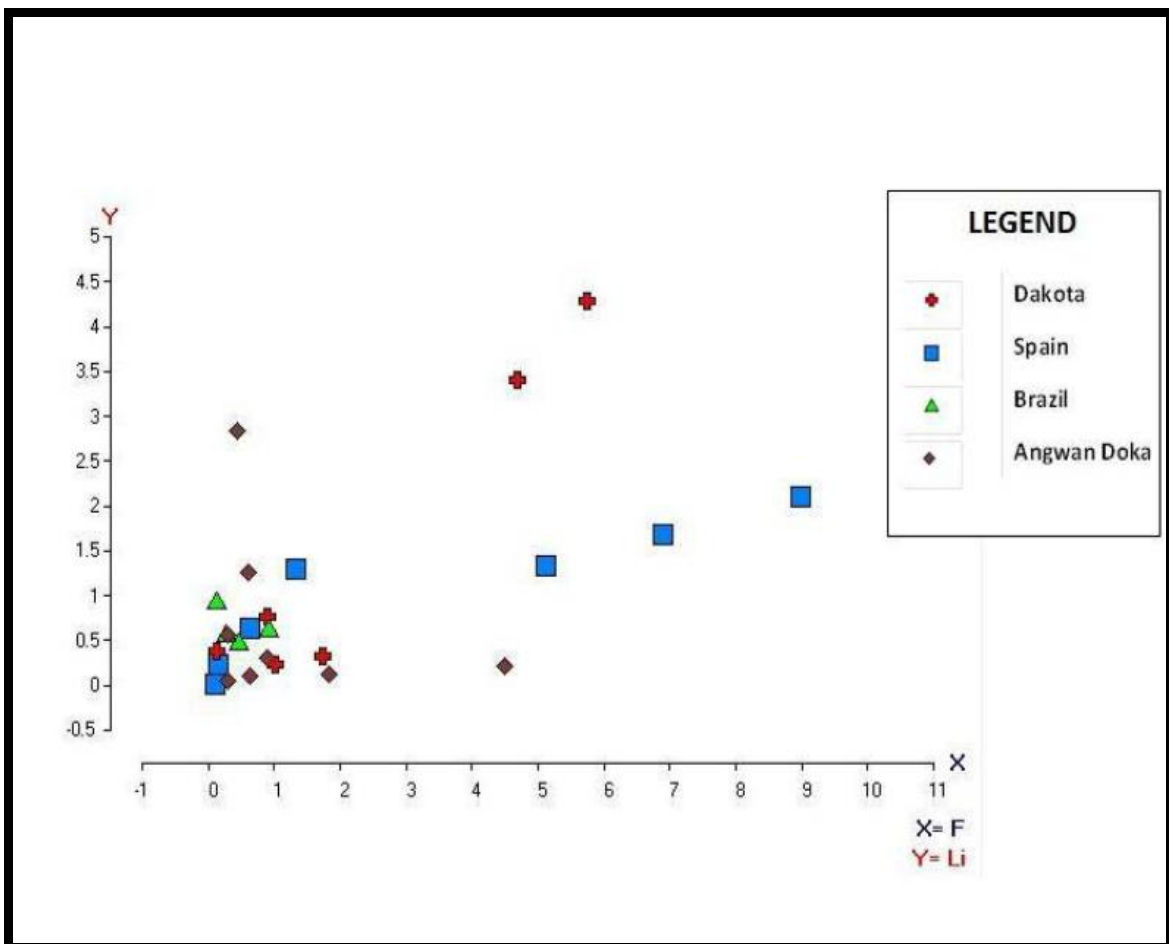


**Figure 4.10: Li and F values of muscovite from gemstone-rich pegmatite from other parts of the world (Jolliff *et al.*, 1986, Viana *et al.*, 2007, Roda *et al.*, 2005)**

## **4.2 RARE EARTH ELEMENTS (REE)**

Knowledge of the behaviour of rare earth elements in aqueous solutions during hydrothermal and metamorphic fluid-rock interaction is critical for the interpretation of REE patterns in hydrothermal minerals. Both REE mobility and immobility have been advocated by many workers (e.g. Menzies *et al.*, 1977, 1979; Muecke *et al.*, 1979; Michard and Albarede, 1986; Brewer and Atkin, 1989; Grauch, 1989; Bau, 1991). The REE distribution pattern of an igneous rock is controlled by the REE chemistry of its source and crystal-melt equilibria which have taken place during its evolution. The REE pattern has important application in identification of the way in which fractionation of individual minerals occurred during magmatic evolution.

In recent years, a rare type of REE fractionation, known as the lanthanide tetrad effect have been advocated. The lanthanide tetrad effect, first described by Peppard *et al.*, (1969) is a separation of rare earth element distribution patterns into four segments. The distribution pattern exhibits distinct sectors (La-Ce-Pr-Nd, Pm-Sm-Eu- Gd, Gd-Tb Dy-Ho, Er-Tm-Yb-Lu) separated at three positions corresponding to (i) between Nd and Pm, (ii) at Gd, and (iii) between Ho and Er. According to Masuda *et al.*, (1987) each tetrad forms a smooth convex or concave pattern, which is further termed the M-type or W-type tetrad effect (Figure 4.11). The M-type pattern has been reported in many granites or pegmatites, which have undergone a high degree of fractional crystallization, hydrothermal alteration and which are associated with economically important

mineralizations (Irber, 1999; Jahn *et al.*, 2001; Zhao *et al.*, 1999). It has been suggested that tetrad effects may be a characteristic indication for the fractional crystallization of REE-rich accessory minerals, such as apatite (Jolliff *et al.*, 1989), garnet and monazite (Zhao and Cooper, 1992) which largely control the solubility of rare earth elements in granitic melts.

Crystals of garnet were recorded in the granodiorite from Angwan-Doka study area. It also occurs in the aplitic rock, forming layers in the aplite and border zones. Garnet is a group of minerals having similar physical and crystalline properties with general chemical formula  $X_3Y_2(SiO_4)_3$ , where X represents divalent ions such as Ca, Mg,  $Fe^{2+}$  (ferrous iron), or Mn, and Y represents trivalent ions such as Al, Fe (ferric iron), Cr or in rare instances, Ti. The REE prefer entering the dodecahedral X-sites by substituting Ca, Mg or Fe in the crystal structure of the mineral. With the LREE being incompatible in garnet, the presence of garnet would have brought about smooth and quite steep tetrad effect from La to Lu. According to London (2008), the presence of garnet in the crystallizing fluid depleted the HREE relative to the LREE especially Yb which is very compatible in garnet. The lack of increase in Th, Y, HREE and the high P content which is typical of S-type granite is characteristic of the granodiorite thus reflecting its inheritance from a P-rich pelitic-greywackeous source.

The crystallization of garnet and phosphate minerals especially apatite, amblygonite, monazite with general chemical formula  $REE(PO_4)$  and xenotime within the pegmatite zones, being the dominant factor controlling the species of REE (Bau, 1991) is of great significance. Monazite is noted to be LREE selective, having preference for the elements La (1.16 Å) to Gd (1.053) whereas xenotime (with simplified formula  $YPO_4$ ) is



HREE selective, incorporating elements between Tb (1.04 Å) and Lu (0.977 Å). Irber (1999) however accepted the discontinuity at Nd, being modeled by monazite fractionation and garnet fractionation to have cause an enhanced Er discontinuity but insisted that it is not necessarily related to fractionation. Bau (1996) is of the opinion that tetrad effect is caused by complexation of the REE with ligands such as H<sub>2</sub>O, CO<sub>2</sub>, F and Li. This led to the suggestion that the tetrad effect of highly evolved peraluminous magmas and granite-related rare metal deposits may result from melt-fluid interaction between magmatic high-temperature hydrothermal systems (Bau, 1996 and 1997; Irber, 1999; Liu and Zhang, 2005) and the transitional nature of volatile-rich evolved magmatic liquids. Tetrad effect is thought to be due to extensive magmatic differentiation, during which there was intense interaction between the residual melts and aqueous hydrothermal fluid, probably rich in F and Cl (Jahn *et al.*, 2001).

Irber (1999) proposed a quantification method which determines the deviation of REE pattern with tetrad effect from a hypothetical tetrad effect-free REE pattern. The method is especially developed for granitic rocks, in which only the first and the third tetrad is used for quantification of the tetrad effect and only samples with values  $TE_{1,3} > 1.10$  that the tetrad effect becomes well visible and considered to show the tetrad effect.

Using the quantification method proposed by Irber (1999) the degree of REE tetrad effect for the granitoids was calculated. The  $TE_1$  and  $TE_3$  represent the tetrad effect of the first and the third group of REE respectively. The granodiorite from the study area show increase in the fractionation level with the  $TE_{1-3}$  gradually increasing from the undifferentiated metaluminous Jamaalu granodiorite (Doka 15) with value of  $TE_{1-3}$  as 1.027 to  $TE_{1-3}$  1.032, 1.056 and 1.051 with increasing distance towards the highly differentiated

Angwan-Doka S-type granodiorite. The fact that the  $TE_{1-3}$  increases from Jamaalu to Angwan-Doka with decrease in the ratios K/Rb, Sr/Eu, Zr/Hf and Eu/Eu\* shows that the tetrad effect is controlled by fractionation but the granodiorite exhibits extremely weak tetrad pattern ( $TE_{1-3} > 1.1$ ) may be due to the fact that it has not undergone intense hydrothermal alterations with F complexation. While the biotite granite from the Janta area, believed to be part of the southernmost high-level, highly discordant Mesozoic anorogenic granite ring-complex known as the Younger Granites, recorded higher  $TE_{1-3}$  value of 1.11 and 1.12 and therefore display tetrad effect as proposed by Irber 1999. From the result of experimental study by Tin (2007), the lanthanide tetrad effect in highly evolved granites are attributable to REE fractionation, the effect being particularly strong in fluorine-bearing volatile-rich granites probably because fluorine and water would reduce the viscosity of the crystallizing magmas and therefore facilitates gravitative settling of crystals or the differences in the ionic radii of the REE in the presence of a complexing ligands may have caused the tetrad effect Kawabe (1992).

The chondrite normalized rare earth element data in the granitoid rocks and muscovite from Angwan Doka area are presented in Table 4.1 while the absolute REE tetrad effect in the granitoid rocks and muscovite from Angwan Doka area and biotite granite from Janta area are presented in Table 4.2. Chondrite normalised REE distribution pattern in the granodiorite and biotite granite form Janta area exhibits the four segments of the lanthanide tetrad effect (Figure 4.11). The REE distribution pattern in muscovite from the different zones of the pegmatite dykes in the granodiorite also displays strongly fractionated REE patterns (Figure 4.12).

**Table 4.1 Chondrite normalized rare earth elements data in the granitoids and muscovite from Angwan Doka pegmatite group**

	Host			Barren	Border Zone	Wall Zone	Intermediate zone	Spodumene zone	Core zone
	ADOKA1	ADOKA5	ADOKA8	ADOKA15	ADOKA7	ADOKA14	ADOKA4	ADOKA6	ADOKA13
<b>LaN</b>	103.55	98.71	67.10	106.77	8.71	5.48	2.58	20.65	15.16
<b>CeN</b>	80.32	75.12	53.96	77.97	5.94	2.97	1.49	8.42	11.76
<b>PrN</b>	65.08	60.49	44.18	60.82	4.26	2.26	1.64	11.15	10.57
<b>NdN</b>	50.50	47.17	36.00	45.33	3.00	1.67	1.17	8.00	7.83
<b>PmN</b>	NA	NA	NA	NA	NA	NA	NA	NA	NA
<b>SmN</b>	31.79	29.23	23.59	27.18	2.56	1.03	0.51	3.59	4.10
<b>EuN</b>	19.18	17.82	15.37	16.60	0.68	0.68	0.68	2.45	2.45
<b>GdN</b>	18.15	17.37	14.29	16.22	1.93	0.77	NA	1.93	1.93
<b>TbN</b>	14.77	12.66	10.55	12.66	2.11	NA	NA	NA	NA
<b>DyN</b>	9.32	8.70	7.76	9.01	2.80	0.62	NA	0.62	1.24
<b>HoN</b>	6.96	5.57	5.57	6.96	2.79	NA	NA	NA	NA
<b>ErN</b>	4.76	4.76	4.29	5.24	2.38	0.48	NA	NA	0.95
<b>TmN</b>	4.32	4.01	3.70	4.94	3.09	NA	NA	NA	NA
<b>YbN</b>	3.83	3.35	2.87	4.31	4.31	0.96	NA	NA	0.96
<b>LuN</b>	3.11	3.11	3.11	3.73	4.04	NA	NA	NA	NA
<b>Eu/Eu*</b>	0.80	0.79	0.84	0.79	0.31	0.76	NA	0.93	0.87
<b>LaN/YbN</b>	27.05	29.49	23.37	24.80	2.02	5.73	NA	NA	15.84
<b>LaN/SmN</b>	3.26	3.38	2.84	3.93	3.40	5.35	5.03	5.75	3.70
<b>CeN/YbN</b>	20.98	22.43	18.80	18.11	1.38	3.10	NA	NA	12.29
<b>CeN/SmN</b>	2.53	2.57	2.29	2.87	2.32	2.90	2.90	2.34	2.87
<b>EuN/YbN</b>	5.01	5.32	5.36	3.85	0.16	0.71	NA	NA	2.56
<b>ΣREE</b>	153.79	144.22	105.94	147.72	13.70	6.35	3.05	20.94	22.47

Note: NA – Not available (limit of detection)

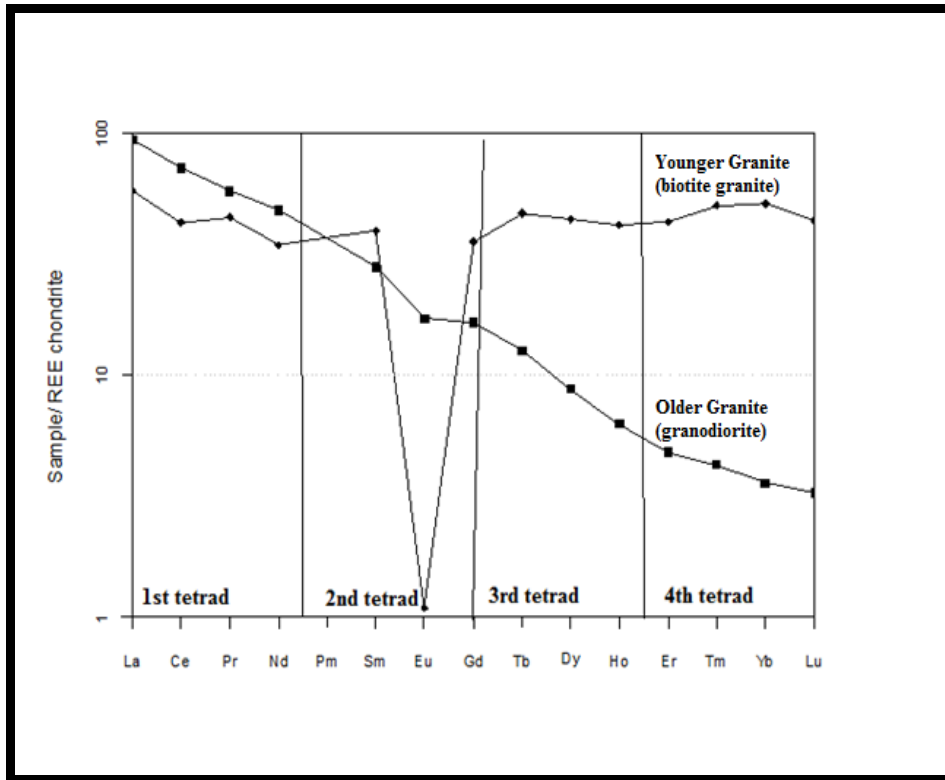


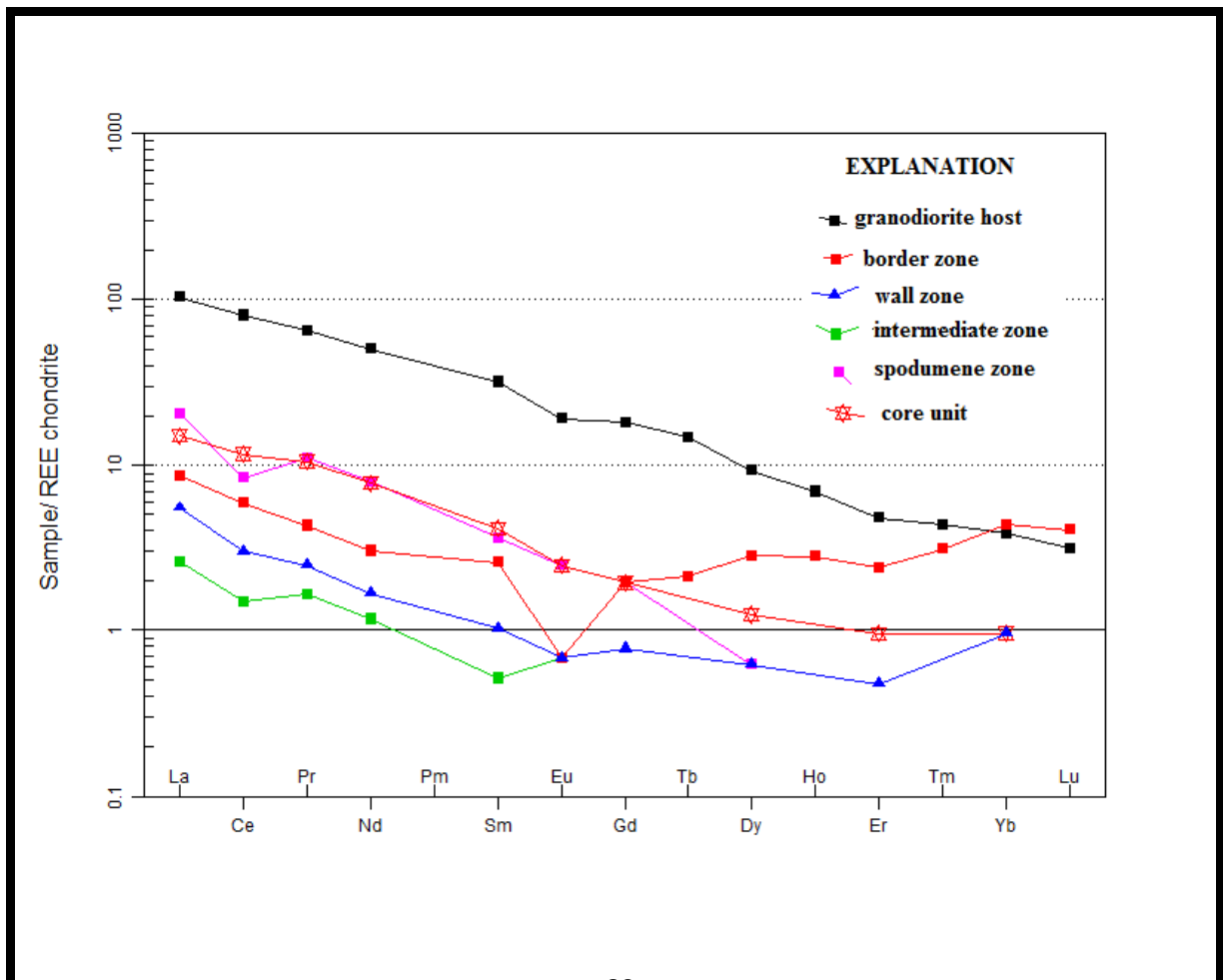
Figure 4.11: Chondrite normalised REE pattern of the granitoids from the study area (showing the four segments of the lanthanide tetrad effect). The biotite granite displays the M-type tetrad effect.

Table 4.2: Absolute values of the REE tetrad effect in the granitoids

	Ce/Cet	Pr/Prt	TE <sub>1</sub>	Tb/Tbt	Dy/Dyt	TE <sub>3</sub>	TE <sub>1-3</sub>
ADOKA1	0.975	1.166	1.066	1.168	0.917	1.035	1.050
ADOKA5	0.964	1.152	1.054	1.111	1.007	1.058	1.056
ADOKA8	0.98	1.146	1.059	1.054	0.960	1.006	1.032
ADOKA15	0.962	1.159	1.056	1.079	0.92	0.996	1.026
ADOKA11	0.798	0.999	0.893	3.717	0.322	1.095	0.989
BAH1	0.872	1.26	1.048	1.291	1.05	1.165	1.105
BAH2	1.021	1.238	1.124	1.25	1.017	1.128	1.126

The average sum of rare earth elements ( $\Sigma$ REE) in muscovite ranges from 13.7 in the border zone (which first crystallized) to 6.35, 3.05 and 20.09 x chondrite in the wall, intermediate and spodumene zone respectively while the core zone/lepidolite unit recorded 22.47. The core zone with  $\Sigma$ REE of 22.47 x chondrite recorded the highest value

because the REE preferentially partition into magmatic liquid relative to the coexisting crystalline assemblage, and thus crystal fractionation resulted in progressive enrichment of those elements in the remaining melt. The simple pegmatite, which was the least fractionated recorded  $\Sigma$ REE of 1.01 while the aplite mark the fractionation of REE-rich mineral such as garnet and apatite with  $\Sigma$ REE of 3.89 x chondrite. The border zone also marked the crystallization of garnet and other phosphates by the high heavy REE concentration relative to the other zones. However, the 1<sup>st</sup> tetrad was distinctly developed in all sample whereas an incomplete or zig-zag pattern developed at the 4<sup>th</sup> tetrad of some samples perhaps due to inadequacy of the analytical data imposed by the analytical method employed (values below detection limit). Only muscovite samples with complete REE was plotted.



**Figure 4.12: REE Chondrite (Boynton 1984) normalised REE patterns of the host granodiorite and muscovite samples from different zones of the pegmatite**

The muscovite samples from the study area possess the tetrad effect similar to the granitic melts. The REE distribution pattern in muscovite further reflects the interaction between melt and coexisting volatile-rich fluid wherein it inherited the REE composition and distribution characteristics of the melt (Bau, 1996; Irber 1999). In line with the view of Zhao *et al.*, (2002) fluid-melt interaction during the late stages of crystallization is the most important factor that controlled the REE fractionation during the evolution of the pegmatite. Trace element data indicate that all of the muscovite from the studied pegmatites show a typical enrichment in LREE inherited from the crust compared to fluid derived from a deep-seated source that are characterised by a strong enrichment in HREE

#### **4.3 NIOBIUM-TANTALUM TIN MINERALIZATION**

Nb, Ta, W and Sn are (rare metals) elements with high charge to ionic radius ratios (HFSE) that do not substitute into common rock forming minerals and thus behave incompatibly during crystallization of silicate melt (Linnen and Cuney, 2005). These elements are concentrated mainly by high degree of fractional crystallization of peraluminous granitic melt enriched in fluxing agent like F, B, P, Li and H<sub>2</sub>O under an increasing alkalinity of the melt, commonly associated with pegmatite of the LCT class (Černý, 1991; London, 2008). The solubility of Nb- and Ta- oxides increases with temperature, increasing alkalinity of the melt and the abundance of fluxing elements in the melt (Linnen, 1998; Linnen and Cuney, 2005). With evolution of a granitic melt, Mn is generally enriched relative to Fe during the fractionation of a pegmatite melt in a closed

system (Černý and Ercit, 1985). The enrichment of Mn in the melt is enhanced by the high activity of fluorine (Černý *et al.*, 1986). Fractional crystallization causes the evolution of columbite–tantalite from ferrocolumbite [ $\text{FeNb}_2\text{O}_6$ ] to manganotantalite [ $\text{MnTa}_2\text{O}_6$ ]. Therefore, columbite should precipitate from the melt earlier than tantalite. From Figure 4.7 to 4.9, muscovite from lepidolite pegmatites are the most impoverished in FeO and MgO while K/Rb versus Rb and Cs shows the trend of evolution in the different zones of the pegmatites. As a consequence of fractional crystallization, Ta/(Ta+Nb) will increase in the melt with fractionation from outer zones to more evolved (London 2008).

As illustrated in the plot of Ta/(Ta + Nb) versus Mn/(Mn + Fe)], (Figure 4.13), the composition of the columbite-tantalite is generally controlled by Fe-Mn substitutions during fractional crystallization, progressing from ferrocolumbite [ $\text{FeNb}_2\text{O}_6$ ] to manganotantalite [ $\text{MnTa}_2\text{O}_6$ ] (Černý *et al.*, 1986). The Nb-Ta content of columbite group mineral can be related to that of micas that coexist with them (Van Lichtenvelde *et al.*, 2008). In Angwan Doka pegmatites, fractionation probably started from Mn-poor ferrocolumbite towards a slightly Mn- and Nb- enriched manganocolumbite and finally to manganotantalite in the more evolved lepidolite zone. According to (Linnen *et al.*, 2005), the solubility of Fe-rich member of the columbite group mineral in a melt is higher than that of Mn-rich mineral, thus the Fe-rich group will be enriched over Mn-rich group but the enrichment of Fe rich group is controlled by the presence of other iron-bearing mineral such as tourmaline and biotite during evolution (London 2008). According to Černý *et al.*, (1985), Ta-dominant species are restricted to the most highly fractionated complex type of rare-element pegmatite.

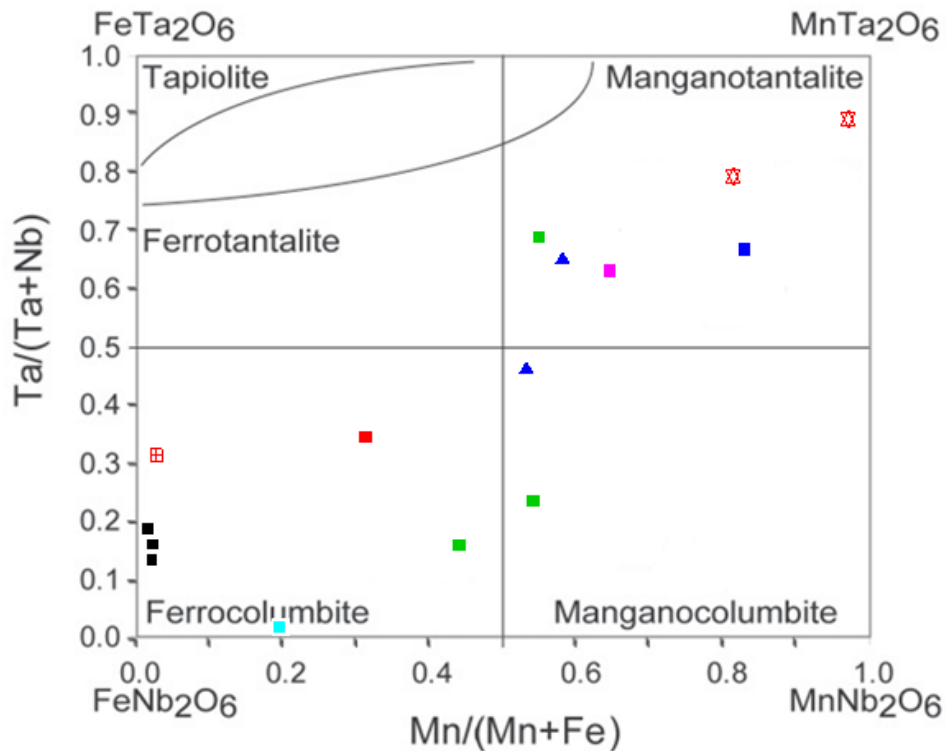


**Figure 4.13: Evolution of the Nb and Ta-oxides in the different pegmatite zones of Angwan Doka pegmatites (after Cerny *et al.*, 1985). Symbols are same as in Figure 4.2.**

Plot of Nb/Nb+Ta against Li also shows very good correlation (Figure 4.14). It should be noted that the Nb-Ta and Sn content increases from the wall zone-intermediate-spodumene pegmatites towards the lepidolite pegmatites with increase in the Li contents. Wolf and London (1993) have reported that high concentration of Li increases the solubility of manganotantalite against manganocolumbite; thus the highest concentration of Ta (352 ppm) was recorded in the lithium most enriched lepidolite zone. The generally low Ta contents in the Angwan Doka pegmatite may be due to the high concentration of phosphate minerals. As lithium was incorporated preferentially in phosphate minerals, Ta enrichment was suppressed due to the low Li concentration (London, 2008; Alfonso, 2003).



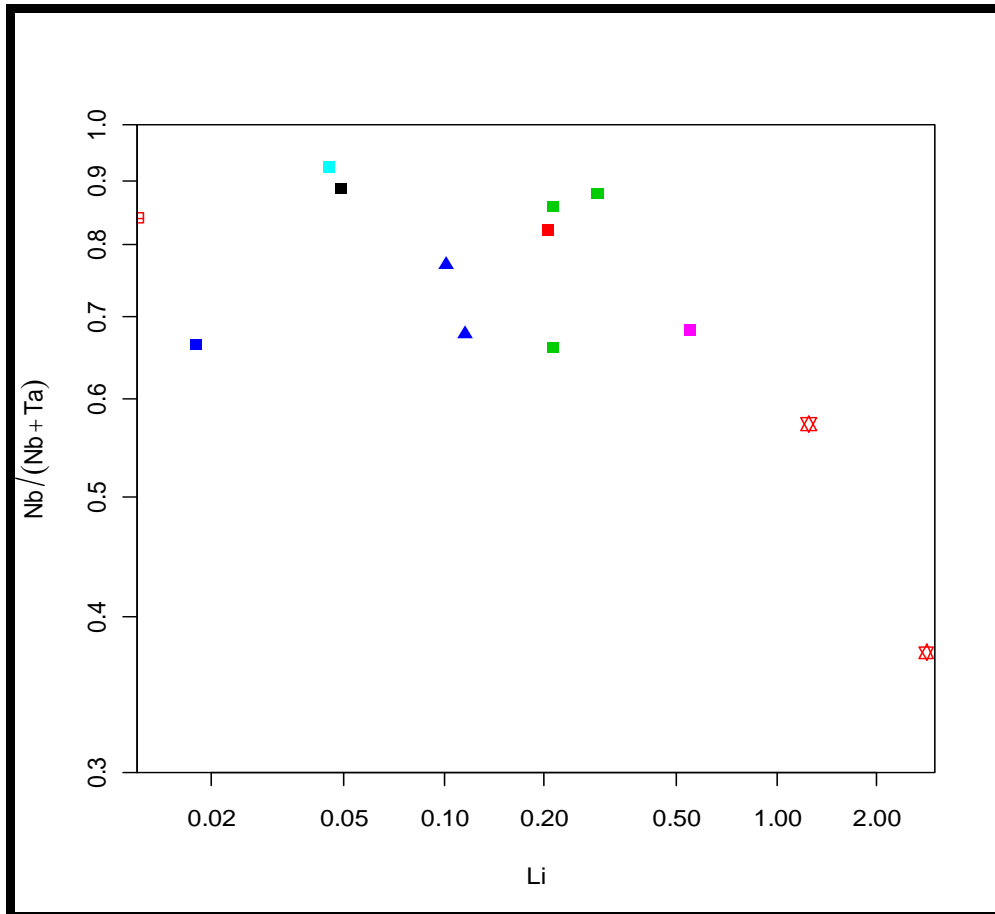
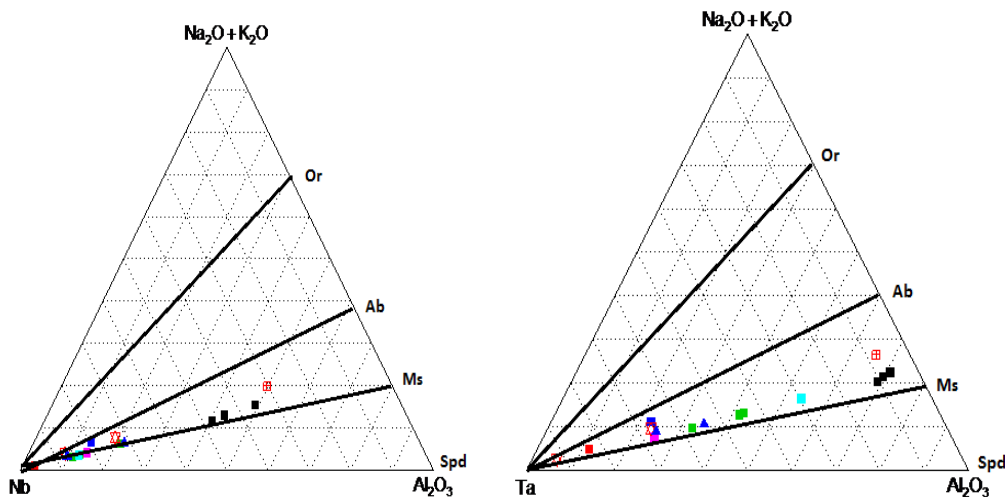


Figure 4.14: Variation plot of Nb/Nb+Ta against Li, in muscovite from pegmatite of the study area (after Anderson, 2013). Symbols are same as in Figure 4.2.

The Nb, Ta and Sn most probably were concentrated in the residual melt during fractionation of the Angwan Doka pegmatite and increased from the granodiorite to the most evolved core zone (Table 3.2). While metasomatic processes appear to have played an important role in the enrichment of Ta, Nb and Sn in the Angwan Doka pegmatites, Nb, Ta enrichment is associated with the albitized border and muscovite-rich replacement zones. The concentration of Nb increased from 90 ppm in the wall zone to 630 ppm in the albitized border zone while 136 ppm Ta is recorded in the albitized border zone, the intermediate zone contain 35 – 58 ppm and increased to 352 ppm in a core zone (Table 3.2). The highest Sn concentration of 886 ppm was recorded in the intermediate zone

(muscovite replacement zones) thus showing that Sn partitioned into the fluid phase that escaped into surrounding zones. The AngwanDoka pegmatite can be considered to be a Sn-bearing pegmatite as the Sn content of 97 through 553 to 886ppm with an average of 510ppm was recorded as compared to the 1350 ppm reported by (Jolliff *et al.*, 1992; Roda *et al.* 1995) which is one of the highest so far reported for muscovite from pegmatites.

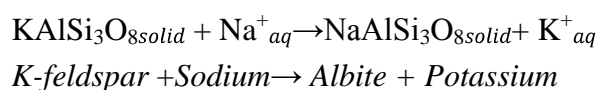
Figure 4.15 is a plot of whole-rock geochemistry of granodiorite and muscovites; it reveals an important association of Nb-Ta and Sn with muscovite- and albite-rich portions of the pegmatite. The lack of correlation of rare-elements with primary K-feldspar and spodumene suggests that metasomatism may have been the dominant process of Nb-, Ta- and Sn-enrichment (Kontak, 2006; Anderson 2013). Both magmatic and metasomatism are, therefore important factor in accumulation of the Nb-Ta- and Sn oxides in AngwanDoka pegmatite.



**Figure 4.15: Ternary plots to demonstrate the association of Ta and Nb enrichments with the albite and muscovite rich parts of the pegmatite (after Kontak, 2006., Anderson,2013). Or = orthoclase, Ab = albite, Ms = muscovite, Kfs = K-feldspar, Spd = spodumene, Ta = tantalum. Symbols are same as in Figure 4.2.**

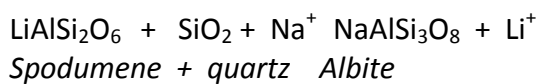
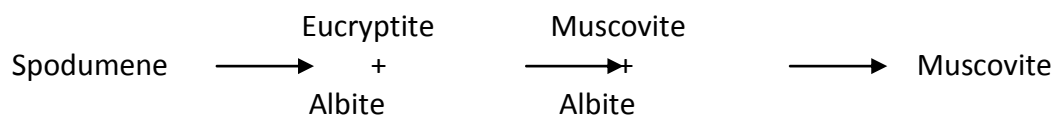
### ***Muscovite-Rich Replacement Zones***

Albitization is a well-known feldspar replacement phenomenon that has been documented in LCT pegmatites from around the world; for example Harding pegmatite, New Mexico, White picacho pegmatite district, Arizona; Moose 11 pegmatite, Canada, Pala district San Diego county, California, USA, the Tanco pegmatite Manitoba Canada. To a large extent, sodic-metasomatism (albitization) has affected the Angwan-Doka pegmatite. According to London and Morgan, (2004); London, (2005) metasomatic reaction involves alkali exchange between Na-rich fluids and K-feldspars due to gradients in chemical potentials and temperature, which results in replacement of early K-feldspar with late pink cleavelandite (platy variety of albite), Anderson (2013). This is illustrated in the following equation.



The K<sup>+</sup> ion released in the above reaction could result in formation of secondary muscovite via hydrolysis reaction due to the low pH of the fluid or muscovite-rich replacement unit composed of fine- to medium-grained muscovite + quartz + albite + perthite observed in the central portions of the pegmatite (the so-called greisenisation) where the late magmatic-metasomatic overprint, and associated sericitisation and muscovitisation in local zones of the pegmatites occurred (Plate XXVI). It is highly likely that the Na-rich fluids reacted with the K- feldspar in the wall zone and spodumene to form albite and micas, as muscovite is a more stable mineral phase in high-F reactions (London, 2008). The process of alteration that affected part of the spodumene-amblygonite zone partially altered it to greenish colour associated with late fracture-fills composed essentially of quartz, different from the fresh and sharply defined spodumene in the spodumene zone. Based on albitization of spodumene and calcic metasomatism of the phosphates, London and Burt

(1982) have noted that metasomatism of the Li- minerals would take place in an alkaline environment. The formation of secondary micas and feldspar in spodumene-montebrazite tourmaline reflects a change from alkaline to relatively acidic postmagmatic fluids, as (K+H)-metasomatism produce greisen-like or sericitic alteration. Generalized alteration (albitization) sequence for spodumene is as shown in the equation below.



London (2008) and Icenhower and London (1995) have proposed that F can accumulate via melting reaction involving biotite and muscovite during anatexis of metapelites. However, the tendency of an LCT pegmatite to contain elevated concentration of F, B, Li, P is a function of their abundance at the source and the nature of reaction (London 1992, 2008) he noted that the concentration of these elements would increase up to saturation level as melt fractionates. Accumulation of F, B, Li and P in magma dramatically changed and increased the composition of the incompatible element in the melt as crystallization progressed. Subsequent crystallization of the pegmatitic zone occurred from a water-rich melt that was saturated with respect to water and volatiles. The saturation of the Angwan-Doka pegmatite with a Li-F-aluminosilicate component is marked, primarily by occurrence of Li-mica and lepidolite in the pegmatite core. In addition, there is a progressive variation from the border zone to the core of the pegmatite involving Fe depletion and Li enrichment. This variation is typical of the general fractionation trend of these elements and in good agreement with observation of London (2008) that

incompatible elements generally increase with evolution, thus resulting in exotic minerals like tourmaline (B,Li), lepidolite (Li), columbite-tantalite (Nb,Ta), beryl (Be) and topaz (F) that are rare in typical granitic melt.

Further, London and Morgan (2004) suggest that the Na-rich metasomatic fluids originate from a late volatile- and sodium-rich melt. London (1986) reported a genetic link between gem tourmaline pocket formation, late-stage boron-rich albitic liquids and adjacent tourmalinization of wall rocks. Webber *et al.*, (1999) also suggested that at the end stages of crystallization, the late stage volatile fluid seeps out into the surrounding and eventually forms replacement minerals. The separated aqueous phase, rich in volatile elements, may form pockets in the lepidolite unit during the last stages of pegmatite crystallization or may seep out along fractures to react with previously crystallized pegmatite or host rocks. Hydrothermal alteration are also widespread in the granodiorite adjacent to the pegmatite as evidence of fluid interaction in the granodiorite is shown by chloritization and sericitization typified by replacement of plagioclase, and fine-grained second-generation muscovites while quartz locally fills fractures in the feldspars.

There is evidence that remobilization of elements during metasomatism (magmatic and/or hydrothermal events) is an important feature of the AngwanDoka pegmatite group (Figure 4.15) and hence the implications for the distribution of economically important Nb-Ta, Sn oxides. Concentration of 211-216 ppm Nb, 352 ppm Ta and 771 ppm Sn were recorded in the lepidolite zone of the pegmatite. The highest values of Nb (630 ppm) and Zn (1260 ppm) occur in the Na-rich border zone where 136 ppm Ta and 573 ppm Sn have been recorded also. In the muscovite-rich replacement zones, concentrations of 113-

262 ppm Nb, 35–68 ppm Ta, 0.21–0.29 wt. % Li, 510–886 ppm Sn, 380–680 ppm Zn, 150–250 ppm of Rb and importantly, 190–712 ppm Cs have been documented.

The Nb-Ta-Sn mineralization is concentrated in the Na-rich (albitized) zone thus suggesting that these elements were mobilized hydrothermally along with Na during metasomatism. Experimental work of (Tin 2007) shows that the potential mechanism for Sn extraction at the final stages of magma crystallization is through alkaline. The intermediate zone which shows characteristic metasomatic and replacement features with elevated Zn and Sn concentration in the secondary muscovite may also reflect the high solubility of these elements in hydrothermal fluids.

The magnitude and complexity (crosscutting) of the pegmatite also suggest multiple extensional events possibly with successive pulses of magma injections. Multiple injections of magma adjacent to previously crystallized pegmatite zones could result in metasomatic alteration of orthoclase to muscovite. These magmatic-metasomatic fluids may have added Nb, Ta, Sn and Zn to the system, and/or remobilized and redeposited the oxides from early generations of columbite-tantalite.

#### **4.4 EVOLUTIONAL TREND AND GEMSTONE MINERALISATION POTENTIAL OF ANGWAN DOKA PEGMATITE**

Tourmaline is a relatively common phase in leucocratic peraluminous granites which starts to crystallize when the aluminum saturation index (ASI) of the magma reaches a value between 1.3 and 1.4 (London 2008). It is also a common constituent of granites and granitic pegmatite. Tourmaline is the largest and most abundant mineralogical host for boron in a variety of geological settings.

Tourmaline is renowned for its spectrum of colours, even within individual crystals and has the appropriate combination of beauty, durability, and rarity to make fine and well sought after gemstones. The tourmaline super group arises from their general chemical formula, currently consisting of 18 species approved by the International Mineralogical Association's Commission on New Minerals, Nomenclature and Classification.

General formula of tourmaline is  $XY_3Z_6[T_6O_{18}][BO_3]_3V_3W$ ,

where  $X = \square$  (vacancy), Na, K, Ca,  $Pb^{2+}$ ,  
 $Y = Li, Mg, Fe^{2+}, Mn^{2+}, Cu^{2+}, Al, V^{3+}, Cr^{3+}, Fe^{3+}, Mn^{3+}, Ti^{4+}$ ,  
 $Z = Mg, Fe^{2+}, Al, V^{3+}, Cr^{3+}, Fe^{3+}$ ,  
 $T = Si, B, Al$ ,  
 $B = B$ ,  
 $V = OH, O$ , and  
 $W = OH, F, O$ .

The Y point is of particular relevance to the tourmalines, as the end-member composition of the Li-bearing gem tourmaline of liddicoatite, rossmanite-elbaite solid solution have the Y site occupied by  $LiAl_2$  e.g. elbaite:  $Na Y (Li_{1.5}Al_{1.5}) Al_6 (Si_6O_{18}) (BO_3)_3 (OH)_3 (OH)$ , in which the Y site is occupied by both Li and Al in a 1:1 ratio.

The transition elements  $Fe^{2+}$ ,  $Fe^{3+}$ ,  $Mn^{2+}$ ,  $Mn^{3+}$ ,  $Ti^{4+}$ ,  $Cu^{2+}$ , and  $V^{3+}$  which act as the most important color-causing agents, or chromophores, in tourmaline occupy the Y and Z site (Hawthorne and Dirlam 2011), and they influence color and color intensity. Much of the chemical complexity of tourmaline has been ascribed to the different sites in the structure and the ease with which several of these sites can incorporate a wide variety of elements.

According to Giller (2003), the end-member ternary plot of X-site occupancy for the Nigerian suite of gemstones shows that the three principal species are the liddicoatite-rossmanite-elbaite solid solution series with a broad diversity of colours. From colourless to near colourless, Pink, red, green to greenish-yellow, reddish to purple and bluish-gray,

while the Y-site chromophoric ternary plot revealed the stone to plot principal in the Mn field.

Magmatic tourmaline appears to be typical of continental collision zones, and seemingly require B-rich source regions (London, 2008; Pesquera *et al.*, 2012). According to London and Manning (1995); London *et al.*, (1996); Wolf and London (1997), if B<sub>2</sub>O<sub>3</sub> is concentrated to a value of ~2 wt% with sufficient Fe and Mg in the melt it would crystallize in tourmaline. It has been noted, however, that tourmaline is unstable in peralkaline, metaluminous and slightly peraluminous melts with an ASI less than 1.2 (Wolf and London 1997; London *et al.*, 1996).

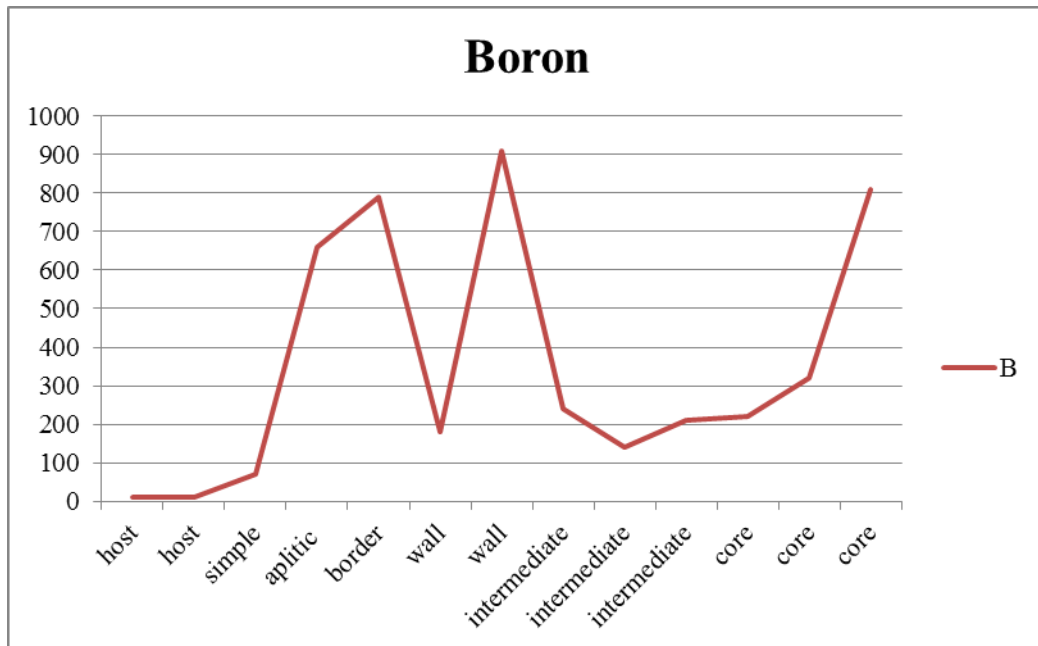
The schorl-enriched wall zone (Doka 7 and 14 respectively) recorded the highest value of boron, 910 ppm. In the schorl-bearing outer border zone and elbaite-mineralized lepidolite unit, boron content of 790 and 810 ppm were recorded respectively. According to Jollif *et al.*, (1986) and Roda *et al.*, (2005), the amount of boron in the different zones of the pegmatite, could serve as indicator of tourmaline enrichment. The absence of tourmaline-bearing pegmatite from Jamaalu area, therefore, could be attributed to the metaluminous nature of the rock as crystallization of tourmaline can only take place in peraluminous granites (London, 2008).

Tourmaline mineralization associated with pegmatite would be found where boron mixes with iron and magnesium from the host rock and upon emplacement (London, 2008). Iron and magnesium diffuse into the pegmatite-forming magma to crystallize tourmaline at the border and wall zones. Tourmaline-rich rocks also form as a result of the metasomatic replacement of Fe and Mg in the rocks by boron-rich hydrothermal fluid. Further, iron (Fe) and magnesium (Mg) play an important role in stabilizing tourmaline in the B-rich melt



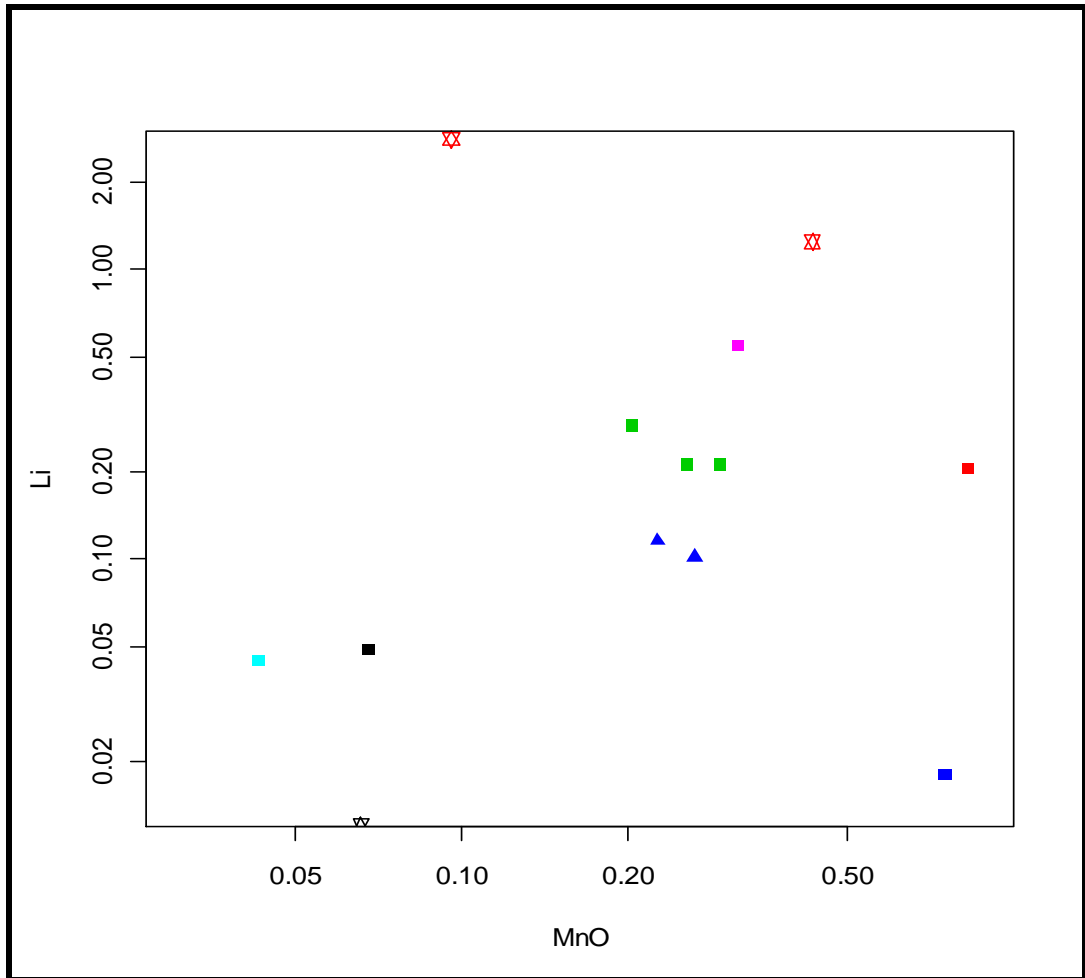
because the normal fractionation trend would have depleted the melt of the required Fe and Mg even before boron reaches sufficient level to stabilize tourmaline.

Figure 4.16 presents a pictorial view of the concentration of boron within the peraluminous Angwan-Doka granodiorite and the pegmatite. The boron concentration in the granodiorite is below detection limit probably because boron preferentially partitions into the fluid phase relative to a granitic melt so that granites do not always reflect the actual magmatic boron (Pesquera *et al*, 2012). The peraluminous residual magma was therefore enriched in B to the point where it started to remove Fe from the enclosing granite wall-rock to produce schorl within the pegmatite-aplite dykes which has a boron content of 660 ppm (Doka 11). Other minerals that broke down to form tourmaline, apart from biotite probably include cordierite, andalusite and garnet. As the content of boron increases with fractionation, it will also reduce with crystallization of tourmaline in an episodic manner whenever B is exhausted (Figure 4.16). The breakdown of these minerals (biotite, cordierite and garnet) in granite liberated Fe and subsequently led to formation of schorl tourmaline in a leucocratic zone adjacent to the pegmatite-aplite dykes or pods. The earlier formed schorl accessory phase in the outer zones indicates the high Fe, Mg, Al value of the fluid. With crystallization of tourmaline phases towards the inner zones, the value of Fe, Mg, Al decreases (Figures 4.7 and 4.8). The simple pegmatite which contains no tourmaline, Doka 10 has Li value of 0.04 % while Doka 11 from the aplitic zone that contains schorl but no elbaite also records very low values (0.018%) of Li despite the high value of boron.



**Figure 4.16: Variation in the boron content within the granodiorite and pegmatite from the study area.**

At the Angwan-Doka area, crystallization of coloured tourmaline (Plate XXIV) was recorded when Li- Mn- F-rich species became stable towards the lepidolite unit of the pegmatite due to fractionation and stabilization of Li, F and Mn (Figure 4. 17), the highest Li and F contents were recorded in the gem-producing lepidolite unit (1.25 and 1.85 wt %; 2.82 and 4.5wt % in Doka 12 and Doka 13 respectively). In addition to having the highest concentration of lepidolite and spodumene, this unit also host moderate quantity of topaz, beryl and other fluorine-bearing mineral together with the gem tourmaline in miarolitic caities. The Angwan-Doka gem tourmaline is generally deep greenish or pinkish-red with green cap (Plate XXIV) indicating late stage Fe enrichment within the core.



**Figure 4.17: Bivariate plot of MnO and Li (after Jollif *et al.*, 1986; Tindle *et al.*, 2006)** Symbols are same as in Figure 4.2.

Due to the decrease in the content of P and Fe-Mg-Mn during crystallization of earlier formed phosphate mineral in the border - intermediate zones and the Fe-schorl tourmaline formation in the wall zone, there was a hiatus between the black schorl tourmaline and the subsequent crystallization of Li-dominant tourmaline in the lepidolite unit. The system ran out of mafic component that would be required for ordinary tourmaline to crystallize in the intermediate zone (Doka 2, 3, 4) which contains moderate values of Li, B and F. It follows, therefore, that fractionation must occur to raise the values

of Li and B needed to crystallize the important Li-dominant gem-tourmaline in inner core zone.

Tourmaline nucleated and grew from a melt oversaturated in B, thus resulting in skeletal crystals (Plate XI). Crystallization of skeletal crystals of tourmaline and schorl in the outer portions of the dykes probably depleted the magma in boron and raised the solidus temperature of the pegmatite forming magma. The low content of Li in the fluid at this point most probably prevented gem elbaite from forming. There was no further crystallization of tourmaline in the phosphate-rich intermediate to spodumene unit owing to the fact that abundance of phosphate is inversely proportional to that of tourmaline or low concentration of B, Fe and MgO within this unit (Alfoso and Melgarejo, 2000). Phosphate generally partitions into the melt until the intermediate levels of differentiation is attained in the pegmatite.

Li- Mn- F-rich species became stable towards the lepidolite unit due to fractionation and stabilization of Li and Mn and thus crystallization of elbaite-liddicoatite (the pink coloured varieties of tourmaline) in the core zone. This sequence of event is consistent with the observation of Černý, (1982); Jollif, (1987); London, (1999); Viana *et al.*, (2007); Roda *et al.*, (2005) and Simmon (2007) on tourmaline-bearing pegmatite in other part of the world.

The highest Li and F contents were recorded in the gem-elbaite producing lepidolite-albite zone (1.25 and 1.85 wt. %; 2.82 and 4.5wt. % in Doka 12 and Doka 13 respectively). In addition to having the highest concentration of lepidolite, this zone also host moderate quantity of topaz and other fluorine-bearing mineral. London (2008), Simmon (2007) and Viana *et al* (2007) have championed the use of Li and F signatures as a

measure of the gem producing capability of pegmatite. The elevated Li content is manifested by the presence of extremely Li-rich mineral phase, such as spodumene in the pegmatite from Angwan Doka area. In the normal sequence of events Li and Ca are decoupled during fractionation of pegmatite because Ca enters minerals in early-crystallizing phase at the border- to wall-zone assemblages whereas Li is concentrated in relatively late-crystallizing phases such as Li-aluminosilicates (spodumene or petalite) and lepidolite (Černý 1991). Apart from elbaite forming in the pegmatite during the fractionation process, the content of Ca in lepidolite zone reflects presence of liddicoatite also. The evolutionary trend of the Angwan-Doka pegmatite group area is quite similar to the evolution of Li-rich pegmatites of the Little Three Pegmatite, California and Bob Ingersoll pegmatite Black hill south Dakota USA as described by Jollif *et al* (1986) and London (2008). The increase of Li activity in the pegmatite has been recorded by tourmaline of the series schorl-elbaite and mica of the series muscovite-Li mica-lepidolite. The saturation of the pegmatite melt with a Li-F-aluminosilicate component is marked by a decrease followed by an abrupt change to a trend of increasing contents of Li and F, with primary occurrence of intermediate-Li mica and lepidolite in the pegmatite core. In addition, there is a general variation from the border zone to the core of the pegmatite involving Fe depletion and Li enrichment. Such variation is in accordance with the general fractionation behaviour of these elements in magmatic systems and is in good agreement with previous studies of tourmaline in pegmatitic system.

The variety of beryl encountered in LCT pegmatites is related to the degree of geochemical fractionation of the pegmatite. Common green beryl typically occurs in the least fractionated pegmatites and along the wall margin while aquamarine, heliodor and

morganite typically occur in pockets in more fractionated rare element enriched pegmatites. Morganite and goshenite are generally restricted to the late stage highly fractionated unit in LCT pegmatite (Černý, 1992).

Beryllium value shows somewhat episodal increase from the early formed outer zones towards the inner zones. Typically, the value increased from 18 ppm in the simple pegmatite to 125 ppm in Na-bearing plagioclase rich aplitic zone and later crystallized into light green coloured crystals in the wall zone where Be is about 20 ppm. Be increased from 20 to 24 ppm in the intermediate zone with no records of Be-mineral until the value increased from 27 to 41 ppm in the core where it crystallized as clear to light pink beryl probably due to the late stage increase in MnO within the lepidolite system. The crystallization of beryl in the wall zone and lately in the albite lepidolite core phases suggest that beryl have formed from a single precipitation event due to repetitive saturation of Be in the melt during the pegmatite fractionation. Evensen and London (2002) explained the interruption of Be in the absence or presence of Ca-plagioclase and muscovite based on the compatibility of these minerals and the buildup of fluxes associated with change in temperature. The generally low level of Be in the Angwan Doka pegmatite group can be explained by the incompatibility of Be in alumino-silicate melt due to the size and charge of Be (Evenson and London 2002). In LCT pegmatite with tourmaline, rose quartz, tryphillite, spodumene and lepidolite, morganite, goshenite and topaz are found in the more complex pegmatites that have albite replacement bodies, more Li mineralization and late stage pockets containing coloured tourmaline e.g. Cruzeiro and the Minas Gerais region, Brazil (London, 2005; Viana *et al.*, 2007).

The value of Cu from the granodiorite ranges from 20 – 30 ppm in Angwan Doka-Jamaalu area where Cu-bearing blue variety tourmaline has been recorded, as indicated by the mine manager (Yusuf) in a personal communication. These results support the observation of Cerny (1991) and London, (1990) that the rare-metals are related to highly differentiated granitic magmas and represent strongly fractionated residual melts rich in silica, alumina, alkali and lithophile elements, water and other volatiles.

Field evidence and petrography indicate that the pegmatite differentiated from the Older Granites. From the broad major, minor and trace element chemistry of the pegmatite, crystallization was largely segmented and progressed inwards towards the core. As crystallization proceeded, the residual melt accumulated in the center of the dyke and became progressively enriched in volatiles (Li, F, B and P) which exsolved to form centrally located primary pockets (see Simmons, 2007 and London, 2008). Two factors are critical in this process. First, the primary melt must initially contain sufficient volatiles so that late-stage exsolution can occur. Second, the pressure regime must not be too high (< 3 kb), as exsolution is inversely proportional to pressure. Simmons *et al.*, (2003) have noted that pockets are most abundant in shallow-level pegmatites and are virtually absent in pegmatites formed under high-pressure conditions. Geochemically the pegmatite from the study area range from barren through Be, Ta, Nb, Sn-bearing to Li, Cs, B, F, K and Rb-rich class. The Angwan Doka pegmatite group can be considered to be shallow level pegmatite thereby yielding miarolitic cavities that contain gem tourmaline, beryl and topaz.

## CHAPTER FIVE

### DISCUSSION

Based on field evidences and geochemical signatures of the host rocks and muscovite from the different zones of the pegmatitic dykes, the area of study is underlain by two genetically different suites of granitoids. The first is related to the consolidation of I-S-type granitoid, composed of granodiorite in Jamalulu to Angwan Doka area which host tourmaline in dykes and pods. The second is A-type granite that occurs to the south of the study area and host gem quality topaz-beryl. These suites of rock differ significantly in their chemistry with respect to their major, minor and trace elements content.

The Angwan Doka granodiorite is peraluminous ( $A/CNK > 1.1$ ) with high content of  $SiO_2$ ,  $K_2O/Na_2O$  ratio, normative corundum, high ratio of  $FeOt/MnO$ , presence of cordierite and tourmaline thus reflecting characteristics of S-type granitoids whereas the



granodiorite in Jamaalu has higher Na<sub>2</sub>O and K<sub>2</sub>O content, presence of hornblende, normative low A/CNK ratio (<1.1) and lower FeO<sub>t</sub>/MnO ratio indicating metaluminous I-type granite affinity and hence involvement of igneous sources in their genesis (Chappell and White, 1992). Figure 3.2 shows that the most distinctive chemical compositional feature resulting from fractionation of felsic I and S type melts is the increase in SiO<sub>2</sub> while P decreases in I type but increase in S type melts (Chappell and White 2001). Discrimination diagram after Batchelar and Bowden (1985) based on field setting and geochemical characteristics of these rocks indicates a pre-plate environment for the granodiorite from Jamaalu whereas in Angwan-Doka, it is mantle fractionates (Figure 3.5).

Geochemical and petrological studies suggest that the Jamaalu and Angwan Doka granodiorite are genetically related. However, the granodiorite in Jamaalu area appears to have some input from igneous derived source whereas in the Angwan-Doka area, the rock had been derived from sedimentary source. It is highly likely that the granodioritic rock in the two areas was produced during the same thermal event and, therefore, the sequence of hornblende-biotite granodiorite and biotite-muscovite ± cordierite granodiorite observed. Diaz-Alvarado *et al.*, (2011), however, was of the opinion that this mineral paragenesis could be a result of reactive bulk assimilation between country rock and biotite granodiorite to form cordierite. The source materials could also be mantle-derived melts during dipping period (subduction) of the crust mixed with crustal anatexic melts which formed a hybrid magma that fractionated into S-type or by the contamination of peraluminous melt prior to emplacement by a metamorphic country rock (see Shearer and Robinson 1988).

Chappell and White (2001) suggested the I-type granites are derived from deeper levels than S-type, from material produced by earlier underplating of the crust and the two types of granite come from source rocks of fundamentally different origin, one formed by

deposition on the crust, the other by accretion beneath the crust, so that there is S-type Sedimentary or Supracrustal and I-type-Igneous or Infracrustal. Petrographic studies indicate that the main constituents, especially the alkali and plagioclase feldspars in the granodiorite are partially altered to sericite while inclusions of muscovite and quartz within orthoclase and plagioclase are also seen in few thin sections. The overgrowth and cross-cutting relationship within plagioclase and formation of sericite in the granitic rocks are closely related to fracture system such as fault and joint considered to have formed by very simple hydrothermal alteration occurring along the fractured zones in the granitic rocks. Shear zone with ductile and brittle deformation that is mainly restricted to the Angwan Doka-Jammalu area and the adjoining schist is common. In addition, undulose extinction of quartz, bending within the plagioclase crystals and intensive fracturing of garnets in Angwan Doka- Jamaalu area indicate regional deformation and an overprinting of the regional stress while foliation could be a result of post-emplacement deformation or by late- to post-magmatic shear zones.

The marked decrease in Sr and increase in Rb towards the more evolved granodiorites of Angwan-Doka area is most probably due to substitution of Rb for K in the feldspar and biotite as fractionation progressed. The granodiorite in Angwan Doka is more fractionated with a decrease in K/Rb ratio ranging from 55-79, REE  $[(Ce/Yb)_N = 20.84-22.43]$ ,  $\Sigma REE = 153$  and minor negative Eu anomalies  $[EuN/Eu^* = 0.8-0.84]$  compared to the Jamaalu granodiorite which is less fractionated with K/Rb 216, REE  $[(Ce/Yb)_N = 18.11]$  and stronger negative Eu anomalies  $[EuN/Eu^* = 0.79]$  indicate fractionation of feldspars. There are no systematic variations in boron content in the granodiorite from Angwan Doka and Jamaalu areas as the boron content is generally below detection limit of the analytical method employed in both rocks. The presence of an inner biotite + tourmaline aureole closer to

the pegmatite could also indicate that Rb-, Cs-, Al-, B-, Li-, and F-rich fluids migrated from the pegmatite into the host-rock at the late stages of crystallization. During this event, whole-rock Rb contents increased from 111 ppm in rock from Jamaalu (Doka 15) to 202-308 ppm in the rock adjacent to the pegmatite (Doka 8,1, and 5) in Angwan Doka area. The high Cs content in the granodiorite do not support derivation of the magmas from a source that had experienced an episode of melting previously, because the highly incompatible Cs would have been lost during the process (e.g. [London, 1995](#)).

Li and F contents show good correlation with some major oxide, for example  $\text{Fe}_2\text{O}_3$ ,  $\text{Al}_2\text{O}_3$ , MgO. Significant changes in Li and F concentration are worthy of note. Some kilometers away from the pegmatite aureole for example, in sample Doka 15 from Jamaalu, Li is 0.012 while F is 0.03 whereas concentration of these elements is considerably elevated in sample Doka1, Li = 0.049 and F = 0.15 thus indicating that abundance of Li is related to the amounts of muscovite in the samples. The strong correlation between Li and F further suggests that the two elements increased with fractionation within the granodiorite. The sharp contact between pegmatite and host also indicate that the granite was completely cold before pegmatite intrusion and consequently there was restricted fluid movement into the host rock while hot pegmatite fluid assimilated and digested the host rock.

Tourmaline occurs as accessory mineral but sometimes it is completely absent in the biotite-rich granodiorite in Angwan Doka area. According to Pesquera *et al.*, (2012), this trend is suggestive of an antipathetic character of tourmaline in the rock. These authors have noted that the granites in which tourmaline occurs as accessory minerals are

generally saturated in quartz and albite, so the SiO<sub>2</sub> activity is fixed while the Na and Ca activity is sufficiently high to promote tourmaline crystallization.

Longfellow (2011) and Candelia (1997) have noted that crystallization at various undercoolings is responsible for the diversity of textures in shallow granitic plutons associated with mineralization. London (2008) attributed textural development in miarolitic pegmatites to crystallization at high undercoolings. Undercooling in these shallow granitic systems is related to thermal effects associated with cooling by conduction and evolution of a hydrous vapor phase. Swanson (2010) attributed the presence of skeletal crystals of quartz and feldspar in pegmatites to mid-crustal emplacement. It has been proven that removal of a fluxing component such as boron or fluorine from the melt by a crystallizing phase can initiate rapid crystallization since the melt is no longer fluxed e.g. crystallization of tourmaline or fluorine-bearing phase can result suddenly in under-cooled melt. This is seen by comb structures and tapered crystals in numerous pegmatites (Černý and Ercit, 2005; London, 2005 and Simmon, 2007).

The variable textures of the granodiorite and pegmatite, in particular the occurrence of skeletal crystals of tourmaline (Plate XI) and graphic intergrowths within the border and wall zone at Angwan-Doka are evidence of undercooled crystallization. Rapid crystallization of the residual melt occurred upon emplacement, thereby producing textures like the graphic intergrowth of quartz and tourmaline in the wall zone (Plate XVII). The graphic texture is known to form from melts that experienced supersaturation in quartzofeldspathic components, usually as a result of rapid cooling, in the endocontact (London, 2005). London *et al.*, (2002) concluded that the rapid growth of tourmaline and quartz would have left a residual melt or fluid thoroughly depleted in Fe and Mg. Černý

(2000) described this process as a “chemical quench”, which depletes the remaining melt in boron and reduces the solubility of water, thereby raising the solidus. This may explain the depleted concentration of boron at the intermediate zones and the absence of tourmaline.

The Angwan Doka pegmatite dykes are closely associated with the Older Granites (S-Type granite) which originated from melting reaction involving mica that impacted the Li, Rb, and Cs to incipient melt. There is an observable change in the chemistry and mineralogy of the pegmatite which differentiated upwards from simple pegmatite in the granodiorite as one moves into zoned albitized body with muscovite and tourmaline towards the granodiorite and the schist. This is consistent with observations of Černý (1992), Stewart (1978) and London (2008) that the most differentiated pegmatite with high Li content form at the cupola farthest way from its source granite. The B, Li and the LILE are similarly concentrated in coarse grained muscovite from the pegmatite dykes, thus indicating inheritance of the trace elements composition from their host that originated from metasedimentary sources due to the trace elements redistribution during devolatilization processes. This view is corroborated by Simmon *et al.*, (1995) who reported that chemical similarities between the host rocks and the pegmatite could signify derivation (insitu) of the pegmatite from their host. London (2008) was of the opinion also that the intrusive pegmatite could interact very extensively with their host, either by assimilation or fluid infiltration such that they acquired the chemical attributes of the host rocks. The composition of the pegmatite-forming minerals suggests that the residual melt became progressively enriched in Cs and Li until the crystallization of the inner-most zone was completed.

The border zone (Doka 7) and part of the wall zone recorded comparatively higher values of  $\text{FeO}_{(t)}$ , MgO, TiO and MnO than the other zones. The relative enrichment of these oxides can be attributed to the enclosing wall rock. Further, the trace element characteristics suggest that pegmatite-forming melt was contaminated by the host rocks through a process of leaching and assimilation while infiltration of fluid from the pegmatite to the host is very minimal and almost negligible.

Based on major and trace element geochemistry, the trend between the granite to the simple pegmatite, wall zone, intermediate zone, spodumene zone and the core zone is very obvious with the granite and simple pegmatite being more primitive and less evolved whereas the spodumene to the core zone are highly evolved and consistent with magmatic evolution. The element fractionation trend clearly marked by systematic increase in Li, F, Rb, Cs from the wall-rock towards the core coupled with alteration of feldspars to clay minerals suggest that crystallization started from outer to inner zones and in a closed system. If crystallization did not occur in a closed system, there would have been no progressive concentration of Li and F from the wall rock contact inward and there would have been no alteration from late stage residual and this phenomenon correlates with the sequence of zoning established by Čerňý (1991) for pegmatitic fields and related granites. Petrographic study of the tourmaline revealed no oscillatory zoning which is characteristic of open systems, where there had been a mixing from different chemical sources. Plagioclase and biotite appear in the crystallization sequence earlier than K-feldspar while tourmaline seems to have crystallized later than the mica, but local occurrence of tourmaline as inclusions in muscovite (Plates VIII and IX) suggests that both minerals may have started crystallizing at the same time or even before the muscovite.

A blue variety (popularly called Paraiba tourmaline) formed by substitution of Mg, Al, Li, and or  $\text{Fe}^{2+}$  by Cu and Mn on the Y-site has also been encountered and reported within a pocket (Doka 13) in the study area (Y. Yusuf, pers. com.). The progressive decrease in biotite and relative increase in percentage of muscovite in the granodiorite as well as tourmaline from border towards the core of the pegmatite dykes may be used as guide for further exploration of tourmaline gemstones within the study area. The increase in the activities of Li, F and B in the pegmatite is recorded by mica in the series: biotite-muscovite- Li mica-lepidolite and tourmaline of the series schorl-elbaite, liddicoatite. This finding clearly corroborates the views of London and Manning (1995) that the presence of tourmaline depends primarily on the B contents in granitic rocks with variable amount of  $\text{Al}_2\text{O}_3$  and (FeO, MnO, MgO). From the systematic enrichment of boron within the studied pegmatite, boron enrichment can be attributed to anatexis of boron-enriched source (mica rich metasediment) followed by magmatic fractional crystallization of the fluid that formed the pegmatite granite.

Considering the internal structure, mineralogical distribution and geochemical data on the granodiorite and muscovite, the proposal of Roda *et al.*, (2012) "from granite to highly evolved pegmatite" is hereby evoked as the petrogenetic model which best explains the origin of the pegmatite from Angwan-Doka area. The pegmatite was formed by magmatic fractionation of the residual fluid that formed the Pan-African granite with the possibility of some direct anatectic input. The high Li-Cs-Ta value in the muscovite (Table 3.3) suggests that the pegmatite group in Angwan Doka area belong to the lithium-cesium-tantalum (LCT) family of the rare element class while the content of Li, Rb, Cs, Be, F, Sn, P, B Ta and Nb in the pegmatite places the group under the albite, spodumene, lepidolite to

elbaite sub-class as proposed by Cerny and Ercit (2005). The pegmatite group in Angwan Doka, Kokoona group can be said to be "heterogeneous" because it consists of the different types and subtypes of LCT family, Rare Element Class pegmatites.

The granitic rock in Janta classified as A-type granite on the basis of chemical composition was emplaced into non orogenic setting. Geochemically, this granite is similar to the topaz-bearing granites in Finland described by Hapaala (1997). This granite worked upwards from great depth intruding and digesting enormously thick highly crystallized older country rocks thereby altering the chemistry of the melt by incorporating trace elements and flux from the basement. The fact that the biotite granite is straddle between post orogenic and syncollisional border (Figures 3.5) and also plots within peraluminous rather than the peralkaline and S-type field (Figure 3.3) are evidences that the rock might have been highly contaminated by pre-existing rocks during ascent and emplacement. The total REE contents ( $\Sigma$ REE) in the biotite granite from Janta area is 137.8 while averagely, it is 139.9 in the granodiorite from Angwan Doka area. The granodiorite from Angwan Doka area display more fractionated light REE enrichment  $(La/Yb)_N = 26.8$  but with heavy REE depleted pattern and weak negative Eu anomaly (expressed as ratio  $Eu/Eu^*$ ) of 0.79 in contrast to the biotite granite with  $Eu/Eu^*$  of 0.02, and  $(La/Yb)_N = 1.12$ , showing relative enrichment of heavy REE. According to Samson and Wood (2005), the heavy REE are normally associated with rocks rich in fluorine.

The magnitude of  $Eu/Eu^*$  anomaly in the granodiorite from Angwan Doka and the associated pegmatite dykes suggests crystallization at a more oxidized environment probably in lower continental crust. According to Rollinson (1993) this anomaly is very common in rocks derived from continental crust and is related to retention of Eu as  $Eu^{2+}$  in



residual plagioclase during partial melting and plagioclase fractionation as  $\text{Eu}^{2+}$  is compatible in plagioclase, while the other trivalent REE are incompatible.

The peraluminous A-type granite which plot distinctively in within-plate (WPG) field On the Rb-(Y+Nb) discrimination diagram after Pearce *et al.*, (1984) is characterized by high alkali content (Figure 3.6). Further, the high Rb content and fractionated nature of the rock with the albitization of the granite caused the granite to plot on the border of post orogenic and syn-collisional diagram (Figure 3.5) of Batchelor and Bowden (1985). Values of the ratios of some ionic twins with similar ionic radius and charge such as K/Rb recorded in the granodiorite from Angwan Doka is 68.8 while it is 74.4 in the biotite granite from Janta thus indicating their derivation from crustal source. Bau (1996) had proposed Y/Ho ratio as a tool for identifying non-charge and non-ionic size controlled magmatic trace element behavior such as found in aqueous systems. Bau and Dulski (1995) suggest the complexation with fluorine as major cause for Y/Ho values  $>28$ . Irber (1996) have reported that peraluminous A-type granites generally show Y/Ho  $> 28$  while peraluminous S-type granites shift to Y/Ho ratios  $<28$ . The Y/Ho ratio is 25.3 and 36 in the granodiorite and the biotite granite respectively. This indicates that the granodiorite in Angwan Doka derived from S-type granitic magma.

In the granitoids from Angwan Doka, Sr/Eu are 188 whereas in the biotite granite it is 6, Zr/Hf ratio of 41.2 was recorded from Angwan Doka while the A-type biotite granites from Janta area with lower ratio of 16.0. This trend indicates that biotite granite in contrast to the granodiorite has been affected by magmatic-hydrothermal alteration and therefore the very strong tetrad effect.

Evidence of postmagmatic alteration abounds in the topaz-bearing granite. This includes reactions involving exsolution and minor recrystallization of alkali feldspar which resulted in partially altered feldspar grains. Subsolidus alteration of biotite to chlorite and of plagioclase to topaz, fluorite, and muscovite further indicates that the postmagmatic fluids have caused great chemical changes in the granite. Postmagmatic reactions have intensely modified its composition. Greisen veins, some of which are mineralized, are associated with the biotite granite. The higher Sn concentration and the low K/Rb ratio are related to the greisenization and enrichment of F (Matheis, 1979 and Kuster, 1990) while the highly depleted Eu is also attributed to intense albitization of the plagioclase. Ogunleye (2006) noted that the prevalence of Sn in the subalkaline granite of the Nigerian anorogenic ring-complex province was due to high level of greisenization brought about by late stage volatile-rich steam of primarily magmatic fluid. Kinnaird (1985) also attributed the high hydrothermal alteration of the granite in Janta area to sodic and potassic metasomatism with albitization, chloritization and argillization processes concentrated at the roof zone of the granite but decreasing with depth.

Alteration of plagioclase to sericite is restricted to the core and generally uneven within the individual crystal (Plates XXX and XXXI); either varying with the intensity of the hydrothermal fluid or due to micropores within the plagioclase crystals (Katzir *et al.*, 2006). The highly fractionated nature of the granite with associated Nb, Ta, Sn and W mineralization suggest that late stage magmatic fluid with high volatile content was responsible for the various alteration processes that the granite has undergone rather than an external hydrothermal fluid. The autometasomatic albitization of the granite in Janata area was rather pervasive than vein controlled. Topaz and beryl gemstones from

Janta area have formed in pegmatite, the presence of magmatic topaz is indicated by crystallized melt inclusions entrapped in some topaz and topaz may also form during the process of greisenization due to the high temperature acidic silica- and fluorine-rich hydrothermal fluid which reacted with the Al leached from feldspar in the granitic rocks to produce the gem quartz, beryl and topaz associated with cassiterite in the area.

## CHAPTER SIX

### CONCLUSION AND RECOMMENDATIONS

#### 6.1 CONCLUSION

Based on petrography, mineralogy and geochemistry, it is highly likely that the granodioritic rocks in the two areas were produced during the same thermal event and, therefore, the sequence of hornblende-biotite granodiorite and biotite-muscovite  $\pm$  cordierite granodiorite observed. The source materials could also be mantle-derived melts during dipping period (subduction) which formed a hybrid magma that fractionated into S-type. The K/Rb and K/Cs ratio, REE chemistry and the gradual increase in Rb, Cs, K, Nb, Ta, Li, F, P, Ti and U from Jamalua to Angwan-Doka indicate fractional crystallization.

Field evidence and petrography indicate that the pegmatite differentiated from the Older Granites. From the broad major, minor and trace element chemistry of the pegmatite, crystallization was largely segmented and progressed inward and northward towards the core. Element fractionation trend clearly marked by systematic increase in Li, F, Rb, Cs indicates crystallization started from outer border zone to lepidolite probably in a closed system. If crystallization did not occur in a closed system, there would have been no

progressive increase and enriched in volatiles (Li, F, B and P) which exsolved to form centrally located primary pockets.

The systematic increase in elements from the granodiorite to the pegmatite and the similarity in all trends shown in the plots of figures used in this study reveal the importance of chemical fractionation as the main influencing factor on the overall crystallization of the granodiorite and pegmatite from the study area. This is consistent with an internal fractionation model. The petrogenic model “from granite to highly evolved pegmatite” is therefore proposed for the granitoids.

Geochemical trend indicate an evolution from a ferrocolumbite to manganotantalite within the different zones of AngwanDoka pegmatite. Niobium, tantalum and Tin are concentrated by extreme fractional crystallization in a flux-rich melt, fractionation trends of muscovite indicate that the pegmatite crystallized from the margins inward thus mineralization are primarily magmatic, alteration led to complex internal zonation with muscovite-rich replacement zones. These late zones are further enriched in Nb-Ta and Sn, indicating that magmatic–metasomatic processes played a role in metal enrichment

The increase in B, Li, F and Mn, Ti, content of the muscovite from the border zone towards the core zone therefore show a convergent evolutionary trend from the Fe-rich tourmaline (schorl-dravite) at the border zone and wall zone to elbaite with a high rossmanite component in the lepidolite zone. This petrogenetic model could serve as a potential indicator for the presence of gem tourmaline in pegmatite and a basis for a more comprehensive evaluation of the gemstone-bearing capacity of other less-known or hitherto less explored pegmatite fields in Nigeria.

The geochemical data combined with occurrence of gem pocket crystals, and the empirical similarity and higher content of these elements in muscovite from Angwan-Doka

pegmatite compared to the Cruzeiro (Governador Valadares region) Eastern Boborema Pegmatite Province of Brazil (EBPP), clearly demonstrate the existence of complex gem-bearing granitic pegmatite capable of supporting commercial mining activities.

The high Li-Cs-Ta value in the muscovite suggests that the pegmatite group belongs to the lithium-cesium-tantalum (LCT) family of the rare element class. The content of Li, Rb, Cs, Be, F, Sn, P, B Ta and Nb in the pegmatite places the pegmatites in the albite, spodumene, lepidolite to elbaite sub-class as proposed by Černý and Ercit (2005).

## **6.2 RECOMMENDATIONS**

- i. Li, B and O isotope signature is an appropriate tool for gaining insight into the physico-chemical conditions required for the tourmaline mineralization. It is important to undertake a study solely devoted to establishing the isotopic signatures of these basic elements in the gem tourmaline from Angwan Doka pegmatite group. The data that would be generated from this would have broad and wider applicability in clearly establishing the granite-pegmatite crystallization processes, hydrothermal and magmatic fluid phases and the presence as well as effect of mixing from the magmatic and metasomatic fluid.
- ii. To acquire compositional information on tourmaline, non-destructive chemical analysis of the mineral should be done using Electron probe micro-analyzer (EPMA). In addition, analysis of crystal-lattice preferred orientations which would enable the determination of variation in chemical constituents relating to ionic

- substitutions, and hence crystallization of the different species of tourmaline should be undertaken.
- iii. There should be detailed evaluation of economic potential of the entire Kokoona pegmatite field, as more commonly; each group carries several economic mineral (commodities). It is recommended here that exploitation of minerals should be based on bulk mining production of all primary minerals without any unnecessary wastage in view of a growing demand for these minerals e.g. feldspars in ceramic and glass industries, mica in the expanding cosmetic industry and rare-metals. Further, this is to discourage the selective mining method that leads to unstable walls and pit that are unsafe for working condition.
  - iv. Most importantly, gem minerals originating from pegmatite which are of tremendous importance in the jewelry and mineral collection industries are actively sought by the worldwide gem industry. Thus the demand for natural gems has elevated miarolitic granitic pegmatites to a level of economic significance that far exceeds their geological abundance. The scope of gemstone mining in Nigeria is still limited by the inadequate knowledge on the available resources and the capacity of the local market. This, therefore, calls for proactive approach that would engender value addition by way of providing relevant mineral assessment data which would make the business more attractive to foreign investors and the export market.

## REFERENCES

- Abaa, S. I (1991): Hydrothermal fluids responsible for the formation of precious minerals in the Nigeria Younger granite province. *Mineralium Deposita* 26, 34-39.
- Adekeye, J. I. D. and Akintola O. F. (2007). Geochemical features of rare-metal pegmatite in Nasarawa area Central Nigeria. *Journal of Mining and Geology*, Vol. 43(1) pp. 1–21.
- Aga, T. and Ashano E. C., (2008). Enhancing the value of Nigerian gemstone through lapidary, *Continental Journal of Earth Sciences*, 3 pp. 71-76
- Ajibade, A. C (1980) Geotectonic evolution of the Zungeru Region, Nigeria. Unpublished Ph.D. Thesis, *University of Wales*,

- Ajibade, A. C. and Wright J. B. (1989). The Togo-Benin Nigerian Shield: Evidence of crustal aggregation in the Pan-African belt. *Tectonophysics*.
- Akintola, O.F., Adekeye, J.D., 2008. Mineralization controls and petrogenesis of the rare metal pegmatites of Nasarawa area Central Nigeria. *Earth Science Research Journal* 12, pp. 23 -32.
- Alfonso, P and J.C. Melgarejo 2000: Boron versus phosphorus in granitic pegmatite: the Cap de Creus case (Catalona, Spain). *Journal of the Czech Geological Society*, Vol. 45, Issue 1-2, 131-141.
- Anderson, O.M., Lentz, R. D., MCFarlane R. M., and Falck, H (2013) : A geological, geochemical and textural study of a LCT pegmatite: implications for the magmatic versus metasomatic origin of Nb–Ta mineralization in the Moose II pegmatite, Northwest Territories, Canada. *Journal of Geosciences*, 58 (2013), 299–320.
- Ball E., (1980). An example of very consistent brittle deformation over a wide intra-continental area: The late Pan-African Fracture system of the Tuareg and Nigerian Shield. *Tectonophysics*, 61, pp. 363-379.
- Bau, M., (1991). Rare-earth element mobility during hydrothermal and metamorphic fluid – rock interaction and the significance of the oxidation state of europium. *Chemical Geology* 93, pp. 219– 230.
- Bau, M. (1996) Controls on the fractionation of isovalent trace elements in magmatic and aqueous systems: evidence from Y/Ho, Zr/Hf and lanthanide tetrad effect. *Contributions to Mineralogy and Petrology*. 123, pp. 323–333.
- Bau, M. (1997).The lanthanide tetrad effect in highly evolved felsic igneous rocks—A reply to the comment by Y. Pan. *Contrib. Mineral. Petrol.* **128**, 409–412.
- Bau, M. and Dulski, P. (1995) Comparative study of yttrium and rare-earth element behaviours in fluorine- rich hydrothermal fluids. *Contrib. Mineral. Petrol.* **119**, 213–223.
- Batchelor, R. A & Bowden P (1985): Petrogenetic interpretation of granitoid rock series using multicationic parameters. *Chemical Geology* 48, pp. 43-55.
- Birkett, T. C and Sinclair, W. D. (1989): Rare-metal replacement deposits (skarns and fenites) associated with alkali and carbonate complexes. In: mineralized intrusion-related skarn systems (D.R. Lentz, ed.). *Mineralogical Association of Canada. Short course handbook* 26, 445-474.
- Boynton, W. V (1984) Cosmochemistry of the rare earth elements: meteorite studies. In: Henderson P (eds), *Rare Earth Element Geochemistry*. Elsevier, Amsterdam, pp 63-114



- Brewer, T.S., Atkin, B.P., (1989). Elemental mobilities produced by low-grade metamorphic events: a case study from the Proterozoic supracrustals of southern Norway. *Precambrian Research*, 45, pp. 143–158.
- Candelia, P. (1997): A review of shallow, ore-related granites: textures, volatiles and ore metals. *Journal of Petrology*, Vol. 38, No. 12, pp. 1619-1633.
- Černý, P., (1991): Fertile granite of Precambrian rare-element pegmatite field: is geochemistry controlled by tectonic setting or source lithology? *Precambrian Research* 51, pp. 429-468.
- Černý, P., (1991): Rare-element granitic pegmatites. Part I: Anatomy and internal evolution of pegmatite deposits. Part 2: Regional to global environments and petrogenesis. *Geoscience Canada*, 18, pp. 49–81
- Černý, P., (1992): Geochemistry and petrogenetic features of mineralization in the rare-element granitic pegmatites in the light of current research. *Applied Geochemistry* Volume 7, pp. 393-416.
- Černý, P., (1982): Petrogenesis of granitic pegmatite. Mineralogical Association of Canada Short Course Handbook 8, 1982.
- Černý, P., and Ercit, T. S., (2005): The classification of granitic pegmatites: revised. *Canadian Mineralogist*, 43: 2005-26.
- Černý, P. and Hawthorne F. C., (1982): Selected peraluminous minerals. Mineralogical Association of Canada Short Course Handbook 8, 1982.
- Černý, P., and Burt, D. M., (1984): Paragenesis crystallochemical characteristics and geochemical evolution of the micas in the granite pegmatite. *Reviews in Mineralogy and Geochemistry*, Vol. 13, pp. 257-297.
- Černý P, Ercit T.S (1985): Some recent advances in the mineralogy and geochemistry of Nb and Ta in rare-element granitic pegmatites. *Bull Minéral* 108: 499–532
- Černý, P., Robert E and Alan J (1985): Extreme fractionation in rare element granitic pegmatites: selected examples of data and mechanisms *Canadian Mineralogists*, Vol.23, pp. 381- 421
- Černý, P., Meintzer E. R, Anderson A. J, (1985): Extreme fractionation in rare element granitic pegmatite: selected examples of data and mechanism. *Canadian Mineralogists*, Vol. 23, pp. 381-421.
- Chappel W. B, White R. J. A (2001): Two contrasting granite type: 25 years later, *Australian Journal of Earth sciences* 48, 489-499

- Dada S.S (2006): Proterozoic evolution of Nigeria. In: Oshin O (ed.), The basement complex of Nigeria and its mineral resources (A Tribute to Prof. M. A. O. Rahaman), Akin Jinad and Co., Ibadan, pp. 29 - 44.
- Danbatta U. A. (2008): A review of the evolution and tectonic framework of the schist belts of western Nigeria, West Africa. *Africa Geoscience Review*, Vol. 15, No, 2, pp145-158.
- Dahl P.S, Wehn D. C, Feldmann, S. G (1993): The systematics of trace-element partitioning between coexisting muscovite and biotite in metamorphic rocks from the Black Hills, South Dakota, USA. *Geochimica et Cosmochimica Acta* 57, pp. 2487-2505.
- Diaz-Alvarado., Antonio Castro., Carlos Fernandez., Ignacio Moreno-Ventas (2011): Assessing bulk assimilation in cordierite-bearing granitoids from the central system batholiths, Spain: Experimental, geochemical and geochronological constraints. *Journal of Petrology*, Volume 52, pp. 223-256.
- Eby, G. (1990): The A-type granitoids: A review of their occurrence and chemical characteristics and speculation on their petrogenesis. *Lithos*, Vol. 26, Issue 1-2, pp. 115-134.
- Ekwueme, B. N. and Matheis, G. (1995): Geochemical and economic value of pegmatites in the Precambrian Basement of Southeast Nigeria. In: Swats, R.K., Chandra, R. (Eds.), Magmatism in relation to diverse tectonic setting. Oxford B.H. Publishing Co. New Delhi, pp. 375-392
- Emmerman, R, Diara L, Schneider J (1975): Petrologic significance of rare earth distribution in granites. *Contributions to Mineralogy and Petrology*, 52, pp 267- 283.
- Ercit, T. S. 2005. REE-enriched granitic pegmatite. in rare- elements geochemistry and ore deposits. Geological Association of Canada, *Shortcourse Notes 17*, pp. 257-296.
- Evenson, J. M and London D. (2002): Experimental silicates mineral partition coefficient for beryllium and the beryllium cycle from migmatite to pegmatite. *Geochimica et Cosmochimica Acta*, 66, pp. 2239-2265.
- Falconer, J. D. (1911): The Geology and Geography of Northern Nigeria. *Macmillan, London*.
- Ferre, E. C, Caby R, Peucat J. J, Capdevila I. R, and Monie P. (1998): Pan-African post collisional ferro-potassic granite and quartz-monzonite plutons of Eastern Nigeria. *Lithos*, 45, 255-278
- Fitches, W R, Ajibade A.C, Egbuniwe i. G, Holt R. W and Wright J. B (1985): Late proterozoic schist belt and plutonism in NW Nigeria, *Geological society of London* 142, 319-337

- Garba, I. (2002): Late Pan-African Tectonics and origin of Gold Mineralisation and Rare-Metal Pegmatites in the Kushaka Schist Belt, North-Western Nigeria. *Journal of Mining and Geology*, 38 (1), pp. 1-12.
- Garba, I., 2003. Geochemical discrimination of newly discovered rare-metal bearing and barren pegmatites in the Pan-African (600 ± 150 Ma) basement of northern Nigeria. *Applied Earth Science (Transactions of the Institution of Mining and Metallurgy B)*, 112, pp. 287 - 292.
- Garba, I. (1996). Tourmalinization related to late Proterozoic-Early Palaeozoic late gold mineralization in Bin Yauri area, Nigeria. *Mineralium Deposita* 31:201-209.
- Giller, B. 2003: An overview of tourmaline mineralogy from gem tourmaline producing pegmatite district in Africa. M. Sc. Thesis, University of New Orleans, 204 p.
- Grant, N. K., (1970) Geochronology of Precambrian basement rocks from Ibadan, South-Western Nigeria. *Earth Planetary Science Letter* 10, pp. 19–38.
- Grant, N. K. (1971). A compilation of radiometric ages from Nigeria. *Journal of Mining and Geology*, Vol. 6, pp. 37 – 54.
- Grauch, R.I., (1989). Rare earth elements in metamorphic rocks. In: Lipin, B.R., McKay, G.A. (Eds.), *Geochemistry and Mineralogy of Rare Earth Elements. Review in Mineralogy*, Vol. 21, pp. 147– 167.
- Groat, L.A. (2007) *Geology of Gem Deposits*. In: L.A. Groat, (ed.). Mineralogical Association of Canada Short Course, Volume, 37, 280 pp.
- Hapaala, I. (1997): Magmatic and post magmatic processes in tin mineralized granites: topaz-bearing leucogranites in the Eurajoki Rapakivi granite stock, Finland. *Journal of Petrology*, Vol. 12, pp 1645-1659.
- Hawthorne, F. C, Dirlam D. M (2011) Tourmaline the indicator mineral: From atomic arrangement to Viking navigation. *Elements* 7: 307-312
- Icenhower, J.P and London, D (1995): An experimental study of element partitioning between biotite, muscovite and coexisting peraluminous granitic melt at 200Mpa (H<sub>2</sub>O). *American Mineralogists*, 80, pp. 719-734.
- Irber, W. (1999): The lanthanide tetrad effect and its correlation with K/Rb, Eu/Eu\*, Sr/Eu, Y/Ho and Zr/ Hf of evolving peraluminous granite suits. *Geochimica et Cosmochimica Acta*, 63, pp. 489–508.

- Irvin, T. M and Baraga (1971): A guide to the chemical classification of common volcanic rocks. *Canada journal of Earth sciences* 8:523-584
- Jacobson, R. R. E., Snelling, N. J. and Truswell, J. F. (1963). Age determination in the geology of Nigeria, with special references to the Older and Younger Granites. *Overseas Geology and Mineral Resources*, No. 9, pp. 168 –182.
- Jacobson, R. and Webb, J. S. (1946). The pegmatite of central Nigeria. Geological Survey of Nigeria Bulletin, No. 23.
- Jahns. R.H.1982. Internal evolution of pegmatite bodies. Mineralogical Association of Canada Short Course Handbook, Vol. 8, pp. 293-327.
- Jahns R. H. and Burhmam C. W. (1969). Experimental studies of pegmatites genesis 1. A model for the derivation and crystallization of granitic pegmatites. *Economic Geology*, 64, pp. 843-864.
- Jahn, B. M., Wu, F., Capdevila R., Martineau F., Zhao Z., and Wang Y: (2001): Highly evolved juvenile granites with tetrad REE patterns: The Woduhe and Baerzhe granites from the Great Xing'an Mountains in NE China. *Lithos* 59, pp. 171-198.
- Jolliff, B.L, Papike J. J. and C. K. Shearer (1986): Tourmaline as a recorder of pegmatite evolution: Bob ingersol pegmatite, Black hill south Dakota. *American Mineralogist* 71, pp. 472-500
- Jolliff, B. L., Papike J.J and Shearer C. K, (1987): Fractionation trends in mica and tourmaline as indicators of pegmatite internal evolution: Bob Ingersoll pegmatite, Black Hills, South Dakota. *Geochimica et Cosmachimika Acta*, Vol. 51, pp. 519 -534
- Jolliff, B. L., Papike, J. J. and Shearer, C. K. (1989) Inter-and intro-crystal REE variations in apatite from the Bob Ingersoll Pegmatite, Black Hills, South Dakota. *Geochimica et Cosmochimica Acta*, 53, 429–441.
- Janousek, J., Farrow C.M, Erban V (2013): *Geochemical Data tool kit R, version for windows 2000-2013*
- Kawabe, I. (1992) Lanthanide tetrad effect in the Ln<sup>3+</sup> ionic radii and refined spin-pairing energy theory. *Geochemical Journal* 26, 309–335.
- Kinnaird, J.A. (1981) Geology of the Nigerian Anorogenic Ring Complexes 1:500,000 geological map. *John Bartholomew and Sons*
- Kinnaird, J. A (1984): Contrasting styles of Sn-Nb-Ta-Zn mineralization in Nigeria. *Journal of African Earth Sciences*, Vol. 2, pp.81–90.

- Kinnaird, J. A. (1985): Hydrothermal alteration and mineralization of the alkaline anorogenic ring complexes of Nigeria. *Journal of African Earth Sciences*, Vol. 3:229–251.
- Kolbe P and Taylor, S.R, (1966): Major and trace element relationship in granodiorite and granite from Australia and south Africa. *Contributions to Mineralogy and Petrology*, 12, pp. 202-222
- Kontak, D.J, (2006) Nature and origin of an LCT-suite pegmatite with late-stage sodium enrichment, Brazil Lake, Yarmouth County, Nova Scotia, I. Geological setting and petrology. *Canadian Mineralogists* 44: 563–598
- Kroner A. and Stern R. J (2005): Pan-African Orogeny. In: R. C. Selley, L. Robin, M. Cocks, and I R. Plimer (eds.). *Encyclopedia of Geology*. Vol 1, Elsevier, Amsterdam, pp. 1 - 12.
- Kusky T. M., Abdelsalam M. G., Tucker R. D., Stern R. J., (2003): Evolution of the East Africa and related orogens and assembly of Gondwana. *Precambrian Research*, 123, pp. 81-337.
- Küster, D., (1990): Rare-metal mineralization of wanba, Central Nigeria-their formation in relation to the Pan-African granites. *Mineralium Deposita* 25, pp. 25-33.
- Liu C. and Zhang H. (2005).The lanthanide tetrad effect in apatite from the Altay No. 3 pegmatite, Xingjiang, China; an intrinsic feature of the pegmatite magma. *Chemical Geology*, 214, pp. 61-77.
- Linnen, R. L (1998) The solubility of Nb–Ta–Zr–Hf in granitic melts with Li and Li + F: constraints for mineralization in rare metal granites and pegmatites. *Econ Geol* 93: 1013–1025
- Linnen, R.L, Cuney M (2005) Granite-related rare-element deposits and experimental constraints on Ta–Nb–W– Sn–Zr–Hf mineralization. In: Linnen RL, Sampson IM (eds) *Rare-Element Geochemistry and Mineral Deposits*. Geological Association of Canada, Short Course Notes17: pp 45–68
- Longfellow K. M and Swanson S. E (2011): Skeletal tourmaline undercooling and crystallization history of the Stone Mountain granite, Georgia, USA. *Canadian Mineralogist* Vol. 49, pp. 341-357.
- London, D. (2005): Granitic pegmatite: An assessment of current concept and direction for the future. *Lithos*, 80, pp. 281-303.
- London D (2005): Geochemistry of alkali and alkaline earth elements in ore-forming granites, pegmatite and rhyolites. In: Robert L and Samson M (Eds.), *Rare-element geochemistry and mineral deposit*, pp. 17- 44.

- London D (2008): PEGMATITES. Canadian Mineralogist Special Publication 10, Mineralogical Association of Canada
- London D (1990): internal differentiation of rare-element pegmatite; a synthesis of recent research. In: H.J Stern and J.L Hannah (Eds.). Geological Society of America Special Paper, Vol. 246, pp. 35-50
- London, D., 1985. Pegmatites of the Middletown district, Connecticut. 77<sup>th</sup> Annual Meeting, New England Intercollegiate Geological Conference, Yale University. *Connecticut Geological and Natural History Survey Guidebook*, Vol. 6, pp. 509 – 533.
- London, D.1986: Formation of tourmaline rich gem pockets in miarolitic pegmatite. *American Mineralogists* 71, pp. 396-404.
- London D, Morgan G.B. VI (2012): The pegmatite puzzle. *Elements* 8: 263-268.
- London, D. and Morgan, G.B. 2004. Alkali fractionation and feldspar zonation in granitic pegmatites. Geological Society of America, Denver, CO.
- London D, Burt, D. (1982): Lithium minerals in pegmatite, In: Černý, P., (Ed.,) Grnitic Pegmatite in Science and industry. Mineralogical Association of Canada Short Course Handbook 8, pp. 97 -133.
- London D and Burt M. D., 1982: Alteration of spodumene, montebrasite and lithiophilite in pegmatite of the white picacho District Arizona: *American Mineralogists*, Vol. 67 pp. 97-113.
- London, D., and Manning, D. A. C., (1995). Chemical variation and significance of tourmaline from Southwest England, *Economic Geology* 90, pp. 495-519.
- London, D., Morgan, G.B. VI, and Wolf, M.B. (1996b): Boron in granitic rocks and their contact aureoles. *Mineralogical Society of America Reviews in Mineralogy*, 33, pp. 299-330.
- London, D., Wolf, M.B., Morgan, G.B. VI, and Gallego Garrido, M. (1999a): Experimental silicate phosphate equilibria in peraluminous granitic magmas, with a case study of the Alburquerque Batholith at Tres Arroyos, Badajoz, Spain. *Journal of Petrology*, 40, pp. 215-240
- London, D., Hervig, R.L., and Morgan, G.B., VI (1988): Melt-vapor solubilities and element partitioning in peraluminous granite-pegmatite systems. *Contributions to Mineralogy and Petrology*, 99, pp. 360 - 373.
- Lukkari, Sari. (2002). Petrography and geochemistry of the topaz-bearing granite stocks in Artjärvi and Sääskjärvi, western margin of the Wiborg rapakivi granite batholith, *Bulletin of the Geological Society of Finland* 74, Parts 1–2, 115–132.

- Maniar, P. D. and Piccoli, P. M. (1989). Tectonic discrimination of granitoids. *Geological Society of America Bulletin* 101, pp. 635 – 643.
- Martin, R. F., De Vito C., (2005): The patterns of enrichment in felsic pegmatites ultimately depend on tectonic setting. *Canadian Mineralogist*, Vol.43: 2027-2048
- Matheis, G., (1979): Geochemical exploration around the pegmatite Sn-Nb-Ta mineralization of southwestern Nigeria. *Geological Society of Malaysia Bulletin* 11, 333-351.
- Matheis, G. (1987). Nigeria rare-metal pegmatites and their lithological frame work. *Journal of Geology*, 22, pp. 271–291.
- Masuda, A., Kawakami, O., Dohmoto, Y. and Takenaka, T. (1987) Lanthanide tetrad effects in nature: two mutually opposite types, W and M. *Geochemical Journal* 21, pp. 119–124.
- Matheis, G. and Caen-Vachette, M. (1983). Rb-Sr Isotopic study of rare metal bearing and barren pegmatites in the reactivation zone of Nigeria. *Journal of African Earth Sciences*, Vol. 1, pp. 35 - 40.
- McCurry, P., (1971). Pan-African Orogeny in Northern Nigeria. *Geological Society American Bulletin*, 82, 3251-3262.
- Menzies, M., Balnchard, D., Jacobs, J., (1977). Rare earth and trace element geochemistry of metabasalts from the Point Sal ophiolite, California. *Earth Planetary Science Letter* 37, pp. 203– 215.
- Menzies, M., Seyfried Jr., W., Blanchard, D., (1979). Experimental evidence of rare earth immobility in greenstones. *Nature* 282, pp. 389 – 399.
- Muecke, G., Pride, C., Sarkar, P., (1979). Rare-earth element geochemistry of regional metamorphic rocks. In: Ahrens, L.H. (Ed.), *Origin and Distribution of Elements*, Vol. I. Pergamon, Oxford, pp. 449– 463.
- Middlemost, E, A K (1985): *Magma and magmatic rocks*. Longman London
- Michard, A., Albarede, F., (1986). The REE content of some hydrothermal fluids. *Chemical Geology*, 55, 51– 60.
- Nabalek P.I, Russ-Nabalek, C. and Denison J.R (1992): The generation and crystallization conditions of the Proterozoic Harney peak leucogranite, Black hills South Dakota U.S.A. In petrological and geochemical constrain. *Contributions to Mineralogy and Petrology*, 110, pp. 173-191.

- O'Connor J.J. (1965): A Classification for granites rich igneous rocks based on feldspar ratio. US Geological Survey Professional Paper 525-B: B79-B84
- Ogunleye, P. O. (2003). Trace element geochemistry of the niobium-rich Arfvedsonite granites of the northern Nigerian Anorogenic ring complexes. Ph.D. Thesis, (unpubl.), Ahmadu Bello University, Zaria, Nigeria, 188 p.
- Ogunleye, P. O, Garba .I, Ike E.C (2006): Factors contributing to enrichment and crystallization of niobium in pyrochlore in the Kaffo albite arfvedsonite granite, Ririwai complex, Younger Granite province of Nigeria 2006. *Journal of Africa Earth Sciences*, Vol. 44, pp.372-382
- Okunlola, A.O. and Ocan O.O., 2009: Rare metal (Ta-Sn-Li-Be) distributin in pre Cambrian pegmatite of Keffi area, Central Nigeria. *Nature and Science*, 7 pp. 90-99.
- Okunlola, O. A., (2005): Metallogeny of Tantalum- Niobium Mineralization of Precambrian Pegmatites of Nigeria. *Mineral Wealth* 137: 38-50.
- Pearce, J. A., Harris, N. B. W. and Tindle, A. G. (1984). Trace element discrimination diagrams for the tectonic interpretation of granitic rocks, *Journal of Petrology*, Vol. 25, Part 4, pp. 956 – 983.
- Peccerillo, A and Taylor S. R(1976): Geochemical of Eocene calc-alkaline volcanic rocks from the Kastamonu area, Northern Turkey. *Contribution to Mineralogy and Petrology*, 58: 63-81.
- Pesquera Alfonso, Jose Torres-Ruiz, Antonio Garcia-Casco and Pedro P. Gil-Crespo (2012): Evaluating the Controls onTourmaline Formation in Granitic Systems: a Case Study on Peraluminous Granites from the Central Iberian Zone (CIZ), Western Spain. *Journal of Petrology*, 54, Issue 3, pp. 609-634.
- Pedrosa-Soares, A.C., De Campos p., Noce, C., Silver, L.C., Novo, T., Roncato, J., Medeiros, S., Castaneda, C., Queiroga, G., Dantas, E., Dussin, I., and Alkmim, F. (2011): Late Neoproterozoic-Cambrian granitic magmatism in the Araçuaí orogen (Brazil), the Eastern Brazilian Pegmatite Province and related mineral resources. *Geological Society Special Publication* 350: 25-5.
- Peppard, D. F., Mason, G. W. and Lewey, S. (1969). A tetrad effect in the liquid-liquid extraction ordering of lanthanides (III), *Journal Inorganic and Nuclear Chemistry* 31, 2271– 2272.
- Pinto, C. P. and Pedrosa-Soares, A.C. (2001). Brazilian gem provinces. *Australian Gemologist*, 21, 12-16.



- Pitcher, W. S. (1993). The nature and origin of granite. Blackie Academic and Professional, London, pp. 218 – 237.
- Rahaman, M. A, Emofureta W. O, Caen Vachetta M (1983): The potassic granites of the Igbetti area: Further evidence of polycyclic evolution of the Pan-African belt in southwestern Nigeria, *Free. Res.* 22, 25-92.
- Rahaman, M. A (1988) Recent advances in the study of the Basement Complex of Nigeria. In: P. O. Oluyide, W. C. Mbonu, A. E. Ogezi, I. G. Egbuniwe, A. C. Ajibade and A. C. Umeji. Proceedings of the 1<sup>st</sup> Symposium on the Precambrian Geology of Nigeria. Geological Survey of Nigeria, Kaduna, pp. 11 - 43.
- Roda, encarnación, Alfonso pesquera, pedro p. gil-crespo, José torres-ruiz, François fontan (2005): Origin and internal evolution of the Li-F-Be-B-P-bearing Pinilla de Femoselle pegmatite (Central Iberian Zone, Zamora, Spain) *American Mineralogist*, Volume 90, pp. 1887–1899.
- Rollinson, H. R., (1993). Using geochemical data: Evaluation, presentation, interpretation, Longman Science and Technical co-published with John Wiley & Sons, Inc. New York, pp. 133 – 213.
- Samson, I.M. and Wood, S. (2005): The rare-earth elements behaviour in hydrothermal fluids and concentration in hydrothermal mineral deposits, exclusive of alkaline settings. In: R.L. Linnen, and Samson, I.M., (eds.), Rare-element geochemistry and mineral deposits: Geological Association of Canada, GAC Short Course Notes 17, p. 269-297.
- Shand, S.J., 1943. Eruptive Rocks. Their Genesis, Composition, Classification, and their relation to ore deposits with a Chapter on Meteorite. John Wiley and Sons, New York, 444p.
- Shearer, K. C, Robinson P. (1988): Petrogenesis of metaluminous and peraluminous tonalite within the Merrimack synclinorium: Hardwick tonalities Central Massachusetts. *American Journal of Science*, Volume 288-A, pp. 148-195.
- Shmakin, W. B 1979: Composition and structural state of K-feldspar from some U.S pegmatite. *American Mineralogists*, Vol. 64, pp. 49-56.
- Simmons, W. B, Pezzotta F, Shigley JE, Beurlen H (2012) Granitic pegmatites as sources of colored gemstones. *Elements* 8: 281-287
- Simmons, W.M., B.Lee M.T, Brewster R.H (1987) Geochemistry and evolution of south plate pegmatite system Jefferson county Colorado. *Geochimica et Cosmochimica Acta*, 51, pp 455-471.

- Simmons, W.B and Webber, K.L., Falster, A.U and Nizamoff, J.W (2003): Pegmatology, pegmatite, mineralogy, petrology and petrogenesis. Rubellite Press, New Orleans, Louisiana.
- Simmons W.B (2007): Gem-bearing pegmatite's. In: Groat LA (ed.) *Geology of Gem Deposits*. Mineralogical Association Canada Short Course 37, pp. 169-206.
- Simmons, S., 2007. Pegmatite genesis: Recent advances and area for future research. *Granitic pegmatites: The state of the Art International Symposium 6<sup>th</sup> – 12<sup>th</sup> May 2007, Porto, Portugal*.
- Simmons, W. B., Foord, E.E., Falster, A. Uand Kings, V.T (1995): Evidence for anatectic origin of granitic pegmatite, Western Maine, USA, *Geological Society of America, Abstract with programmes 27,411*. In London D (2008): PEGMATITES. Canadian Mineralogist Special Publication 10, *Mineralogical Association of Canada 2008*.
- Stewart, D.B, (1978): Petrogenesis and mineral assemblages of lithium-rich pegmatite. *Geological Society of America, Special Paper 76, 159*.
- Swanson, S.E. (2010): Undercooling in deep pegmatites: an example from Spruce Pine, North Carolina. *Geological Society of America, Abstr. Programs 42, 53*.
- Taylor, S.R., McLennan, S.M., 1985. The continental crust: its composition and evolution. Blackwell, Oxford, 312 p.
- Tin Quach Duc (2007): Experimental studies on the behaviour of rare earth elements and tin in granitic systems 2007. *On line M. Sc. Thesis*
- Turner D. C, (1983): Upper proterozoic schist belt in the Nigeria sector of the Pan African- province of West Africa. In: C. A Kogbe *Geology of Nigeria 2<sup>nd</sup> Revised Edition*. Rock view publication company, Jos Nigeria, PP 93-109
- Tindle. G. A, Selway, B. J, Breaks, W. F (2005): liddicoatite and associated species from the mcombe spodumene-subtype rare-element granitic pegmatite, northwestern Ontario, Canada. *The Canadian Mineralogist* Vol. 43, pp. 769-793 (2005)
- Van Breeman, O. and Bowden, P., (1973). Sequential age trends for some Nigerian Mesozoic granites. *Nature*, 242, pp. 9 – 11.
- Viana, R.R., Jordt-Evangelista, H., and Stern, W.B., 2007. Geochemistry of muscovite from the pegmatite of the Eastern Brazilian pegmatite province: a clue to petrogenesis and mineralization. *European Journal of Mineral* 19, pp. 745-755.
- Van Lichtervelde M., Gregoire M., Linnen R., Beziat D., Salvi. S., (2008): Trace elements geochemistry by laser ablation ICP-MS of micas associated with Ta mineralization in the Tanco pegmatite, Monitoba, Canada. *Contrib mineral petro* 155:791-806.

- Webber, K.L., Simmons, W.B., Falster, A.U., Foord, E.E., 1999. Cooling rates and crystallization dynamics of shallow level pegmatite–aplite dikes, San Diego County, California. *American Mineralogists* 84, 708–717.
- Wolf, M.B. and London, D. (1997): Boron in granitic magmas: stability of tourmaline in equilibrium with biotite and cordierite. *Contributions to Mineralogy and Petrology*, 130, 12-30.
- Wright, J.B., (1970). Controls of mineralization in the Older and Younger Tin Fields of Nigeria. *Economic Geology*. 65, 945-951.
- Zhao, J. X. and Cooper J. (1992): Fractionation of monazite in the development of V-shaped REE patterns in leucogranite systems: Evidence from a muscovite leucogranite body in central Australia. *Lithos* 30, 23–32.
- Zhao, Z., Masuda A., and Shabani M. (1992) Tetrad effects of rare-earth elements in rare-metal granites. *Chinese Journal of Geochemistry*, 12, pp. 221-233
- Zhao, Zhenhua, xiong xiaolin, Han Xiaodong, Wang Yixian, Wang Qiang, Bao Zhiwei<sup>1</sup> and Borming Jahn (2002): controls on the REE tetrad effect in granites: evidence from the Qianlishan and Baerzhe granites, China. *Geochemical Journal*, Vol. 36, pp. 527 - 543.